

*UNIVERSIDAD DE GRANADA
FACULTAD DE CIENCIAS*

*Departamento de Física Aplicada
Grupo de Física de Fluidos y Biocoloides*

*Estabilidad y actividad interfacial de
emulsiones modelo con interés en
alimentación funcional*



Roberto Tejera García

TESIS DOCTORAL

DIRECTORES

Dr. D. Miguel Ángel Cabrerizo Vílchez
Catedrático de Física Aplicada

Dra. Dña. María José Gálvez Ruiz
Prof. Titular de Física Aplicada

Dr. D. Antonio Martín Rodríguez
Prof. Titular de Física Aplicada

Grupo de Física de Fluidos y Biocoloides
UNIVERSIDAD DE GRANADA

Roberto Tejera García

Trabajo presentado para aspirar al grado de Doctor en Ciencias Físicas,
Doctor Europeus. Granada, 2008

A mis padres, mi hermana

A mi mujer

It is by logic that we prove, but by intuition that we discover

Henri Poincaré

Agradecimientos

Quisiera mostrar mi más sincero agradecimiento a las personas que me han ayudado, empujado y animado para la realización de este trabajo.

En primer lugar, agradezco a mis directores de tesis, María José Gálvez Ruiz, Miguel Ángel Cabrerizo Vílchez y Antonio Martín Rodríguez por la confianza que han depositado en mí y por haberme guiado por este camino dándome todo el apoyo posible y los mejores consejos. Quiero agradecerles especialmente su paciencia con mis momentos de terquedad y el trato tan cercano que siempre hemos tenido. También quiero agradecer especialmente a Roque Hidalgo Álvarez todo el apoyo que me ha dado desde el primer momento y el servirme como punto de referencia en todos los niveles.

Agradezco a mis compañeros todos los momentos que hemos pasado. Todas las charlas con mis amigos me ayudaron a entender los problemas, a enfocar sus posibles soluciones y sobre todo a disfrutar el tiempo que he tenido la suerte de poder compartir con ellos. Muchas gracias a Pedro Gea por el tiempo que hemos pasado juntos desde hace ya muchos años y por todos los conocimientos que me supo transmitir, incluido su pragmatismo. Gracias también a Sándalo Roldán con quien he tenido conversaciones que me han enriquecido tanto a nivel científico como personal y me han enseñado esa siempre creciente ilusión por la física que nunca perderemos.

A Arturo Moncho por ser genial y por haberme ayudado con muchos de los problemas que se han presentado. Muchas gracias por todos los momentos que he disfrutado y que espero seguir disfrutando, aunque no sea tan a menudo, con Manolo (que nunca consiguió aniquilarme aunque sabe que lo intentó con todas sus fuerzas), Javier, Teresa, Cedric, Juanjo, Juan Carlos, El Moro, Fernando Martínez (que me pasó el notebook de Lompado), Jose Manuel, Fernando Vereda (que con un martillo y un soldador arregla tres electrodos de zetapals, en un minuto y perdiendo solo dos dedos). Gracias a todos mis compañeros, a Jose Arturo, Catalina, Ceci, Alberto, Julia, María, Ana Belén y a los últimos fichajes. A Miguel Ángel Rodríguez Valverde por haberme enseñado a moverme en un laboratorio, por sus inestimables consejos y aclaraciones y por todo el tiempo que me dedicó durante la realización de mi tesina. Gracias también a Francisco Martínez, Artur, Juan Luis, Delfi, José Callejas, Juan de Vicente y Rafael.

También quisiera mostrar mi especial agradecimiento a la Dra. Dña. Cristina Otero Hernández y a su grupo de investigación en el departamento de Biocatálisis del Instituto de Catálisis y Petroleoquímica del CSIC por habernos donado generosamente los lípidos estructurados empleados en este trabajo.

I wish to thank very specially to Professor Paavo Kinnunen, for taking me into his group and make me feel as in family from the beginning. Thank you to Juha-Matti, Chris, Pavol, Rohit, Sanjeev, Karen & Juha, Yegor, Mikko Parry and to Kristiina for all your support and friendship.

A mi broder Joaquín, de quien siempre he recibido buenos consejos, apoyo incondicional y una gran amistad. Y a mis amigos Rodrigo, Atún y a Che por haber estado siempre a mi lado dando alegría y buenos momentos.

Finalmente quiero agradecer a mi familia todo lo que me han dado (que ha sido todo). A mis padres y a mi hermana que han sufrido mis momentos buenos y malos y siempre han estado conmigo. A Minna, por haber hecho que este trabajo fuese posible, por ser mi mujer, mi vida y mi ilusión.

El presente trabajo se ha desarrollado dentro del Grupo de Física de Fluidos y Biocoloides del Departamento de Física Aplicada de la Universidad de Granada, gracias a la ayuda de la Consejería Innovación, Ciencia y Empresa de la Junta de Andalucía y de los proyectos AGL2004-01531 y MAT2007-66662-C02-01 del Ministerio de Ciencia y Tecnología.



Prólogo

Los aceites y grasas han formado siempre parte de nuestra dieta a lo largo de la historia. Sin embargo, solo en las últimas décadas se les ha empezado a prestar una mayor atención. Evolutivamente nuestros paladares se fueron desarrollando para favorecer la obtención de un máximo de energía de los alimentos que ingeríamos. Solo los individuos que se abastecían con las mayores cantidades de energía estaban preparados para sobrevivir a enfermedades o hambrunas. De esta forma, al hombre actual le resultan sabrosas las comidas con elevado contenido calórico. De entre todos los alimentos, aquellos que alcanzan las mayores cotas energéticas son los aceites y las grasas. Pudiendo llegar hasta cerca de los 4000kJ por cada 100g, algunos aceites como el de girasol pueden utilizarse incluso como combustible en los motores Diesel. Los aceites y las grasas nos resultan sabrosos. Las empresas de comida rápida se dieron cuenta de ello y los introdujeron ampliamente en sus productos haciendo que, a día de hoy sus franquicias se extiendan, al ritmo de pegadizos slogans, por todos los países del mundo. En muchas partes han llegado incluso a imponerse sobre las dietas tradicionales locales.

Este elevado aporte calórico, que durante una parte muy cercana de nuestra historia significó una señal de salud, se ha convertido en la actualidad en un problema. Los nuevos estilos de vida más sedentaria, junto con el excesivo consumo de estos alimentos han dado lugar a la proliferación de enfermedades como las afecciones coronarias,

arteriosclerosis o trombosis. Las grasas, debido a la saturación de sus cadenas hidrocarbonadas, han demostrado ser especialmente perjudiciales para la salud cuando se consumen en exceso. La manipulación industrial de estos productos ha dado una vuelta de tuerca más a estos problemas introduciendo las comúnmente conocidas como grasas *trans*-. Este tipo de grasas aparece en los procesos industriales de hidrogenación parcial de aceites para la producción de margarinas y demás derivados. Con estos procesos se favorecen características tales como su punto de fusión o su mejor almacenaje. Sin embargo, a parte de incrementar el grado de saturación haciéndolas menos densas y más insaludables, el principal problema para la salud radica en la alteración que se produce en la geometría de los enlaces simples de estos aceites que da lugar a interacciones adversas con nuestro organismo. Este tipo de grasas se han asociado con enfermedades como la diabetes, el cáncer o incluso con la infertilidad y han demostrado su efecto perjudicial en el sistema cardiovascular. Como alternativa a este tipo de grasas semisólidas han aparecido recientemente otro tipo de grasas en las que no se hidrogenan las cadenas de ácidos grasos sino que simplemente se reemplazan por otras ya saturadas. Éste es un proceso enzimático de transesterificación catalizado por la presencia de una lipasa que da lugar a grasas semisólidas en las que no aparecen los enlaces simples *trans*-. En este trabajo realizaremos un estudio in-vitro sobre las distintas características de las emulsiones producidas con estas grasas estructuradas y observaremos como se lleva a cabo una simulación del proceso digestivo de las mismas.

ÍNDICE

I. Introducción	19
II. Objetivos y Esquema	27
III. Breve Resumen y Discusión de Resultados	31
IV. Conclusiones y Perspectivas	39

CAPÍTULO 1:

Interfacial study of interactions between lipases and bile salts

<i>Abstract</i>	53
1. Introduction	55
2. Materials and Methods	57
2.1. <i>Chemicals</i>	57
2.2. <i>Interfacial tensiometry</i>	59
2.3. <i>Theoretical background</i>	63
3. Results and Discussion	65
3.1. <i>Kinetics of single adsorption of bile salts and lipases</i>	65
3.2. <i>Kinetics of mixed adsorption of bile salts and lipases</i>	70
3.3. <i>Kinetics of sequential adsorption of mixed bile salts and lipases</i>	75
4. Conclusions	82
<i>Refences</i>	85

CAPÍTULO 2:

Physical characterization and emulsion stability of semisolid fats from olive oil and fully hydrogenated fats

<i>Abstract</i>	89
1. Introduction	90
2. Materials and Methods	92
2.1. <i>Chemicals</i>	92
2.2. <i>Emulsions preparation</i>	94
2.3. <i>Theoretical approach</i>	95
2.4. <i>Following the breaking of the emulsions with Turbiscan</i>	98
3. Results and Discussion	102
3.1. <i>Effect of the type and concentration of BS on the stability of emulsions with triolein</i>	102
3.2. <i>Effect of the STAG type on the stability of emulsions with NaTC</i> ..	110
4. Conclusions	122
<i>Refences</i>	124

CAPÍTULO 3:

Turbidimetric and interfacial study of lipolysis in O/W emulsions of triolein and of semisolid structured fats stabilized with bile salts

<i>Abstract</i>	127
1. Introduction	129

2. Materials and Methods	133
2.1. <i>Chemicals</i>	133
2.2. <i>Emulsions preparation</i>	136
2.3. <i>Following the reaction by turbidimetry</i>	138
2.4. <i>Theoretical approach</i>	140
2.5. <i>Lag phase</i>	153
2.6. <i>Air-water interfacial accumulation of reaction products</i>	154
2.7. <i>Fibrillar formations</i>	155
3. Results and Discussion	157
3.1. <i>Effect of the oil and lipase concentrations on the kinetics of lipolysis</i>	157
3.1.1. <i>Reaction with NaTC</i>	157
3.1.2. <i>Reaction with NaTDC</i>	164
3.2. <i>Effect of the NaTC and CaCl₂ concentrations on the kinetics of lipolysis</i>	169
3.3. <i>Effect of the lipase and NaTDC concentrations on the kinetics of lipolysis</i>	173
3.4. <i>Effect of the type of STAG on the kinetics of lipolysis</i>	180
3.4.1. <i>Reaction with STAG from sesame oil and fully hydrogenated soybean oil</i>	181
3.4.2. <i>Reaction with STAG from olive oil and fully hydrogenated palm oil</i>	185
4. Conclusions	189
Refences	192

APÉNDICE A:

Basic Concepts

A.1. <i>Interfacial Energy</i>	199
A.2. <i>Young-Laplace Equation</i>	201
A.3. <i>Pendant Drops</i>	203
A.4. <i>Interfacial Adsorption</i>	207
A.5. <i>Emulsions</i>	209

APÉNDICE B:

Experimental Techniques

B.1. <i>Axisymmetric Drop Shape Analysis (ADSA)</i>	213
B.2. <i>Emulsions stability</i>	215
B.3. <i>Emulsions preparation</i>	218
B.4. <i>Batch turbidity measurements</i>	220
B.5. <i>Batch surface tension measurements</i>	222
B.6. <i>Emulsion droplet sizing</i>	224

I. Introducción

Los ingredientes de un sistema alimentario determinan las propiedades del mismo. Con el fin de mejorar las características de un alimento se ensayan diferentes procesados de estos ingredientes. Gran parte de los productos alimentarios son sistemas multifase, es decir, contienen dos o más fases inmiscibles (fase acuosa, oleosa o gaseosa) dando lugar a emulsiones o espumas líquidas [1] que son termodinámicamente inestables [2]. Es en esta inestabilidad donde radica el principal problema para la caracterización de estos sistemas ya que la fase dispersada solo lo estará durante un período de tiempo finito. Este tiempo depende de las características de la interfaz que separa ambas fases por lo que el estudio de interfases fluidas constituye uno de los ámbitos de investigación más importante dentro del campo de los coloides alimentarios [3]. Numerosas líneas de investigación que se han abierto desde hace tiempo en este sentido [4]. Gran parte de los estudios realizados hasta la fecha presentan sin embargo la dificultad de ajustar correctamente los resultados experimentales a los modelos propuestos para emulsiones. Existen además problemas relacionados con las innovaciones o modificaciones que se tienen que introducir en los distintos dispositivos experimentales para producir la interfaz aceite-agua, así como con la mayor complejidad de los estudios planteados en este tipo de interfaz frente a los realizados en la interfaz aire-agua [5].

A la dificultad de caracterización de estos sistemas hemos de añadir el hecho de que a gran parte de los productos alimentarios actuales se les exige que posean ciertas propiedades funcionales y que presenten una serie de atributos: una textura adecuada, buen sabor, color, etc. En este sentido los retos de la industria alimentaria son muy amplios, ya que no sólo se trata de mejorar las formulaciones tradicionales o existentes, sino de formular nuevos productos tales como alimentos instantáneos o semipreparados, con bajo contenido en grasas, enriquecidos con algún componente (vitaminas, calcio, esteroides vegetales, ácidos grasos poliinsaturados), alimentos para dietas hospitalarias -alimentos funcionales- o infantiles, etc.

Los omega-3

Los alimentos funcionales, o nutracéuticos, son aquellos que aportan beneficios a la salud o que reducen el riesgo de sufrir ciertas patologías. Junto a su valor nutricional, aporta valores profilácticos (preventivos) o terapéuticos. Este tipo de alimentos constituyen el área de mayor crecimiento potencial en la industria alimentaria, en particular los aceites, lípidos y fosfolípidos. Los aceites esenciales contienen ácidos grasos omega-3 y 6 que el organismo no puede sintetizar, que son imprescindibles para mantener la salud y que deben ingerirse en la dieta. El cuerpo transforma este tipo de ácidos en poderosos agentes como los eicosanoides (prostaglandinas y leucotrienos). La alimentación occidental es muy deficiente en estos ácidos y esta tendencia se continúa agravándose, existiendo un balance desproporcionado entre la ingesta de omega-3 y 6 (5-

6 veces inferior). Es por ello que en la última década, la industria alimentaria y la farmacéutica han mostrado un interés creciente por la preparación de productos enriquecidos en ácidos grasos poliinsaturados (PUFA) que permitan una ingesta de omega-3/omega-6 en la razón necesaria para potenciar sus propiedades nutricionales y terapéuticas. Conjuntamente se está llevando a cabo un gran despliegue científico respecto a los llamados lípidos estructurados: triacilglicéridos modificados por métodos químicos o enzimáticos, mediante alteración de su composición en ácidos grasos y/o la distribución de éstos en la molécula de glicerol. Entre ellos figuran: huevos enriquecidos a partir de gallinas con dieta rica en omega-3 y o productos lácteos donde la grasa ha sido sustituida por aceites extraídos de productos marinos. Los aceites de pescado son importante fuente natural de PUFA omega-3. Otro ácido nutracéutico es el ácido linoleico conjugado (CLA): mezcla de isómeros posicionales y geométricos del ácido linoleico.

La tercera parte de los cánceres y enfermedades coronarias están relacionados con la dieta [6]. En humanos, la ingesta diaria de omega-3 *eicosapentenoico* (EPA) y *docosahexenoico* (DHA) reducen patologías coronarias inhibiendo la producción de agentes bloqueantes y facilitando la producción de agentes antibloqueo. Reducen arteriosclerosis, cáncer, diabetes, hipertensión arterial y estados depresivos. DHA es esencial para el funcionamiento del ojo y el sistema nervioso. El carácter anticarcinogénico y antioxidante del CLA se debe a la inhibición competitiva de la biosíntesis del ecosanoico y a inhibir la formación de peróxidos. Revisiones sobre la repercusión omega-3 han sido publicadas por Simopoulos [7] y Nettleton

[8]. 5.5 gramos/semana de EPA y DHA reduce 50% riesgo de infarto [9]. El mínimo consumo de CLA es 3.5 g/día [10]. Por todo ello, tanto consumidores amantes de dietas saludables como individuos con riesgo potencial para ciertas enfermedades han aumentado su interés por nutrientes con propiedades terapéuticas. A parte de todos estos beneficios, los glicéridos con residuos EPA y DHA se absorben en el torrente sanguíneo humano mejor que sus etil ésteres [11] y la estabilidad oxidativa de los ácidos n-3 en forma glicérido es muy superior a la de su forma libre [12]. Así los nutracéuticos deberían contenerlos como glicéridos.

Posibles aplicaciones alternativas a las nutricionales son el uso de inyecciones parenterales de emulsiones lipídicas ricas en ácidos omega-3 (ej., inyección intravenosa), de enorme interés en clínica para el tratamiento de las disfunciones en la absorción de grasas en nutrición enteral [13].

El aceite de oliva

El aceite de oliva es el aceite típico de la dieta Mediterránea, rico en monoinsaturados (>70% ácido oleico) y resistente a la fritura/cocción. Se considera el mejor para la dieta por su alta estabilidad y propiedades de aroma, sabor, y por sus componentes minoritarios: polifenoles, aldehidos, cetonas, ésteres, ácidos, furanos y terpenos. Por contra, aceites ricos en saturados son más estables pero incrementan el colesterol “malo” promotor de las lipoproteínas de baja densidad LDL, mientras que los aceites ricos en PUFA (ej., soja) son los más lábiles a la oxidación y a la temperatura (riesgo en almacenamiento, no útiles para cocción y frituras). La sustitución selectiva de determinados ácidos presentes en aceites y grasas puede

minimizar sus efectos indeseables. Mediante su incorporación regioselectiva en la molécula del glicerol es posible potenciar los efectos beneficiosos de los PUFA. Dada su abundancia, precio asequible, alto contenido en monoinsaturados y demás propiedades, el aceite de oliva resulta idóneo como materia prima para la obtención de aceites enriquecidos en omega-3, que permitan mejorar el balance en la dieta cotidiana moderna entre ácidos esenciales omega-3 y omega-6, sin renunciar a las aportaciones propias del aceite de oliva.

Lípidos estructurados

Nuevos alimentos y/o aditivos funcionales a partir de subproductos alimentarios baratos, como residuos de la industria del pescado y del aceite de oliva, están siendo investigados. Dada su composición (glicéridos de máximo valor en PUFA) estos productos presentan un carácter terapéutico y profiláctico. La tecnología enzimática es la más idónea para obtener estos productos de alto valor añadido ricos en ácidos omega-3 y omega-6. Las reacciones enzimáticas transcurren en condiciones suaves que reducen la oxidación de los PUFA (muy lábiles por su gran insaturación) y, mediante su incorporación regioselectiva en la molécula del glicerol se puede llegar a un máximo aprovechamiento de sus propiedades fisiológicas y terapéuticas para el organismo. Glicéridos enriquecidos en PUFA para su aplicación como nutracéuticos pueden ser obtenidos mediante hidrólisis, alcoholisis, acidólisis, glicerolisis y transesterificación de aceites de pescado, aceites de semillas, y aceites de microorganismos [14, 15, 16, 17, 18, 19].

Por otro lado, la disminución de la presencia de enlaces insaturados con isomería *trans* en grasas provenientes de la hidrogenación parcial de aceites es uno de los objetivos fundamentales de la industria alimentaria moderna. En los últimos años, se están explorando procesos de transesterificación enzimática parcial entre una grasa saturada y un aceite, de gran utilidad para obtener grasas semisólidas de distinta textura y plasticidad [20, 21]. Las lipasas permiten el cambio deseado en la estructura del triacilglicérido en una sola etapa selectiva, basada en su especificidad por tipo de ácido graso y posición en el glicerol. La redistribución selectivamente ciertos ácidos grasos en triacilglicéridos da lugar a otros con una textura y punto de fusión definidos [22, 23]. De esta forma pueden obtenerse grasas más sanas que las que se encuentran usualmente en las margarinas y aderezos que consumimos, ricos en ácidos grasos *trans*. De la transesterificación entre subproductos de aceite de oliva o pescado y grasa hidrogenada pueden obtenerse grasas semisólidas con diferentes propiedades y aplicaciones, de diverso carácter plástico, ricas en ácido oleico, de alta estabilidad oxidativa y sin ácidos *trans*. Esta tecnología ya está siendo utilizada a nivel industrial por la multinacional Unilever empleando la lipasa inmovilizada del hongo *Rhizomucor miehei* que comercializa Novozymes [24].

Caracterización físico-química de emulsiones de lípidos estructurados

Desde el punto de vista físico las emulsiones quedan encuadradas dentro de los llamados fluidos complejos y se definen como “sistemas heterogéneos constituidos por dos fases inmiscibles, de tal manera que una

de las fases se encuentra dispersa en la otra en forma de gotas de tamaño coloidal” [25]. Los lípidos introducidos en la dieta van a formar parte de una serie de sistemas coloidales antes de que puedan ser absorbidos por la mucosa del intestino delgado. La primera emulsión se forma en el estómago con ayuda de fosfolípidos (ingeridos o segregados en el mismo estómago). Esta emulsión se mantiene durante varias horas y posteriormente pasa al duodeno, donde se incorporan los distintos componentes de la bilis. De esta forma se constituye una nueva emulsión con propiedades físico-químicas diferentes, consecuencia de la incorporación de sales biliares, colesterol y más fosfolípidos. Este proceso ha sido estudiado durante varias décadas desde un punto de vista bioquímico, sin embargo, el papel de la emulsión en esos procesos ha recibido poca atención por parte de los investigadores, posiblemente motivado no sólo por la complejidad del sistema real sino también por la necesidad de la utilización de técnicas muy específicas de elevado coste y por el carácter interdisciplinar de la investigación.

Distintos grupos de investigación especializados en nutrición [26, 27, 28] han defendido los efectos positivos que aportarían estudios en el campo de las emulsiones, invitando a que se abran nuevas áreas de investigación que puedan resolver los problemas actuales de aplicación y desarrollo de nuevos alimentos funcionales o nutracéuticos, o como transportadores de fármacos [29]. De hecho, desde hace varias décadas existe una rama de la físico-química de coloides que se dedica a la alimentación (Food Colloid) con potentes grupos de investigación como por ejemplo los de P. Wilde (Institute of food Research, Norwich, Gran Bretaña), R. Miller (Max Planck Institute of Colloids and Interfaces, Golm,

Alemania), Dickinson (Procter Department of Food Science, University of Leeds, Gran Bretaña), D. Langevin (Laboratoire de Physique des Solides, Université Paris, Francia), J.M. Rodríguez Patino (Dept. de Ingeniería Química, Universidad de Sevilla, España), que analizan las propiedades de los distintos componentes de emulsiones, geles o espumas, si bien la mayoría de los esfuerzos se centran en la preparación y/o conservación de los alimentos. La caracterización interfacial de la interfaz líquido-líquido de las emulsiones resulta una tarea complicada que debe de llevarse a cabo conjuntamente con estudios dinámicos de tensión interfacial fuera del sistema emulsificado. Estos estudios de las propiedades de la interfase se revelan hoy en día como muy útiles para el estudio de las emulsiones puesto que la formación y estabilización de estos sistemas depende fuertemente de la cantidad de moléculas adsorbidas en la interfaz así como de su disposición y de cambios conformacionales que sufren una vez adsorbidas [30, 31].

La caracterización de emulsiones con los nuevos lípidos estructurados que empiezan a ser incorporados por la industria alimentaria se revela como parte fundamental para el desarrollo de estrategias que controlen y optimicen los procesos de su degradación y absorción por el organismo, mejorando su aplicabilidad en nutrición y/o en nanomedicina como liberadores de fármacos.

II. Objetivos

El principal objetivo de esta tesis doctoral es el análisis de los mecanismos que controlan el comportamiento de sistemas coloidales integrados por grasas semisólidas estructuradas procedentes de procesos de transesterificación de aceites insaturados y grasas completamente saturadas. Se pretende llevar a cabo una caracterización físico-química, en condiciones similares a las fisiológicas, de emulsiones con estos triacilglicéridos estructurados enriquecidos en ácidos grasos insaturados, es decir productos con valor añadido, prestando especial atención a sus propiedades físicas. Esta caracterización se basará en la determinación del tamaño medio de gota y polidispersidad así como de su estabilidad coloidal en función de la composición triacilglicérido-emulsionante fisiológico. Para ello se utilizarán técnicas de dispersión de luz dinámica y estática. La estabilidad será posteriormente relacionada con las propiedades físicas de las interfases estudiadas mediante tensiometría utilizando un tensiómetro de gota pendiente adaptado para este propósito [32]. Con este tensiómetro, que funciona como una balanza de superficies de penetración, se estudiará el comportamiento interfacial de emulsionantes biológicos como las sales biliares en diferentes interfases. Finalmente se realizan análisis de las cinéticas de hidrólisis enzimática interfacial de los triacilglicéridos estructurados anteriores. En este estudio se considerará el efecto de la concentración y composición de las sales biliares y triacilglicéridos sobre la reacción de hidrólisis. Además de los lípidos estructurados objeto de este

trabajo, se utilizarán fases oleosas como la trioleína y los aceites de oliva o sésamo. Estos triacilglicéridos serán estudiados para ser considerados como punto de referencia en la evaluación de las mejoras funcionales de los nuevos productos estructurados. Con el fin de obtener resultados exactos del comportamiento interfacial de tensioactivos fisiológicos en interfaces oleosas se ha llevado a cabo una purificación previa de las fases oleosas utilizadas.

La caracterización de estas sustancias se centra en tres aspectos interrelacionados:

i) Adsorción, interacción y competencia interfacial entre lipasas y sales biliares centrándose en el posible desplazamiento o asociación interfacial de ambos compuestos. Se realizarán experimentos de adsorción individual de las distintas sales biliares que se utilizan para estabilizar las emulsiones de triacilglicéridos en agua. También se llevarán a cabo experiencias de adsorción competitiva de las distintas sustancias. La disposición de capilares coaxiales en nuestro tensiómetro automatizado permitirá realizar estudios de adsorción secuencial para la caracterización de las interacciones en interfases aire-agua. Estos estudios presentan la ventaja de que el complejo lipasa-sal biliar se forma sólo en la interfaz y la interacción de estos compuestos en el seno de la dispersión no influirá en los mecanismos de adsorción. Los estudios de adsorción se realizarán en la interfaz agua-aire, manteniendo el área o la presión interfacial constante [33]. Los valores de presión interfacial de equilibrio encontrados para cada concentración de

lipasa y de sal biliar dependerán no solo de la naturaleza de la proteína usada sino de la naturaleza de la fase oleosa [34, 5, 35]. Es por ello que en esta primera parte de este trabajo solamente se considerará la interfaz aire-agua. El interés fundamental de este estudio reside, una vez más, en la carencia de investigaciones como las aquí planteadas, de sistemas mixtos y en la interfaz aire-agua así como en su utilidad para el diseño de emulsiones. La formación y estabilización de las mismas dependen fuertemente de la cantidad de cada compuesto adsorbida así como de la formación de redes en la interfaz y de cambios conformacionales durante o tras la adsorción [30, 31].

ii) Caracterización coloidal de emulsiones constituidas por lípidos estructurados incluyendo tamaños de gota, polidispersidad y estabilidad (procesos de agregación y separación de fases). Se prepararán emulsiones con ayuda de un homogeneizador “DiAx 900, Heidolph” utilizando un protocolo con distintos ciclos de agitación a una temperatura controlada. Se modificará la composición lípido-agua aunque siempre se buscará la preparación de emulsiones aceite en agua (o/w). Los tamaños medios y polidispersidad de estas emulsiones será obtenidos mediante técnicas de dispersión dinámica de luz como el dispositivo ALV-NIBS/HPPS que utiliza la luz retrodispersada por la muestra para caracterizar emulsiones muy concentradas o con grandes tamaños de gota. La estabilidad de las emulsiones se medirá haciendo uso del dispositivo Turbiscan MA2000. El análisis de la luz transmitida además de la retrodispersada a lo largo de distintas posiciones en la célula de medida permite determinar la evolución

temporal del tamaño de partícula y distinguir los mecanismos que conducen a la inestabilidad de las emulsiones tales como floculación, coalescencia, cremado o sedimentación.

iii) Se propone un estudio del proceso de degradación (hidrólisis) de estos lípidos estructurados catalizado mediante una lipasa en emulsiones bajo condiciones similares a las fisiológicas [36]. Aunque es conocido que las propiedades físico-químicas de absorción e hidrólisis de los lípidos estructurados difieren de los lípidos no-modificados [37, 38], en la bibliografía no se encuentran estudios comparativos de degradación de este tipo de productos. Utilizando una nueva metodología para la caracterización de las cinéticas enzimáticas, desarrolladas especialmente para este trabajo, se realizarán análisis cinéticos comparativos de la hidrólisis de lípidos naturales y estructurados. Esta metodología novedosa basada en los cambios de turbidez de la muestra durante la reacción que permite la medida simultánea de hasta 96 reacciones con distintas concentraciones de los distintos componentes. En estos estudios se consideraran las distintas variables que pueden influir en la reacción como por ejemplo la estructura del triacilglicérido o la composición en emulsionantes biológicos.

III. Breve Resumen y Discusión de Resultados

Capítulo 1. Interfacial study of interactions between lipases and bile salts

En este capítulo se abordaron los distintos tipos de interacciones que tienen lugar entre lipasas y sales biliares tanto en el seno de la dispersión como a nivel interfacial. Si bien la actividad catalítica y estabilizante de estos compuestos está restringida a la región interfacial, no está todavía completamente claro si se producen o no interacciones en la subfase o si, de producirse, dan lugar a agregados que activan la lipasa y aumenten su adsorción o inhiben su actividad lipolítica. Diversos trabajos han estudiado la actividad interfacial de estos compuestos tanto de forma individual como conjunta en interfaces puras. Sin embargo estos estudios no permiten clarificar la cuestión de a que nivel se están produciendo las interacciones entre estos compuestos. Solamente con estudios comparativos entre la adsorción simple, combinada y secuencial de ambos compuestos, como los realizados en este capítulo, es posible distinguir la naturaleza de dichas interacciones. Esta información es particularmente relevante a la hora de encontrar diferencias en la actividad de la lipasa sobre diferentes sustratos. Todos los estudios de adsorción llevados a cabo en este capítulo están realizados en la interfaz aire-agua con el objeto de evitar que la actividad hidrolítica de la lipasa de lugar a productos de reacción que interfieran con los resultados. Esta aproximación se supone que no es relevante con respecto a las posibles interacciones que pudieran tener lugar en la subfase y

permite acercarnos de una forma relativa a los fenómenos interfaciales que tienen lugar entre estos componentes. Los experimentos se llevan a cabo con el tensiómetro de gota pendiente adaptado que hemos presentado anteriormente. La posibilidad de intercambio de subfase que ofrece este dispositivo ha sido utilizada en los estudios de adsorción simple y conjunta midiendo la tensión interfacial de una interfaz de buffer pura e introduciendo posteriormente, a través de un intercambio de subfase, los componentes de forma individual o mezclados. Con ello se consigue un registro de las cinéticas de adsorción desde los primeros instantes del proceso. Los estudios de adsorción secuencial se apoyan en estos resultados para compensar la imposibilidad del registro de estos primeros instantes. En estos estudios se observa la adsorción individual de uno de los compuestos y una vez establecida una capa interfacial de éste se lleva a cabo un intercambio de la subfase introduciendo el segundo componente. Estos estudios se realizan intercambiando el orden de adsorción de los componentes y permiten estimar el grado de penetración interfacial de cada uno así como las posibles interacciones interfaciales entre ellos. La lipasa utilizada fue la *Mucor Miehei* y las sales biliares, taurocolato sódico y taurodeoxicolato sódico. En los resultados obtenidos en este capítulo se observa un fuerte efecto sinérgico entre la adsorción de ambos componentes que da lugar a una mayor presión interfacial cuando se adsorben conjuntamente. Independientemente del orden de adsorción se observa la penetración de cada compuesto en la interfaz poblada por el segundo dando lugar a las mismas presiones interfaciales finales. Esto hace suponer que no se produce desplazamiento de la lipasa por el surfactante sino que está

ocurriendo algún tipo de interacción entre ambos componentes. La similitud entre las presiones interfaciales obtenidas tanto para adsorción conjunta como secuencial de iguales concentraciones de estos compuestos ratifica la hipótesis de que la interacción entre ambos tiene lugar a un nivel interfacial principalmente.

Capítulo 2. Physical characterization and emulsion stability of semisolid fats from unsaturated oils and fully hydrogenated fats

En este capítulo se llevan a cabo estudios comparativos sobre la estabilidad de emulsiones preparadas con trioleína, aceite de oliva y de sésamo y con distintos triacilglicéridos estructurados consistentes en grasas semisólidas procedentes de la transesterificación de aceite de oliva o sésamo y aceites completamente hidrogenados de palma o soja respectivamente. Estos estudios se realizan observando las variaciones de turbidez que se producen en las distintas posiciones de la muestra a lo largo del proceso de rotura de la emulsión. Para ello se emplea un dispositivo Turbiscan Classic en el que se introducen cuidadosamente de forma sistemática las distintas emulsiones obteniéndose una superposición de distintas curvas turbidez/altura correspondientes a distintos tiempos del proceso de rotura. A partir del análisis de estas curvas es posible estimar el tipo de mecanismo de rotura que domina el proceso. En todos los casos estudiados se observa la aparición conjunta de procesos de cremado y coalescencia simultáneos. Para distinguir entre ellos se consideran distintas partes de la muestra. En la parte inferior, la desaparición de substrato debida a la migración de las gotas será

principalmente representativa del proceso de cremado aunque también estará influida por la coalescencia que esté teniendo lugar. Con objeto de cuantificar esta coalescencia se considera la parte superior de la muestra en la que, debido a las altas concentraciones de triacilglicérido en emulsión, la concentración de fase oleosa será muy similar desde los primeros instantes del proceso de rotura. Es en esta parte donde podremos estimar la velocidad de ruptura de la emulsión debida casi exclusivamente a la coalescencia entre las gotas de triacilglicérido. Es importante aclarar que debido a las limitaciones de esta técnica, basada en la dispersión estática de luz, y a la concurrencia de distintos mecanismos de ruptura, no es posible la obtención de resultados cuantitativos que permitan precisar los niveles de estabilidad. Sin embargo la información cualitativa obtenida con este instrumento resulta de suma utilidad a la hora de comparar el efecto de distintas variables en la estabilidad de la emulsión como es nuestro interés en este caso. En una primera parte de este capítulo se lleva a cabo un estudio sobre el efecto del tipo de surfactante y la concentración de éste en la estabilidad de emulsiones de trioleína en presencia de distintas concentraciones de taurocolato y de taurodeoxicolato sódico. Los resultados obtenidos muestran un comportamiento muy diferente dependiendo del tipo de surfactante. Las emulsiones con taurocolato sódico muestran una mayor estabilidad, para concentraciones similares, que aquellas con taurodeoxicolato sódico. Esto se cree que es debido a un fenómeno depletivo producido por la aparición micelas a menores concentraciones de esta segunda sal biliar. En la segunda parte se estudia el efecto del tipo de triacilglicérido estructurado en la estabilidad de emulsiones estabilizadas con taurocolato sódico. La tendencia

general observada muestra que la estabilidad de las emulsiones depende no solo del grado de saturación de los ácidos grasos en cada triacilglicérido sino también del origen del aceite empleado para su síntesis. En el caso de emulsiones con grasas procedentes de aceite de sésamo y soja se observa que la estabilidad aumenta significativamente con el grado de saturación del triacilglicérido correspondiente mientras que en aquellas procedentes de aceites de oliva y palma se observa un valor intermedio de saturación para el que la estabilidad de la emulsión es mínima. En este caso se plantea un efecto combinado de la densidad y tensión interfacial para la aparición de dicho valor óptimo.

Capítulo 3. Turbidimetric and interfacial study of lipolysis in O/W emulsions of triolein and of semisolid structured fats stabilized with bile salts

Al contrario que en los capítulos anteriores, los experimentos realizados en este capítulo final fueron realizados en el Helsinki Biophysics and Biomembrane Group de Finlandia bajo la supervisión del profesor Paavo Kinnunen. En este capítulo se presenta el estudio de la lipólisis de lípidos estructurados en emulsión. Para ello se ha diseñado una metodología basada en los cambios de turbidez de las emulsiones durante el proceso de lipólisis, así como en la acumulación de productos de reacción en la interfaz aire-agua superior de la muestra, que permite obtener unos parámetros cinéticos de reacción y comprobar de forma cualitativa la cantidad final de productos de reacción que se han liberado a lo largo del proceso. El diseño y

utilización de esta metodología tiene dos ventajas fundamentalmente. La primera es que permite el estudio de 96 reacciones simultáneamente. Llevar a cabo este número de experimentos con técnicas tradicionales como las titrimétricas podría ser una labor de semanas mientras que con este protocolo se puede llevar a cabo en menos de una hora, dependiendo de las condiciones experimentales. La segunda ventaja, y más importante, es la posibilidad de estudiar el efecto de múltiples variables sobre la reacción con una misma emulsión. Esto evita las complicaciones propias de trabajar con sistemas en constante proceso de ruptura como las emulsiones, cuyas características además están altamente influenciadas por pequeñas variaciones en las condiciones del proceso de fabricación (temperatura, posición del instrumento dispersante, etc). Las emulsiones utilizadas en este capítulo fueron preparadas usando un dispositivo de focalización de ultrasonidos Covaris S-Series. Emulsiones finas y altamente monodispersas fueron obtenidas a partir de los mismos aceites y grasas semisólidas presentadas en el capítulo segundo. El efecto sobre las cinéticas o el grado de reacción de variables tales como las concentraciones de lipasa, aceite, sal biliar, iones Ca^{2+} o los tipos de substrato o de sal biliar, fue considerado a lo largo de los diferentes experimentos. De entre los resultados observados cabe destacar que, bajo determinadas condiciones se encontraron indicios de diferentes mecanismos de activación de la lipasa. Estos mecanismos ya fueron propuestos por diferentes autores y están basados en la formación de complejos activos de lipasa y micelas de sal biliar y en la formación de oligómeros lipásicos en la interfaz con una configuración activa. Como productos secundarios de este tipo de interacciones aparecen una serie de

precipitados fibrilares que muestran características similares a complejos amiloides. En cuanto a las sales biliares, se observa que el taurocolato sódico potencia la actividad lipásica mientras que el taurodeocolato sódico la inhibe. Las distintas concentraciones necesarias para la formación de micelas, así como el distinto tamaño de estas, hacen suponer que las micelas de taurodeocolato sódico no tienen las características adecuadas para la formación de estos complejos activos con la lipasa utilizada. Esta suposición está justificada por las observaciones de la estructura de este tipo de complejos llevadas a cabo por diferentes autores.

IV. Conclusiones y Perspectivas

Las conclusiones y resultados más relevantes extraídos de esta tesis doctoral se enumeran a continuación:

Capítulo 1: Estudio interfacial de las interacciones entre sales biliares y lipasa

1. Las cinéticas de adsorción de las sales biliares taurocolato sódico y taurodeoxicolato sódico en la interfaz aire-agua se desarrollan en dos fases principalmente. En la fase inicial se produce una adsorción muy rápida debida a los altos coeficientes de difusión de estas moléculas. A continuación se produce una adsorción secundaria y mucho más lenta que parece estar controlada por reordenamiento de las moléculas en la interfaz o por la formación de agregados micelares en la subinterfaz.
2. Ambas sales biliares, taurocolato y taurodeoxicolato sódico, alcanzan unas presiones de saturación interfacial similares tras largos periodos de adsorción. Sin embargo, la adsorción de taurodeoxicolato sódico en la interfaz aire-agua da lugar a presiones superficiales iniciales, tras la primera fase de adsorción, mayores que la adsorción de taurocolato sódico. Esto parece ser debido al mayor carácter anfifílico de este tipo de compuestos, causado por el defecto del grupo hidróxido en la posición 7 de la molécula, que da lugar a la formación una película interfacial más compacta que la formada en el caso del taurocolato sódico.

3. Las concentraciones micelares críticas obtenidas a partir de las isotermas de presión superficial frente a concentración en subfase son aproximadamente 10mM en el caso del taurocolato sódico y 1mM en el caso del taurodeoxicolato sódico. Las áreas interfaciales correspondientes a estas presiones, suponiendo adsorción de Gibbs, son 0.8 nm^2 y 1.1 nm^2 respectivamente.
4. Las cinéticas de adsorción de la lipasa *Mucor Miehei* en la interfaz aire-agua presentan tres regímenes distintos de adsorción característicos en este tipo de proteínas. El primero es un régimen de inducción en el que la aparición interfacial de moléculas de lipasa no afecta de forma significativa a los valores de tensión interfacial registrados. En el caso de esta lipasa el periodo de inducción aparece solamente para concentraciones bajas en la subfase y su duración es de unos pocos segundos. El segundo periodo se corresponde con un rápido incremento de la presión superficial que se supone controlado por difusión y en el que empiezan a producirse interacciones de las moléculas de lipasa en la interfaz. La duración de este periodo depende de la concentración de lipasa en la subfase y puede ir desde unos pocos segundos hasta más de una hora. Finalmente aparece un periodo de colapso interfacial caracterizado por unos incrementos de presión superficial mucho más lentos en los que se supone que se producen unos cambios conformacionales de la capa de proteínas así como la formación de multicapas o estructuras tipo gel.
5. En la adsorción de mezclas de *Mucor Miehei* y taurocolato sódico se produce una rápida adsorción inicial que da lugar a unas presiones interfaciales superiores a las que cabría esperar por la adsorción conjunta de

ambos compuestos. La formación de complejos lipasa-sal biliar con un mayor carácter anfifílico que el de los elementos por separado se propone como posible explicación de este efecto sinérgico. Periodos de interacción molecular y de colapso interfacial son también observados en este tipo de adsorción conjunta. Sin embargo, las cinéticas de incremento de presión superficial a lo largo de estos periodos parecen estar controladas por la presencia interfacial de los complejos anteriores.

6. En la adsorción secuencial de lipasa sobre interfaces preabsorbidas con sal biliar desaparecen los periodos de inducción observados en la adsorción sobre interfaces puras.

7. Independientemente del orden de incorporación, se observa que cada compuesto es capaz de penetrar la interfaz preabsorbida con el primero.

8. La comparación de las cinéticas de adsorción competitiva y secuencial indica que la formación de complejos lipasa-sal biliar se produce tanto en la subfase como en la interfaz. En este segundo caso, la formación de estos complejos parece estar fuertemente condicionada por la orientación interfacial de las moléculas de ambos compuestos.

Capítulo 2: Caracterización física y estabilidad de emulsiones con grasas semisólidas estructuradas a partir de aceites insaturados y grasas completamente hidrogenadas

1. El incremento de la concentración de sal biliar confiere una mayor estabilidad a las distintas emulsiones disminuyendo tanto la coalescencia como la separación de fases por cremado.

2. Las emulsiones de trioleína estabilizadas con taurocolato sódico presentan una separación de fases por cremado más rápida que las estabilizadas con taurodeoxicolato sódico. El mayor carácter anfifílico de esta segunda sal biliar así como la formación de micelas a concentraciones más bajas de esta segunda sal biliar es propuesta como una posible causa para este comportamiento.
3. A las concentraciones estudiadas de sal biliar aparecen unos tiempos de retraso en la coalescencia de la parte superior de las emulsiones de trioleína que parecen ser representativos de unos periodos de ordenamiento del las gotas de emulsión antes de que la coalescencia domine la separación de fases.
4. La mayor coalescencia en la parte superior de la muestra para concentraciones similares de sal biliar en el caso del taurodeoxicolato sódico hace suponer la presencia de un efecto depletivo fomentado por la presencia de micelas de esta sal biliar.
5. La estabilidad de las emulsiones con grasas semisólidas estructuradas se ve incrementada a mayores concentraciones de taurocolato sódico en la subfase.
6. La estabilidad de las emulsiones con grasas semisólidas estructuradas procedentes de aceites de sésamo y soja es mayor cuanto mayor es el grado de saturación de la fase dispersa en ausencia de taurocolato sódico. Cuando la concentración de esta sal biliar aumenta, estas diferencias se van haciendo menores hasta alcanzar ciertas concentraciones donde la influencia del tipo de aceite sobre la estabilidad de la emulsión es inapreciable.

7. La estabilidad de las emulsiones con grasas semisólidas estructuradas procedentes de aceites de oliva y palma presenta un mínimo para los grados intermedios de saturación en los enlaces de las cadenas de ácidos grasos. La explicación de este mínimo de estabilidad puede ser un posible efecto combinado de las diferencias tensiones interfaciales y densidades de este tipo de grasas.

Capítulo 3: Estudio turbidimétrico e interfacial de la lipólisis en emulsiones O/W de trioleína y grasas semisólidas estructuradas estabilizadas con sales biliares

1. Se ha propuesto una nueva metodología basada en estudios de dispersión de luz, turbidimétricos e interfaciales para el seguimiento y caracterización de los procesos de lipólisis de triacilglicéridos en emulsión. El protocolo de aplicación de esta tecnología se desarrolla en los siguientes pasos:

1.1. Inicialmente se realiza una primera caracterización del sistema emulsionado de la que se obtiene la información de la distribución de tamaños de gota. En los estudios llevados a cabo en esta tesis, esta caracterización se llevó a cabo usando técnicas de dispersión dinámica de luz.

1.2. A continuación se da inicio a la reacción añadiendo la lipasa al sistema y se registran los cambios de turbidez que se van produciendo.

- 1.3. Se utiliza la información de la distribución inicial de tamaños para estimar los cambios que ha sufrido el radio medio de gota a lo largo de la reacción utilizando los cambios de turbidez registrados. A partir de estos cambios en el tamaño se obtienen dos parámetros cinéticos: La velocidad máxima de reacción interfacial y la aceleración inicial de la reacción interfacial.
 - 1.4. Una inspección final de las tensiones interfaciales aire-agua permite estimar de forma cualitativa el grado de reacción que ha tenido lugar a partir de la mayor o menor acumulación de productos de reacción en dicha interfaz.
-
2. Con la metodología propuesta se puede hacer el seguimiento de reacción de hasta 96 experimentos simultáneamente.
 3. Con esta metodología se evitan los problemas clásicos del estudio de cinéticas de reacción lipolítica en emulsiones como el cambio de la configuración de la emulsión, entre distintos experimentos, producida por fenómenos de envejecimiento o por pequeñas diferencias en el protocolo de fabricación.
 4. De la aplicación del protocolo propuesto al estudio de la reacción lipásica en emulsiones de trioleína estabilizadas con taurocolato sódico y con taurodeoxicolato sódico se obtienen que en todos los casos la velocidad máxima de reacción aumenta con la concentración de lipasa en la subfase. Además, de los diferentes experimentos se obtienen las siguientes conclusiones:

- 4.1. En emulsiones estabilizadas con taurocolato sódico (20mM) se observan unas altas velocidades máximas de reacción interfacial que tienden a disminuir con el aumento de fase oleosa en emulsión. Esta disminución parece ser debida a una menor concentración interfacial de lipasa.
- 4.2. En emulsiones estabilizadas con taurodeoxicolato sódico (20mM) se observan una fuerte inhibición de la actividad lipásica que desaparece solamente a elevadas concentraciones de sal biliar. La manifiesta incapacidad de esta sal biliar para formar complejos activos con la lipasa junto con su mayor carácter anfifílico parecen ser las causas de este comportamiento.
- 4.3. A concentraciones de taurocolato sódico por debajo de su concentración micelar crítica se observa una fuerte inhibición de la actividad lipásica que se recupera e incrementa a concentraciones superiores. La formación de complejos activos lipasa-micela de sal biliar pueden explicar este fenómeno.
- 4.4. La presencia iónica de Ca^{2+} incrementa ligeramente las cinéticas enzimáticas pero en una medida mucho menor de lo que lo hace la concentración de taurocolato sódico.
- 4.5. Para emulsiones estabilizadas con distintas concentraciones de taurodeoxicolato sódico se observa un máximo de actividad para concentraciones de sal biliar intermedias. La concentración de sal biliar correspondiente a esta máximo disminuye ligeramente con la concentración de lipasa en reacción. La formación de complejos inactivos lipasa-micela de sal biliar junto con una mayor activación

lipásica por oligomerización interfacial se proponen como responsables de este fenómeno.

4.6. Bajo determinadas condiciones se puede observar la precipitación de agregados fibrilares que presentan características similares a las de complejos fibrilares amiloides. Es este trabajo se plantea la posibilidad de su posible formación por la agregación interfacial de oligómeros activos de lipasa.

5. En el caso de reacción en emulsiones producidas con grasas semisólidas estructuradas procedentes de aceites de sésamo y de soja se observa un claro descenso de la velocidad máxima de reacción con el mayor grado de saturación del substrato emulsificado en emulsiones estabilizadas con ambas sales biliares.

6. En el caso de reacción en emulsiones producidas con grasas semisólidas estructuradas procedentes de aceites de oliva y de palma se observan tendencias diferentes en las emulsiones estabilizadas con taurocolato sódico frente a aquellas estabilizadas con taurodeoxicolato sódico. En las primeras se observa nuevamente un descenso de las cinéticas enzimáticas con el grado de saturación de substrato emulsificado mientras que la baja estabilidad de las emulsiones con aceite de oliva y taurodeoxicolato sódico hace que no sea posible observar esta tendencia en las segundas.

Las perspectivas futuras de este trabajo de investigación son numerosas. Los estudios realizados con nuestro dispositivo de intercambio de subfase permiten dar un nuevo enfoque a la formación de complejos activos lipasa-sal biliar que hasta ahora solo se suponía que ocurría en la subfase. Por otro lado, a medio-largo plazo, los resultados obtenidos relacionados con las propiedades coloidales y de degradación de lípidos estructurados podrán ser considerados para la formulación de emulsiones con aplicación en nutrición. Por lo tanto este trabajo supone una potencial mejora para la viabilidad técnica y económica de la preparación de *nutracéuticos* y para el desarrollo del conocimiento funcional de los mismos con particular énfasis en la interrelación composición-funcionalidad-aplicación. Estudios como el presentado en esta tesis pueden ayudar a la mejora de la viabilidad industrial de estos productos en los que se consigue la revalorización de materias primas baratas (subproductos de orujo de oliva, aceites de sardina o atún) o grasas libres de ácidos *trans* (grasas totalmente hidrogenadas) mediante su biotransformación selectiva. Nuestra caracterización puede permitir desarrollar estrategias que controlen y optimicen los procesos de degradación y absorción de estos lípidos en el organismo (nutrición) y su aplicabilidad como liberadores de fármacos (nanomedicina).

La metodología desarrollada para el registro de la actividad enzimática por lotes se presenta como una potente herramienta que puede abrir nuevos caminos para el entendimiento de problemas que son objeto de controversia desde hace ya mas de treinta años como los mecanismos de activación lipásica. Finalmente hay que mencionar que gran parte de las

hipótesis planteadas en este trabajo quedan en el aire a la espera de poder ser ratificadas con nuevos estudios complementarios que serán realizados en trabajos futuros.

Referencias

1. Mackie AR et al. *In situ measurement of the displacement of protein films from the air/water interface by surfactant*. Biomacromolecules 2001;2:1001
2. Wilde PJ. *Interfaces: their role in foam and emulsion behaviour*. Current Opinion in Colloid & Interface Science 2000;5:176
3. Wang L et al. *Interfacial properties of an amphipathic alpha-helix consensus peptide of exchangeable apolipoproteins at air/water and oil/water interfaces*. J Biol Chem 2003;278:37480
4. Dickinson E. *Food colloids*. Current Opinion in Colloid & Interface Science 2002;7:410
5. Miller R et al. *Dynamics of protein and mixed protein/surfactant adsorption layers at the water/fluid interface*. Adv Colloid Interface Sci 2000;86:39
6. Parodi PW. *Conjugated linoleic acid and other anticarcinogenic agents of bovine milk fat*. Journal of Dairy Science 1999;82:1339
7. Simopoulos AP. *Omega-3-Fatty-Acids in Health and Disease and in Growth and Development*. American Journal of Clinical Nutrition 1991;54:438
8. Nettleton JA. *Omega-3 fatty acids and health*. Chapman and Hall, New York 1995
9. Siscovick DS et al. *Dietary intake and cell membrane levels of long-chain n-3 polyunsaturated fatty acids and the risk of primary cardiac arrest*. JAMA 1995;274:1363
10. Ip C et al. *Mammary cancer prevention by conjugated dienoic derivative of linoleic acid*. Cancer Res 1991;51:6118
11. Lawson LD and Hughes BG. *Human absorption of fish oil fatty acids as triacylglycerols, free acids, or ethyl esters*. Biochem Biophys Res Commun 1988;152:328
12. Boyd LC et al. *A Rapid Method for Determining the Oxidation of N-3 Fatty-Acids*. Journal of the American Oil Chemists Society 1992;69:325

13. Adolph M. *Lipid emulsions in parenteral nutrition*. Annals of Nutrition and Metabolism 1999:43:1
14. Torres CF et al. *Lipase-catalyzed ethanolysis of borage oil: a kinetic study*. Biotechnol Prog 2004:20:756
15. Otero C et al. *Continuous enzymatic transesterification of sesame oil and a fully hydrogenated fat: effects of reaction conditions on product characteristics*. Biotechnol Bioeng 2006:94:877
16. Arcos JA et al. *Kinetics of the lipase-catalyzed synthesis of glucose esters in acetone*. Biotechnol Bioeng 2001:73:104
17. Gill I and Valivety R. *Polyunsaturated fatty acids .2. Biotransformations and biotechnological applications*. Trends in Biotechnology 1997:15:470
18. Gunstone FD. *Movements towards tailor-made fats*. Progress in Lipid Research 1998:37:277
19. Macrae AR. *Tailored Triacylglycerols and Esters*. Biochemical Society Transactions 1989:17:1146
20. Toro-Vazquez JF et al. *Crystallization kinetics of palm stearin in blends with sesame seed oil*. Journal of the American Oil Chemists Society 2000:77:297
21. Zhang H et al. *Production of margarine fats by enzymatic interesterification with silica-granulated Thermomyces lanuginosa lipase in a large-scale study*. Journal of the American Oil Chemists Society 2001:78:57
22. Torres CF et al. *Catalytic transesterification of corn oil and tristearin using immobilized lipases from Thermomyces lanuginosa*. Journal of the American Oil Chemists Society 2002:79:775
23. Lopez-Hernandez A et al. *Lipase-catalyzed transesterification of medium-chain triacylglycerols and a fully hydrogenated soybean oil*. Journal of Food Science 2005:70:C365
24. Quinlan P and Moore S. *Modification of triglycerides by lipases: process technology and its application to the production of nutritionally improved fats*. Inform 1993:4:580
25. Binks BP. *Modern Aspects of Emulsion Science*. The Royal Society of Chemistry, London 1999
26. Fillery-Travis A and Wickham M. *Colloidal aspects of lipid digestion and absorption*. Curr Top Colloid Interface Sci 1999:3:103
27. O'Driscoll CM. *Lipid-based formulations for intestinal lymphatic delivery*. European Journal of Pharmaceutical Sciences 2002:15:405

28. Holman RT. *The slow discovery of the importance of omega 3 essential fatty acids in human health*. Journal of Nutrition 1998;128:427S
29. Carpentier YA et al. *Recent developments in lipid emulsions: Relevance to intensive care*. Nutrition 1997;13:S73
30. Kahlweit M et al. *How to Study Microemulsions*. Journal of Colloid and Interface Science 1987;118:436
31. Bos MA and van Vliet T. *Interfacial rheological properties of adsorbed protein layers and surfactants: a review*. Adv Colloid Interface Sci 2001;91:437
32. Wege HA et al. *Axisymmetric drop shape analysis as penetration film balance applied at liquid-liquid interfaces*. Colloids and Surfaces A-Physicochemical and Engineering Aspects 1999;156:509
33. Maldonado-Valderrama J et al. *Dynamics of protein adsorption at the oil-water interface: comparison with a theoretical model*. Colloids and Surfaces A-Physicochemical and Engineering Aspects 2005;261:85
34. Graham DE and Phillips MC. *Proteins at Liquid Interfaces .1. Kinetics of Adsorption and Surface Denaturation*. Journal of Colloid and Interface Science 1979;70:403
35. Wustneck R et al. *Interfacial dilational behaviour of adsorbed beta-lactoglobulin layers at the different fluid interfaces*. Colloids and Surfaces B-Biointerfaces 1999;15:263
36. Beisson F et al. *Methods for lipase detection and assay: a critical review*. European Journal of Lipid Science and Technology 2000;102:133
37. Small DM. *The Effects of Glyceride Structure on Absorption and Metabolism*. Annual Review of Nutrition 1991;11:413
38. Oliveira FL et al. *Triglyceride hydrolysis of soy oil vs fish oil emulsions*. JPEN J Parenter Enteral Nutr 1997;21:224

Capítulo 1

Interfacial study of interactions between lipases and bile salts

Abstract

Lipases and bile salts are two main compounds present during the digestion of triacylglycerides. Their activity is restricted to the oil-water interface on the digestive emulsion where lipases hydrolyze the oil drops reducing their size from mesoscopic to microscopic scale and where bile salts give extra stability against phase separation in the system. The interfacial adsorption of bile salts and lipases on pure interfaces has been widely studied but their combined interfacial behavior is still not completely clear nowadays.

In this work, we study the way lipases and bile salts interact at the air-water interface by means of a continuous recording of the surface tension during their individual, simultaneous and sequential interfacial adsorptions. The sequential absorption is done in two steps. First, one compound is adsorbed at the air-water interface until the surface relatively covered with an interfacial layer and then the subphase is exchanged by a solution of the second compound. In this manner, the interfacial interaction between both compounds is studied by monitoring the change in the

interfacial pressure caused by the adsorption of the second compound on the already occupied interface. The comparison of the kinetics of interfacial pressures increase in the simultaneous and sequential adsorptions helped us to clarify whether the lipase-bile salt interactions were taking place in the bulk or at the interface by the separation of the region where both compounds take contact. *Mucor miehei lipase* was chosen as a model interfacial activated lipase and sodium taurocholate and taurodeoxycholate were the bile salts.

There was observed a strong synergetic effect between the lipase and the bile salt that made us propose a model for this interactions in which the interfacial formation of lipase-BS complexes is taking place. The experimental protocol followed arises as a useful tool in the clarification of the interfacial interactions between digestive compounds and provides key information towards the further understanding of these systems.

1. Introduction

The digestion of triacylglycerides (TAG) is a complicate multi-phase and multi-stage process [1] that takes place at the oil/water interface of the digestive emulsion along the digestive tract of most vertebrates. The process consists in the hydroxylation of the ingested TAG catalyzed by different digestive lipases (triacylglycerol acylhydrolases, EC 3.1.1.3). This reaction cleaves them into monoacylglycerols (MAG), diacylglycerols (DAG) and free fatty acids (FA), all of them with relative amphiphilic character. Since this process takes place at the oil-water interface, the interfacial area will be a primary factor in its efficiency. The digestive emulsion is very polydisperse and presents a very large oil-water interface guaranteeing a maximum efficiency which goes up to 94% of TAG absorption in the case of human being [1]. Emulsions, however, are by definition unstable systems in a continuous breaking process consisting in the separation of the oil and water phases. The exponential decrease in the interfacial area caused by the emulsion breaking process may decrease dramatically the reaction efficiency during digestion. Bile salts (BS) help to reduce this breaking process at duodenum by setting at the oil-water interface incrementing the interfacial charge and preventing the droplet coalescence by electrostatic repulsion. Their interfacial presence helps to maintain the maximum oil-water interfacial area achieved after the digestive emulsification for a maximum rate of lipolysis. Both compounds have high interfacial activity and a high performance as emulsifiers and interfacial catalyzers. Due to this

interfacial activity, these compounds present competitive interfacial adsorption. This competition is suggested by some authors as responsible of the lack of lipolytic activity of pancreatic lipase when bile salts are present [2]. Only the presence of a proteinic cofactor (colipase) allows the lipolysis to take place working as a bridge between both compounds.

The different kind of interactions between these compounds, depend on different factors like the type or concentration of BS, the ionic strength in the continuous phase or the pH [3, 4]. These interactions affect directly to the way in which they are adsorbed at interfaces. Different works have been dedicated to study the interfacial activity of lipases and BS separately [5, 6, 7], however, few works have studied their competitive adsorption and interfacial interactions [8]. This is necessary since the interfacial presence of each compound is conditioned by the interfacial fraction of the second and affects to the interfacial quality and stability regulating, therefore, the rate of lipolysis. As Tiss et al. states, *“One widely adopted hypothesis is that an adsorbed bile salt monolayer counteracts the interfacial binding of the pancreatic lipase. In other words, bile salts and lipase compete for adsorption at the interface”* [6]. In order to clarify and provide more information about the interfacial interactions of BS and lipases we have studied the interfacial interactions, at the air-water interface, of a fungal lipase and a BS by recoding their kinetics of adsorption when they are pure, mixed or sequentially adsorbed. The use of a fungal lipase is done for simplicity since this kind of lipases, due to their specific structure, do not precise the presence of a lipase cofactor to guaranty their lipolytic activity in presence of BS.

Using interfacial tensiometry, we characterize the interfacial activity of these compounds finding information about which compound has a bigger interfacial activity or how it is affected by the presence of the second compound. This is a particularly useful technique to characterize interfacial activated lipases. These robust globular proteins can perform small and reversible conformational changes upon interfacial adsorption without performing any strong irreversible denaturation under non-aggressive conditions.

2. Materials and Methods

2.1. Chemicals

Trizma buffer (0.05M) with pH 7.4 was prepared every day using freshly deionized (0.054 mS) filtered water (Milli RO/Milli Q, Millipore Inc., Jaffrey, NH). NaCl (150mM) and CaCl₂ (20mM) were added to the buffer preparation and bacterial contamination was avoided by adding NaN₃ (7.7mM).

Sodium taurocholate (NaTC) and sodium taurodeoxycholate (NaTDC) bile salts were purchased from Sigma (St. Louis, MO). Their purity of the former BS was above 95% and 97% respectively. These water-soluble molecules have a rigid 5 β ring structure (see Fig.1) and present an amphiphilic character with a hydrophobic α -face and a hydrophobic β -face [9].

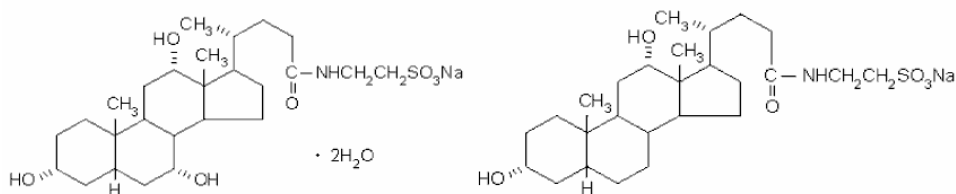


Figure 1. Molecular structure of the bile salts NaTC (left) and NaTDC (right).

Due to their structure they form micelles in a non-usual stepwise way [10]. The micellar sizes can vary from R_h around 20 \AA^3 to $13 \times 10^3 \text{ \AA}^3$ [11, 9] depending on the different conditions like BS concentration or pH. In our case NaTDC will form slightly bigger micelles than NaTC [12].

The lipase *Mucor Miehei* (MML) was also from Sigma. This lipase is a fungal lipase with 269 residues and a globular protein structure that makes it soluble in aqueous solutions. MML have a molecular weight of 29472 Da and dimensions of $7.1 \times 7.5 \times 5.5 \text{ nm}$. Its structure and conformational changes were firstly obtained by Brady et al. [12]. This lipase has been presented as a model for the typical property of many lipases known as interfacial activation [13, 14, 15, 16]. This activation consists in a small reversible change on the molecular structure of the lipase upon its interfacial adsorption. It can be considered as a reversible surface denaturation of the lipase [17]. The conformational change exposes a catalytic active site that would be covered otherwise permitting its contact with the substrate by conditioning the orientation of the lipase at interfaces [18]. This is supposed to be the reason for the drastic enhancement of the lipase activity when the substrate is forming or present at an interface

instead of in monomeric form [19]. In our experiments concentration of MML was estimated by UV spectrophotometry at 280 nm using a DU 7040 (Beckman Coulter, Inc. Fullerton, USA) spectrophotometer and a molar extinction coefficient of $42000 \text{ cm}^{-1}\text{M}^{-1}$. The MML isoelectric point was estimated to be between 3.8-4.7 for MML [20].

Fresh solutions were prepared before every experiments set using the buffer solution and different concentrations of BS and MML. The experiments were performed at 23 °C and all the solutions were filtered with a $0.2\mu\text{m}$ PFTE membrane. The glassware was cleaned by plentiful rinsing of pure water after one day with sulphuric acid (96% purity). All the chemicals were stored according to the manufacturer instructions.

2.2. Interfacial tensiometry

Interfacial tension measurements are frequently used in combination with other methods like fluorescent [20] or radioactive [21] dispersed phase labeling or microscopic interfacial observations like Brewster angle (BAM), atomic force (AFM) [22] or confocal laser scanning (CLSM) microscopy [23]. However the use of interfacial tensiometry by itself can offer a very useful information, in a fast and precise way [24, 25, 26], for the characterization of the interfacial adsorption of different compounds with interfacial activity. Since lipases and bile salts have a high interfacial activity, it is possible to study dynamically their adsorption and interactions at interfaces through the registration of the interfacial tension variations

during the process. The measured interfacial tension can be used to obtain the estimated interfacial pressure, π , using the relation $\pi = \gamma_0 - \gamma$, where γ_0 and γ are the interfacial tension at the clear and adsorbed interface respectively. In this work, we have performed measurements of interfacial tension, at the air-water interface, employing two different techniques.

Batch measurements of relatively stable air-water interfacial pressures were carried out using a Delta-8 multichannel microtensiometer (Kibron Inc., Helsinki, Finland). This technique employs eight Wilhelmy wires for a quick automatic measurement of the air-water interfacial tension for up to 96 samples simultaneously. It performs non-dynamic measurements and is equipped with an auto-cleaning heating-based system that prevents the contamination between the different samples measurements.

The measurements of the kinetics of adsorption of the different compounds were carried out using a Langmuir-type pendant drop film balance equipped with a double capillary for drop subphase exchange [27]. This balance uses the ADSA technique [28], assuming that the geometry of a pendant drop is completely axisymmetric with respect to the vertical hanging axe. With this technique is possible to obtain the values of interfacial tension and area from the image analysis of the drop profile. The experimental set performs automatic recording the pendant drop shape, extracting the drop profile and fitting it to theoretical profiles that would be obtained for a same density pure liquid, leaving the interfacial tension as an adjusting variable. The theoretical profiles used for the fitting are obtained by integration of the Young-Laplace equation which predict the shape of a

liquid-fluid interface and that is given by:

$$\Delta P = \gamma \left(\frac{1}{R_1} + \frac{1}{R_2} \right) \quad (1)$$

being ΔP , the pressure difference along the interface and R_1 and R_2 the main curvature radii that correspond with the maximum and minimum curvature radii at this point of the interface. The system is controlled by the software DINATEN [29] that regulates at real time the volume of the drop keeping constant the interfacial tension or the interfacial area depending on the experiment. This is done by means of a modulated logic PID algorithm (proportional, integral, and derivative control). The technique allows performing real time interfacial tension measurements to register dynamic processes like the interactions of different compounds at the interface. The pendant drop is set inside a glass cuvette (Hellma GmbH & Co, Müllheim, Germany) avoiding external interferences and its temperature is controlled by an external thermostat bath. There is also the possibility of assay the kinetics of adsorption of one compound on an interface already adsorbed with a second compound. This can be done since the system is equipped with a double coaxial capillary that enables the drop subphase exchange by the simultaneous injection and extraction of the same volume (see Fig. 2). The speed and volume exchange are adjusted, depending on the interfacial composition, for a maximum removing of subphase components with a minimum perturbation to the interfacial configuration. The coaxial capillary is connected to two micro-syringes controlled by the system software. In the case of adsorption of single and mixed compounds, a pendant drop of the

clear buffer is set and the assessment of no interfacial contamination is obtained by the measurement of steady interfacial tension values. The dispersed phase is then introduced by subphase exchange making possible to register the adsorption on the already existing, clear and stable interface.

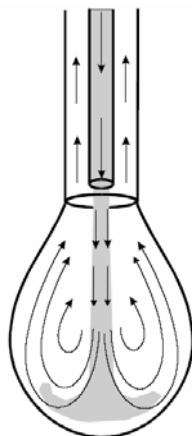


Figure 2. Subphase exchange technique: The subphase volume is replaced at an equal injection-extraction rate keeping the drop volume constant and without perturb the interfacial structure [27].

This is achieved in the similar way as in a normal Langmuir balance but in a more rapid, precise and economic form. In the case of sequential absorption, the first compound was adsorbed at the air-water interface until the surface was well covered and then the second compound was introduced by subphase exchange. In this manner, unique information about the interfacial interaction between both compounds was obtained by monitoring the change in the interfacial pressure caused by the adsorption of the second compound on the already occupied interface. In this work, the system is set to keep a constant interfacial area of 34mm^2 in order to have a good

estimation of the mass exchange at the interface [30]. Before every experiment, all the system capillaries were used with a strong flow of the correspondent experimental solution to minimize the lipase lost due to adsorption on the capillaries. The subphase exchange was made at 5 μ l/s until 400% of the drop volume was exchanged. This were found to be the most suitable conditions [31], for complete remove of the original subphase without perturbation the pre-adsorbed compounds, after performing similar studies (not shown) to those carried out in previous works [27, 30, 32].

2.3. Theoretical background

On the initial moments when amphiphilic compounds are arranging at an interface, the interfacial pressure may be expressed as a function of the interfacial concentration as follows [33]:

$$\pi(t) = R T \Gamma(t) \quad (2)$$

where R is the gas constant and T is the absolute temperature. The rates of interfacial adsorption of bile salts and lipases are initially mainly controlled by diffusion [6, 26]. The relation between the bulk concentration, diffusion coefficient and interfacial pressure for an adsorption process on clear interfaces can be established by [34, 35]:

$$\Gamma(t) = 2\sqrt{\frac{D}{\pi}} \left[c_0 \sqrt{t} - \int_0^{\sqrt{t}} c(0, t-t') d(\sqrt{t'}) \right] + \frac{c_0 D}{r} t \quad (3)$$

where t is time, Γ and c_0 are the interfacial and bulk concentration of the dispersed phase, D is the dispersed phase diffusion coefficient, r^{-1} is the interfacial curvature and t' a dummy integration variable. By assuming this adsorption to be exclusively diffusion controlled and irreversible (perfect sink condition), and considering the curvature term as a small systematic error for low interfacial curvatures, the last expression can be simplified to,

$$\Gamma(t) = 2 c_0 \sqrt{\frac{Dt}{\pi}} \quad (4)$$

By introducing Equation 4 in Equation 2 is possible to obtain a linear relation to fit the initial experimental results and obtain the estimated diffusion coefficients of the dispersed phase [33]. After the necessary time of adsorption, $\Gamma(t)$ will remain steady at Γ_∞ . In this pseudo equilibrium conditions, and diluted solutions, the interfacial pressure and the interfacial and bulk concentrations of the dispersed phase can be related as [36]:

$$\Gamma_\infty = \frac{1}{RT} \frac{d\pi}{d(\ln c_0)} \quad (5)$$

By measuring the interfacial pressures, after long time adsorptions, at different bulk concentrations of the disperse phase will be possible to obtain extra information about the possible correspondent interfacial configurations.

3. Results and discussion

3.1. Kinetics of single adsorption of bile salts and lipase

The kinetics of adsorption at the air-water interface of solutions at different concentrations of NaTC and NaTDC are illustrated in Figure 3. These BS present a very fast initial adsorption that is due to the high diffusion coefficients ($\sim 4 \times 10^{-10} \text{ m}^2/\text{s}$) of these compounds [37, 38]. The values of surface pressure obtained are higher for NaTDC than for NaTC. The reason is the lack of the OH group in the position 7 of the NaTDC molecule that offers it a higher amphiphilic character.

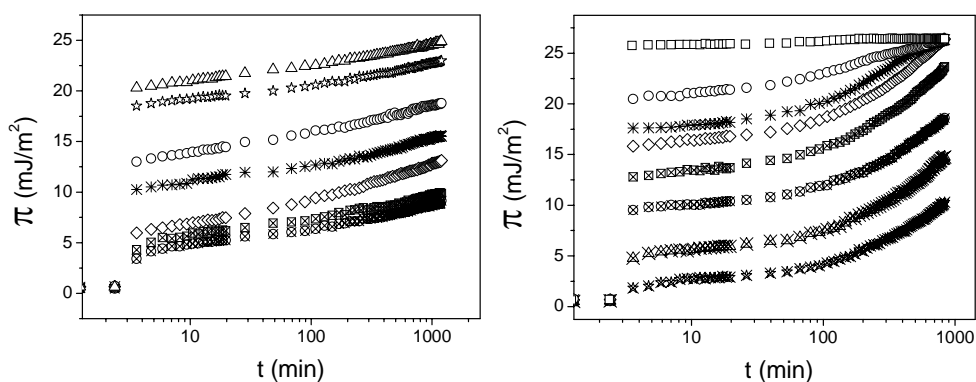


Figure 3. Air water interfacial pressure variation during to the adsorption of NaTC (left) and NaTDC (right) at: 10mM (squares), 8mM (triangles), 2mM (stars), 1mM (circles), 400 μM (asterisks), 200 μM (diamonds), 100 μM (crossed squares), 75 μM (crossed circles), 20 μM (crossed triangles) and 10 μM (crossed stars).

After this primary adsorption, they present a slower increment of the interfacial pressure that is similar in growth for different concentrations of BS.

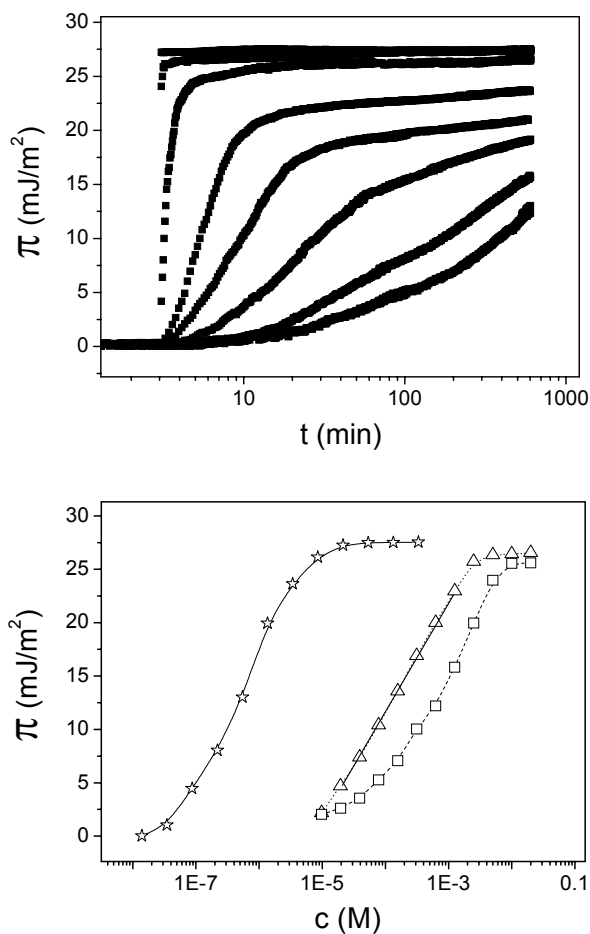


Figure 4. (top) Temporal variation of the air-water interfacial pressures during the adsorption of MML at (from up to down): 60 μ M, 30 μ M, 15 μ M, 3 μ M, 2 μ M, 1 μ M, 0.75 μ M and 0.5 μ M. (bottom) Air-water interfacial pressures depending on the bulk concentration of the dispersed phase after 120 minutes of adsorption of BS (NaTC, squares and NaTDC, triangles) and of MML (stars).

After one hour approximately, the increment of interfacial pressure is quite steady in the case of NaTC (considering the lin-log representation). However, for NaTDC is possible to observe a continuous growth in the interfacial pressure that is possibly due to a different interfacial organization [10]. After 20 hours of adsorption, the interfacial pressure keeps incrementing in a logarithmic growth until reaching the final pressure of saturation found for higher concentrations. This saturation pressure was 25mJ/m^2 for NaTC and 26mJ/m^2 for NaTDC. At this point a stable film of lipase molecules is supposed to be formed [7]. The interfacial pressures after 120 minutes of adsorption were obtained with Delta 8 (see Fig. 4 bottom) and are in fair concordance with the initial interfacial pressures of the isotherms of Figure 3. The obtained final pressures suggest that the critic concentration for the formation of micelles (CMC) in the bulk occurred over 10mM for NaTC and 1mM for NaTDC. These results were in agreement with those obtained by other authors under similar experimental conditions [6, 1]. The estimated interfacial areas per molecule, considering Gibbs adsorption (Eq. 5) are shown in Figure 5 (squares and triangles). As expected, the interfacial area per molecule decreases with the interfacial pressure. These areas are slightly higher for NaTDC than for NaTC when they are at similar pressures. This is due to the flat structure of the BS molecules and the location of the polar groups that, as mentioned, offers to the molecules of NaTDC a higher amphiphilic character. The molecular areas of the BS are estimated to be around 1nm^2 at the collapsing pressures in agreement with the results on the bibliography [6]. The kinetics of adsorption of MML at different concentrations are shown in the Figure 4

(top). Especially for bulk concentrations below $3\mu\text{M}$, these isotherms present the three characteristic regimes observed by another authors during the adsorption of similar globular proteins [39].

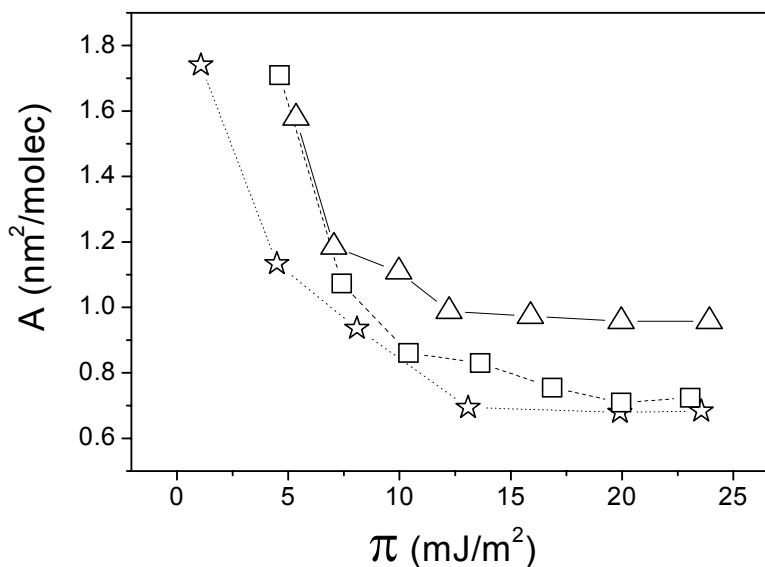


Figure 5. Estimated molecular area occupied at the air-water interface by NaTC (squares), NaTDC (triangles) and MML (stars) depending on the interfacial pressure.

Initial induction periods with a slower interfacial tension increase were found. This lag periods have been suggested to be caused by an initial adsorption of single lipase molecules which barely affects the tension at the interface [21]. Almost no interfacial interactions between the lipase macromolecules are supposed to happen in this period. In our case, these induction periods were found only for the lower concentrations of lipase and they did last for less than 10 seconds in all the cases. By employing the lower concentration isotherms, we estimated using Equations 2 and 4 the

diffusion coefficient of the lipase under our experimental conditions as $D = 1.5 \times 10^{-10} \text{ m}^2/\text{s}$. This result is slightly higher than the typical diffusion coefficients of this type of proteins found by another authors [40, 21].

After the induction period, a second regime appears with a fast increase of the interfacial pressure caused by the further lipase adsorption and arrangement of the lipase layer at the interface. This regime is also diffusion controlled and, therefore, the rate of increase of the interfacial pressure grows with the concentration of lipase. In consequence, the period is shorter for higher bulk concentrations of lipase (see Fig. 4, top). It can last from few seconds, for concentrations of MML over 30mM, until more than one hour for concentrations smaller than 1 μ M. In some experiments, this period ends when the lipase monolayer reaches its maximum pressure and begins to collapse.

At this point, a third period characterized by a lowering in the rate of interfacial pressure increase to a very slow logarithmic growth appears. During this period, conformational changes of the adsorbed layer and a possible gel-like or multilayer interfacial structuring are supposed to be taking place. Now, the increase of interfacial pressure with the bulk concentration is opposite to the ones found in the second period. The increment of interfacial pressure decreases with the increment of the lipase bulk concentration. This final period leads to a final saturating interfacial pressure that corresponds to an unclear interfacial configuration, very similar to the one encountered for different lipases by another authors [41]. The interfacial areas per molecule that would be correspondent (Eq. 2) to the interfacial pressures measured in the kinetics experiments range from

0.05 nm², for the higher lipase bulk concentrations, to 2.5 nm² for the lower. These areas are clearly under the globular size of the lipase molecule suggesting a possible partial layer collapse or interconnection of the unfolded structures of the lipase. The structure of the saturated lipase layer at the high pressures of this period have been suggested by some authors to be a possible interfacial gel-like structure [33]. The formation of this structure can be affected by different factors like the ionic strength or the pH on the bulk [5].

3.2. Kinetics of mixed adsorption of bile salts and lipases

The adsorption with mixtures of two concentrations MML and four of NaTC has also been studied. Temporal increments of the air-water interfacial pressure during the adsorption of these mixtures are shown in Figure 6. The main difference with the adsorption of pure lipase is that now there is a straight initial increment of the interfacial pressure similar to the one observed for the adsorption of pure BS. This could mean that the BS occupies very quickly the interface and the lipase is later adsorbed, in a competitive way, having a much small interfacial area available. However, especially for low concentrations of NaTC, this initial quick adsorption leads to interfacial pressures much higher than the ones that would be expected by the combination of both compounds. At these initial moments of adsorption, the interfacial concentration of lipase is very small. A fast

interfacial formation of lipase-BS complexes, with a possible higher amphiphilic character than the single compounds, is suggested as a possible explanation to these high initial interfacial pressures. This type of complexes have been observed by other authors for different lipases and are supposed to present different conformations depending on different factors like the concentration of each compound [2]. Traditionally the formation of these complexes has been assumed to occur exclusively in the subphase. As we will see from the results of sequential adsorption, the formation of these complexes, at least in our case, should also occur at the interface. The initially reached interfacial pressures increases with the bulk concentration of BS. This could be due to the combination of the interfacial presence of these aggregates and the fast-adsorbed BS molecules. These initial interfacial pressures are slightly higher in the case with a higher concentration of lipase. After this supposed very fast initial interfacial formation of lipase-BS complexes, a period with a slower increase of the interfacial pressure appears. During this later adsorption is possible to distinguish two different periods as we did in the case of single lipase adsorption. We find similarities with the periods of monolayer saturation and interfacial gelation. We must consider that the area of the BS molecule at the interface is still five times smaller than the cross section of the lipase macromolecule. The duration of the first period observed seems to show a slight decrease with the increment of BS concentration and decreases clearly with the higher bulk concentration of lipase. In the case of MML (0.5 μ M), they last for approximately 40 minutes while for MML (1 μ M) these times are reduced to values between 8 and 25 minutes.

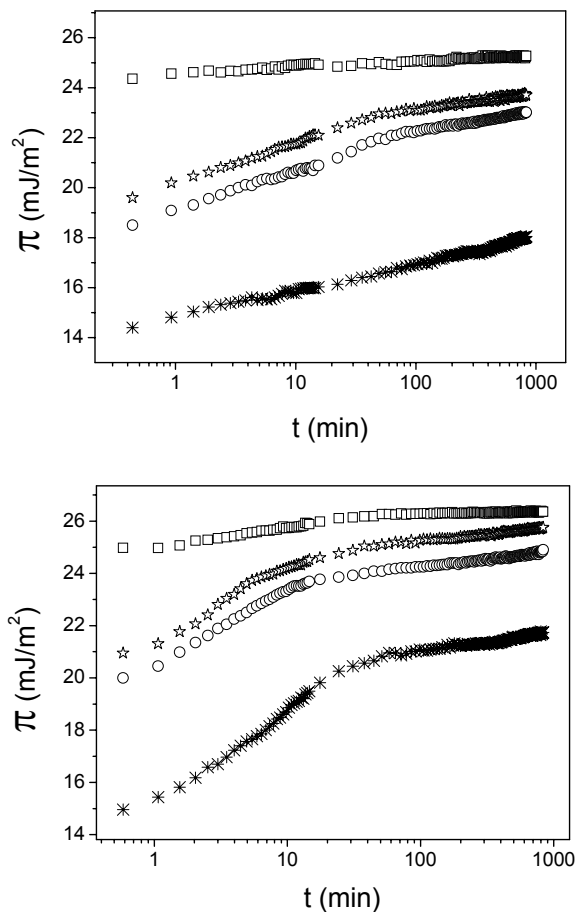


Figure 6. Temporal variation of the air-water interfacial pressure during the adsorption of MML ($0.5\mu\text{M}$, top and $1\mu\text{M}$, bottom) mixed with different bulk concentrations of NaTC (10mM , squares; 1mM , stars; $400\mu\text{M}$, circles; $100\mu\text{M}$, asterisks).

The rates of increment of the interfacial pressures with the time, during the first period, are shown in Table 1. As expected, these rates were always higher for the higher bulk concentration of lipase. For the lower concentrations of BS, the rates of increment are not particularly dependent

on the bulk concentration of BS. This could be indicating that the lipase interfacial penetration has a bigger influence on this increment. In the case of MML (0.5mM), these initial rates are almost double to the ones found when there was single adsorption of lipase.

[NaTC]	MML (0.5 μ M)	MML (1 μ M)
no BS	0.52	5.04
100 μ M	0.95	2.23
400 μ M	0.98	2.12
1 mM	1.05	2.18
10 mM	0.23	0.52

Table 1. Initial rates of increase of the interfacial pressure ($\text{mJ}\cdot\text{m}^{-2}\cdot\text{min}^{-1}$) during the monolayer saturation period for different mixtures of MML and NaTC.

An explanation for this phenomenon may be, as commented before, the fast interfacial formation of more amphiphilic lipase-BS complexes. However, for MML (1 μ M) these rates were almost half of that ones observed in absence of BS. This is just a sigh that, at these concentrations, the lipase penetrates more difficultly the interface populated with BS and lipase-BS complexes than the interface occupied just by the correspondent lipase layer at this higher lipase concentration. The fact that for NaTC (10mM) this rate is almost 10 times slower reinforces the former hypothesis. For both lipase concentrations is possible to find, at NaTC (10mM), an important decrease in the interfacial pressure growth.

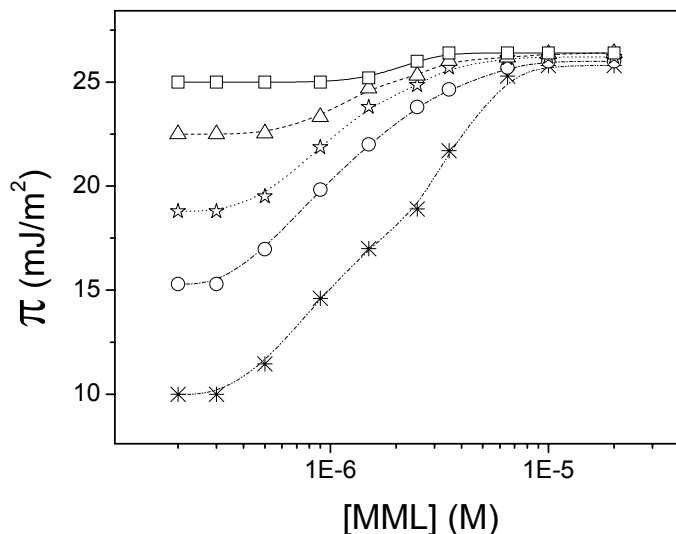


Figure 7. Air-water interfacial pressures after 120 minutes of adsorption of mixtures of NaTC and MML for the following concentrations of NaTC: 10mM (squares), 2mM (triangles), 1mM (stars), 400 μ M (circles) and 100 μ M (asterisks).

This can be explained as a combination of the effects of the possible bulk interactions between the lipase and the new BS micelles that are beginning to appear at this concentration and of the maximum interfacial pressure reached at this concentration of BS that makes much more difficult the interfacial access for the lipase. By considering the final interfacial pressures after 20 hours of adsorption of these mixtures (see Fig. 7) we can see that, for low concentrations of MML, the concentration of NaTC is conditioning the final interfacial pressure. This is in agreement with the conditioning roll of the BS concentration on the interfacial formation of lipase-BS complexes. This means that the effect on the interfacial pressure

of the initial interfacial presence of BS and lipase-BS complexes does not allow the further lipase penetration for these low concentrations. In fact until MML concentrations over $0.3\mu\text{M}$ the presence of the lipase is not affecting to the final interfacial pressure. When the concentration of MML is higher than this value, the effect on the final interfacial pressures depends on the concentration of BS. This is consequent with the fact that the BS concentration is regulating the interfacial pressure at which the lipase is supposed to penetrate the interface later. For concentrations of NaTC below 2mM , the effect of the lipase on the final interfacial pressure is observable for concentrations of MML over $0.3\mu\text{M}$. However, the bulk concentration of lipase necessary to change the interfacial pressure is increasing until $1.3\mu\text{M}$ when the bulk concentration of NaTC is 10mM . Below this concentration, the interfacial layer of BS and lipase-BS complexes is supposed to be too compact as to the bulk complexes to penetrate it.

3.3. Kinetics of sequential adsorption of mixed bile salts and lipases

With the obtained information of competitive adsorption is possible to have a good estimation of how the interfacial interactions between BS and MML are taking place. Nevertheless, additional and complementary information can be obtained by sequential adsorption experiments were each compound is adsorbed on an already populated interface. In this way, we avoid the simultaneous presence of both compounds in the drop subphase. It

is important to notice that no desorption of the lipase neither the BS was observed in any of the experiments after the optimized subphase exchanged with clear buffer.

The results for the sequential adsorption of MML on an interface pre-adsorbed with low concentrations of NaTC are presented in Figure 8. As expected, no induction periods were observed due to the BS presence. For the low concentrations of NaTC used (Fig. 8, top), the lipase is able to penetrate at the interface in a very fast way. This confirms the fact that BS-lipase are interacting at the interface increasing the interfacial pressure possibly by the formation of aggregates. However, for the lower lipase concentration, the initial pressures now are much smaller than the ones obtained with the adsorption of mixtures of these elements at the same concentrations. This fact gives strength to the idea of the important roll of the lipase molecules orientation at the interface on the complexes formation. In the present case of sequential adsorption, the interface is already populated with BS, which means that the initial formation of complexes should be produced by an interfacial incorporation of lipase that is stopped earlier due to a high interfacial BS presence. The fact that the initial interfacial pressures are increasing with the concentration of MML is supporting the former idea. In fact, for MML ($1\mu\text{M}$) the initial pressures are already slightly higher than the ones obtained with the mixture of both compounds reinforcing the assumption of a slowing down of the penetration of the lipase by the complexes at the interface, in a stronger way than the BS molecules. This may be coherent with a possible acceleration on the complexes formation by the orientation that the BS molecules adopt at the

interface. After this very fast initial adsorption, it is again possible to assume process of monolayer saturation and of interfacial gelation. For the lower concentration of BS, the lower concentrations of MML presented very similar initial slopes of around $2.2 \text{ mJ}/(\text{m}^2\text{min})$ for. The regulation of the interfacial pressure on the lipase penetration and complex formation is the possible reason for this similar behavior. For MML ($2\mu\text{M}$) the rate of growth on interfacial pressure is ten times smaller which possibly mean that the interfacial layer formed is too compact for a further penetration of the lipase molecules. Similar behavior has been observed when the interface was pre-adsorbed with a higher concentration of NaTC ($400\mu\text{M}$) (Fig. 8, bottom). This time, however, for the bulk concentration MML ($2\mu\text{M}$) there is what seems to be a very strong decrease of the initial formation of complexes. The initial interfacial pressure is considerably below the ones obtained with smaller amounts of lipase in the bulk. This anomalous behavior may be probably due to the formation of second order aggregates with a less amphiphilic character or even soluble [11]. These aggregates may be formed due to the high concentrations of BS and lipase and to the interfacial orientation of the BS molecules. Nevertheless, this hypothesis must be verified with further experiments in future works. The next step was to consider how the adsorption of NaTC takes place on an interface with MML adsorbed previously. With these experiments, we are able to assess how important was the interfacial orientation of the BS molecules on the formation of complexes in the former results. These results are shown in Figure 9. In this case, we can see how the BS is also able to penetrate the interfacial layer of lipase. Again, there is a very quick initial adsorption,

which this time seems to be helped by the high diffusion coefficient of the BS.

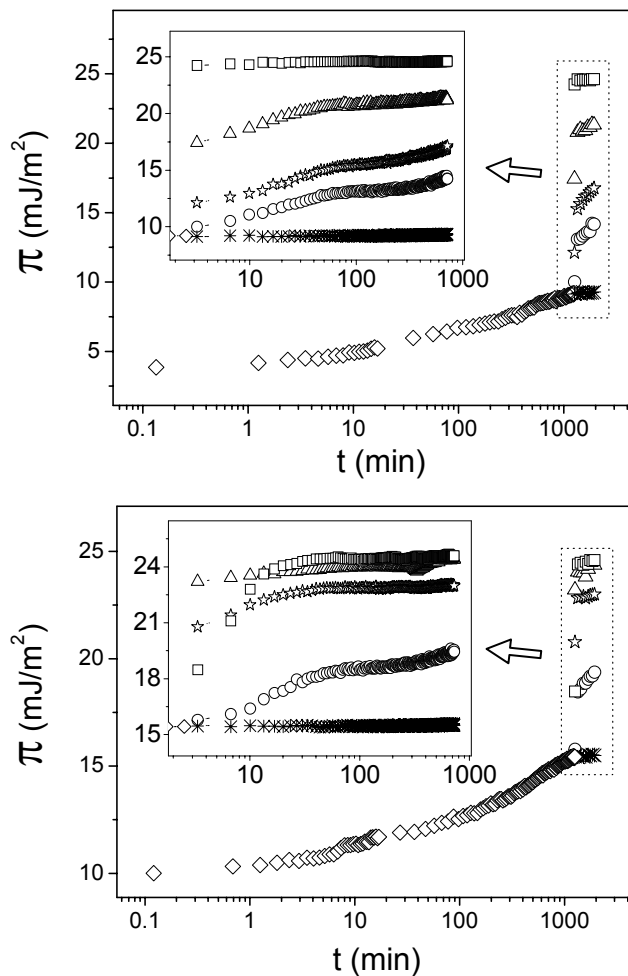


Figure 8. Temporal variation of the air-water interfacial pressure during sequential adsorption of NaTC at 100 μM (top) and 400 μM (bottom) with a subphase exchange, after 20 hours, with the following solutions of MML: 2 μM (squares), 1 μM (triangles), 0.75 μM (stars), 0.5 μM (circles) and exchanging with buffer (asterisks).

Nevertheless, interfacial interactions between the lipase and the BS must be taking place since the reached interfacial pressures are clearly higher than the ones obtained on the diffusion controlled adsorption of the same BS concentration on a clear interface. These initial pressures were, in almost all the cases, higher than the obtained when adsorbing with the same concentration mixtures or even higher than the ones obtained by the reverse sequential adsorption. This could be due to the maximum interfacial formation of complexes when there is a maximum initial presence of lipase at the interface. Therefore, the initial interfacial orientation of the lipase molecules seems to be more important for the formation of complexes than the one of the BS. This is a logical assumption since the lipase is a much more voluminous and flexible molecule that takes longer to change its interfacial orientation. With the higher concentration of BS, these initial pressures are similar to the ones obtained in the case of simultaneous adsorption, which means under our hypothesis, that the initial interfacial formation of complexes is similar in both cases. After this supposed initial complexes formation the interfacial pressure remains stable until the end of the experiment. No further lipase-BS interactions or BS penetration is observed which is a clear prove that the interfacial presence of the lipase is the key factor for the lipase-BS complex formation.

Special attention requires the case of adsorption with the lower concentrations of BS. In this case, there is a slow increase of the interfacial pressure after the drop subphase exchange corresponding, in our opinion, to a later penetration and complex formation that slowly leads to a similar interfacial configuration to the one obtained when adsorbing sequentially in

the reverse way. This is particularly clear when this process occurs with the higher bulk concentration of lipase pre-adsorbed (Fig.9 top) were there is almost no initial formation of complexes.

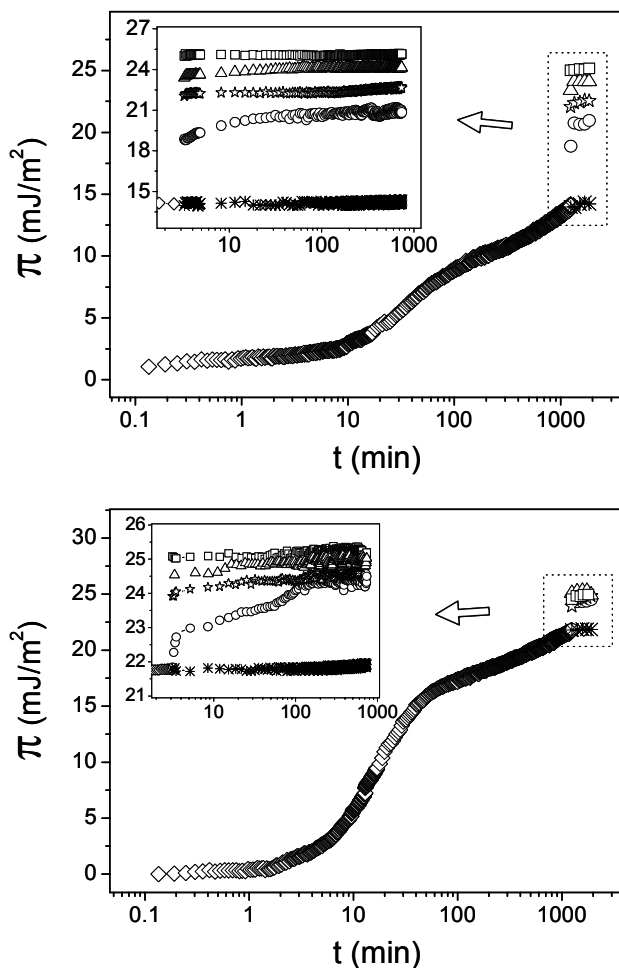


Figure 9. Temporal variation of the air-water interfacial pressure during sequential adsorption of MML at 0.5 μ M (top) and 1 μ M (bottom) with a subphase exchange after 20 hours, with the following solutions of NaTC: 10mM (squares), 2mM (triangles), 1mM (stars), 400 μ M (circles) and exchanging with buffer (asterisks).

A lack of initial access of the BS to the interface, at this low BS concentration, seems to be the main reason for this. The final interfacial pressures after 20 hours of adsorption on interfaces pre-adsorbed with the other compound are shown in Figure 10. These final interfacial pressures always increases with the concentration of each compound until reach a final value that can be considered as saturating pressure for the layer of lipase-BS aggregates. These results show that the bulk concentration of the secondly adsorbed compound necessary to reach these saturating pressures clearly depends on the initial interfacial concentration of the initially adsorbed one.

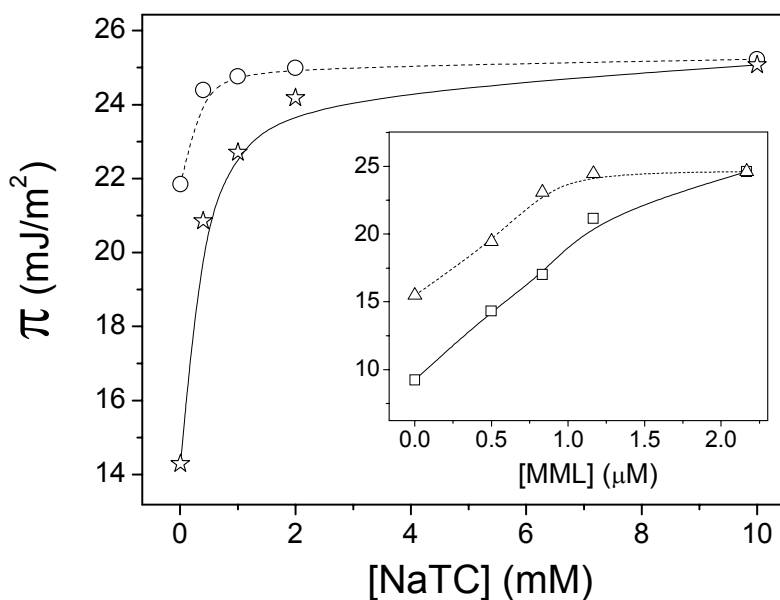


Figure 10. Final air-water interfacial pressures after sequential adsorption of MML on an interface preadsorbed with NaTC (100 μ M, squares and 400 μ M, triangles) and after sequential adsorption of NaTC on an interface preadsorbed with MML (0.5 μ M, stars and 1 μ M, circles).

The bigger importance of the initial interfacial orientation of the lipase molecules is corroborated by the fact that this saturation pressure is reached in a faster way when adsorbing, under the same concentrations, with BS on a lipase pre-adsorbed interface than in the opposite way.

4. Conclusions

Different air-water interfacial interactions between the lipase MML and the BS NaTC have been suggested. A synergetic and fast interfacial formation of lipase-BS complexes with a higher amphiphilic character than the single compounds is proposed. This supposition is based in the fact that initial interfacial pressures were much higher than the ones that would be expected from the diffusion coefficients of each compound separately. The interfacial formation of these complexes, in addition to bulk formation, is supposed after the observation of higher kinetics of adsorption when adsorbing sequentially than when adsorbing simultaneously both compounds. This synergism is attributed to the higher complexes formation due to the initial interfacial orientation of the pre-adsorbed molecules. The initial fast formation of these complexes is followed by a slower one produced by the later interactions between the bulk and interfacial molecules. The interfacial pressure seems to be a key factor for this secondary complexes formation. The obtained experimental results seem to confirm this model. From these results is difficult to consider that any interfacial displacement of one compound by the other is taking place.

The experiments show that the kinetics of formation of these hypothetical lipase-BS complexes at the interface are very dependent on the order in which each compound is incorporated to the interface. However, after long periods of adsorption, the final interfacial pressures are very close suggesting comparable configurations of the interfacial complexes layer (see Fig. 11) despite the order in which the adsorption of each compound was taking place. We consider that the possible formation of this interfacial complexes may be partially responsible of the enhancement that the lipolytic activity of some lipases experience when BS are present in the process.

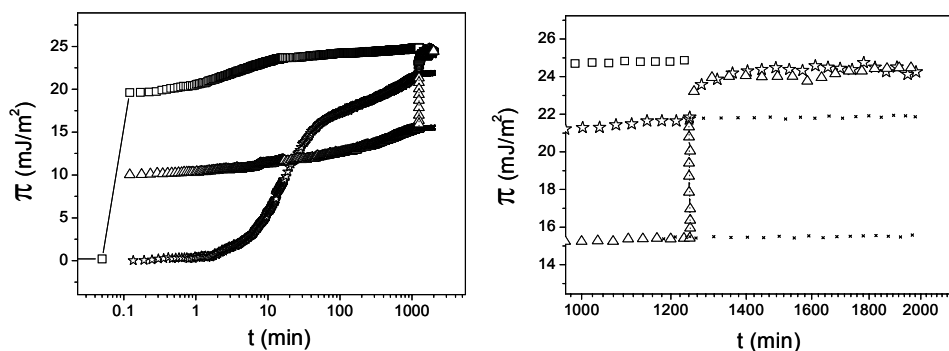


Figure 11. Kinetics adsorption, in terms of the air-water interfacial pressure, of MML ($1\mu\text{M}$) and NaTC ($400\mu\text{M}$) with mixed adsorption (squares) and with sequential adsorption of BS over lipase (stars) and lipase over BS (triangles).

The increment in the lipolytic activity of MML with the concentration of NaTC during the lipolysis in triolein emulsions has been measured in another works [42]. This increment in the activity has traditionally been considered due exclusively to the solubilization of the products of reaction

at the interface forming mixed micelles with the bile salts. In the case of *human* or *porcine pancreatic lipases*, this lipolytic activity in the presence of BS has been observed during in-vitro and in-vivo studies when their respective cofactors were present. However in absence of this cofactors the activity was very inhibited by the presence of the BS [2]. This was explained as the bulk formation of non-amphiphilic lipase-BS complexes that only were incorporated to the interface by the interfacial presence of the colipase. From our point of view, this could also be explained if we consider that these complexes were formed at the interface and subsequently desorbed unless the presence of a cofactor would gives them the amphiphilic character necessary to remain at the interface with a proper orientation. The model that we present is coherent with these theories but, as an initial step, requires complementary studies. More experimental results, including interfacial rheology and labeling or microscopy techniques, are necessary for the characterization of the final interface in order to validate or disqualify this model.

References

1. Fillery-Travis A and Wickham M. *Colloidal aspects of lipid digestion and absorption*. Curr Top Colloid Interface Sci 1999:3:103
2. Momsen WE and Brockman HL. *Inhibition of pancreatic lipase B activity by taurodeoxycholate and its reversal by colipase*. J Biol Chem 1976:251:384
3. Menger FM and McCreery MJ. *Kinetic characterization of bile salt micelles*. J Am Chem Soc 1974:96:121
4. Vogel WC and Zieve L. *A rapid and sensitive turbidimetric method for serum lipase based upon differences between the lipases of normal and pancreatitis serum*. Clin Chem 1963:9:168
5. Blecker C et al. *Two forms of lipase from Mucor miehei exhibit a different behavior at the air-water interface*. Colloids and Surfaces B: Biointerfaces 1995:3:271
6. Tiss A et al. *Surface behaviour of bile salts and tetrahydrolipstatin at air/water and oil/water interfaces*. Chem Phys Lipids 2001:111:73
7. Matubayasi N et al. *Thermodynamic study of gaseous adsorbed films of sodium taurocholate at the air water interface*. Langmuir 1996:12:1860
8. Holmberg K et al. *Interactions between a lipase and charged surfactants - a comparison between bulk and interfaces*. Adv Colloid Interface Sci 2000:88:223
9. BORGSTRO.B. *Dimensions of Bile Salt Micelle . Measurements by Gel Filtration*. Biochimica et Biophysica Acta 1965:106:171
10. O'Connor CJ and Wallace RG. *Physico-Chemical Behavior Of Bile Salts*. Adv Colloid Interface Sci 1985:22:1
11. Pignol D et al. *Critical role of micelles in pancreatic lipase activation revealed by small angle neutron scattering*. J Biol Chem 2000:275:4220
12. Mazer NA et al. *Quasielastic light scattering studies of aqueous biliary lipid systems. Size, shape, and thermodynamics of bile salt micelles*. Biochemistry 1979:18:3064

13. Brzozowski AM et al. *A Model for Interfacial Activation in Lipases from the Structure of A Fungal Lipase-Inhibitor Complex*. Nature 1991:351:491
14. Verger R and Dehaas GH. *Interfacial Enzyme-Kinetics of Lipolysis*. Annual Review of Biophysics and Bioengineering 1976:5:77
15. Derewenda ZS. *A Twist in the Tale of Lipolytic Enzymes*. Nature Structural Biology 1995:2:347
16. Ben SA et al. *Kinetic studies of Rhizopus oryzae lipase using monomolecular film technique*. Biochimie 2001:83:463
17. Haiker H et al. *Rapid exchange of pancreatic lipase between triacylglycerol droplets*. Biochim Biophys Acta 2004:1682:72
18. Jensen MO et al. *Orientation and conformation of a lipase at an interface studied by molecular dynamics simulations*. Biophys J 2002:83:98
19. Sarda L and Desnuelle P. *[Actions of pancreatic lipase on esters in emulsions.]*. Biochim Biophys Acta 1958:30:513
20. Wu XY et al. *Purification and partial characterization of Rhizomucor miehei lipase for ester synthesis*. Applied Biochemistry and Biotechnology 1996:59:145
21. Graham DE and Phillips MC. *Proteins at Liquid Interfaces .I. Kinetics of Adsorption and Surface Denaturation*. Journal of Colloid and Interface Science 1979:70:403
22. Mackie AR et al. *In situ measurement of the displacement of protein films from the air/water interface by surfactant*. Biomacromolecules 2001:2:1001
23. Li W et al. *Surface properties and locations of gluten proteins and lipids revealed using confocal scanning laser microscopy in bread dough*. Journal of Cereal Science 2004:39:403
24. Tripp BC et al. *Adsorption of Globular-Proteins at the Air/Water Interface As Measured Via Dynamic Surface-Tension - Concentration-Dependence, Mass-Transfer Considerations, and Adsorption-Kinetics*. Journal of Colloid and Interface Science 1995:173:16
25. Sengupta T and Damodaran S. *Role of dispersion interactions in the adsorption of proteins at oil-water and air-water interfaces*. Langmuir 1998:14:6457
26. Beverung CJ et al. *Protein adsorption at the oil/water interface: characterization of adsorption kinetics by dynamic interfacial tension measurements*. Biophysical Chemistry 1999:81:59

27. Wege HA et al. *Development of a constant surface pressure penetration Langmuir balance based on axisymmetric drop shape analysis*. Journal of Colloid and Interface Science 2002:249:263
28. Rotenberg Y et al. *Determination of Surface-Tension and Contact-Angle from the Shapes of Axisymmetric Fluid Interfaces*. Journal of Colloid and Interface Science 1983:93:169
29. Holgado-Terriza JA. *Medida de magnitudes dinámicas por análisis digital de interfaces curvas*. PhD Thesis, Granada 2002
30. Maldonado-Valderrama J et al. *Comparative study of adsorbed and spread beta-casein monolayers at the water-air interface with the pendant drop technique*. Langmuir 2003:19:8436
31. Wege HA. *Interacciones físicas en interfaces de interés biológico. Estudio termodinámico y cinético*. PhD Thesis, Granada 2002
32. Ferri JK et al. *Equilibrium and dynamics of PEO/PPO/PEO penetration into DPPC monolayers*. Colloids and Surfaces A-Physicochemical and Engineering Aspects 2005:261:39
33. Messina P et al. *Surface characterization of human serum albumin and sodium perfluorooctanoate mixed solutions by pendant drop tensiometry and circular dichroism*. Biopolymers 2006:82:261
34. Ward AFH and Tordai L. *Time-Dependence of Boundary Tensions of Solutions .I. the Role of Diffusion in Time-Effects*. Journal of Chemical Physics 1946:14:453
35. Makievski AV et al. *Adsorption of protein layers at the water/air interface as studied by axisymmetric drop and bubble shape analysis*. Journal of Physical Chemistry B 1999:103:9557
36. Gibbs JW. *Collected works of J. Willard Gibbs*. Longmans, Green and Co New York 1928
37. Kratochvil JP et al. *Concentration-Dependent Aggregation Patterns of Conjugated Bile-Salts in Aqueous Sodium-Chloride Solutions - A Comparison Between Sodium Taurodeoxycholate and Sodium Taurocholate*. Colloid and Polymer Science 1983:261:781
38. Oh SY et al. *Diffusion-Coefficients of Single Bile-Salt and Bile Salt-Mixed Lipid Micelles in Aqueous-Solution Measured by Quasi-Elastic Laser-Light Scattering*. Biochimica et Biophysica Acta 1977:488:25
39. Wustneck R et al. *Dynamic surface tension and adsorption properties of beta-casein and beta-lactoglobulin*. Food Hydrocolloids 1996:10:395

40. Nesmelova IV et al. *Generalized concentration dependence of globular protein self-diffusion coefficients in aqueous solutions*. Biopolymers 2002:63:132
41. Nitsch W et al. *Lipase Monolayers at the Air-Water-Interface - Interfacial Behavior and Enzymatic-Activity*. Journal of Colloid and Interface Science 1991:141:322
42. Tejera-Garcia R et al. *Turbidimetric and interfacial study of lipolysis in emulsions of triolein in water with bile salts*. to be published 2008

Capítulo 2

Physical characterization and emulsion stability of semisolid fats from olive oil and fully hydrogenated fats

Abstract

We have performed turbidimetric studies of the breaking process of emulsions from natural triacylglycerides and semisolid structured fats with interest in functional foods. Semi-solid triacylglycerols proceeding from the transesterification of poly-unsaturated oils and fully-hydrogenated fats were used as substrate. The sources of oils and fats employed in their synthesis were sesame or olive oil and fully hydrogenated fat from soybean oil or from palm oil respectively. Different concentrations of the bile salt sodium taurocholate have been used for the emulsions stabilization. The fatty acid composition and the degree of saturation have shown to be very important factors on the stability of the emulsions. The effect of the concentration of surfactant on the emulsion stability has shown also to be strongly influenced by the type of oil or fat. Differences in the oil density and in the degree of interfacial adsorption of the surfactant molecules depending on the type of oil phase have been suggested as the main explanation for the differences encountered.

1. Introduction

The quest to obtain delicious and healthy foods has been primary goal in the food industry during the last years. The good characteristics of fats in the enhancement of the flavours in bakery are usually not obtained when using oils. The main reason seems to be changes in the texture of the food due to the different interactions between the flour and the triacylglycerol (TAG) depending on its phase. The higher cost of the natural saturated TAG like butter has made to the food industry to prefer less expensive fats proceeding from the hydrogenation of natural polyunsaturated oils. However, the process of hydrogenation does not lead to a complete saturation of the fatty acid (FA) chains and in many cases introduce some changes in the single bonds making *trans* isomers to appear. These *trans* FA are more difficult to metabolize and they have been recently associated with diseases like Alzheimer, diabetes or cardiovascular problems. Recently is has became usual the use of the term functional food, referring to foods which have some properties regarding to the healing or reducing risk of undergo certain diseases. Some functional foods are produced by manipulating the structure of TAG in order to improve their properties for the health. In some cases the presence of *trans* FA in hydrogenated fats maybe drastically reduced by changing the traditional metal catalysis procedures for lipase catalyzed ones. The high specificity of some lipases allows replace the unsaturated FA by completely saturated ones without producing changes in the way of isomerization of their poly-

unsaturated ones [1]. These kinds of more healthy structured TAG (STAG) are in a constant developing process to be incorporated in the industrial production since they appear as a good alternative versus the traditional unhealthy hydrogenated fats. However, the different aspects about their digestive process are not still completely clear.

The digestive emulsion stability is a very important factor in the metabolization of fats by the human organism. The more stable emulsions will offer a higher oil-water interfacial area and therefore a higher rate of lipolysis. Among other compounds, bile salts (BS) appear as a main stabilizing agent during this process. These compounds not only help to solubilize the reaction products during the interfacial lipolysis but also obstruct the emulsion droplets coalescence by electrostatic stabilization once they are adsorbed at the oil-water interface. The interactions between BS and the oil phase in the digestive emulsion are a very important factor affecting to the stability of the digestive emulsion and therefore to the whole digestive process.

The type of STAG has already been proven to be an important variable affecting to the capability of BS to solubilized the reaction products during lipase lipolysis in emulsions [2, 3]. However, the way in which these interactions affects to the stability of the digestive emulsion is a relevant factor that should be taken into account. The type of oil phase has been shown to be a determinant factor on the emulsion stability in several works [4]. Turbidimetry has been employed in several works to assess the stability of emulsions [5] or to quantify changes in the droplet size [2].

In this work we study the effect that the type and concentration of BS has on the stability of emulsions from triolein. In a second part, we consider how the stability of the emulsion is affected by the type of oil using different STAG with different concentrations of one of the former BS. Performing a turbidimetric analysis of the changes taking place along the height of the emulsions during their breaking process we are able to find important information about the whole phenomena and how is affected by the different variables. The information obtained from the turbidimetric measurements shows how fast the phase separation occurs and the coalescence in the upper part of the system. The stabilizing effect of the BS concentration will be strongly influenced by the type of STAG in emulsion.

2. Materials and Methods

2.1. Chemicals

Trizma buffer (0.05M) with pH 7.4 was prepared every day using freshly deionized (0.054mS) filtered water (Milli RO/Milli Q, Millipore Inc., Jaffrey, NH). NaCl (150mM) and CaCl₂ (20mM) were added to the buffer preparation and bacterial contamination was avoided by adding NaN₃ (7.7mM). Sodium taurocholate (NaTC) and Sodium taurodeoxycholate (NaTDC) bile salts, with purity over 95% and 98% respectively, were

purchased from Sigma (St. Louis, MO). These water-soluble molecules have a rigid 5 β ring structure and present an amphiphilic character with a hydrophilic α -face and a hydrophobic β -face [6]. Due to their structure they form micelles in a non-usual stepwise way [7]. The micellar sizes may vary from R_h around 20 Å to $13 \times 10^3 \text{Å}^3$ depending on the different conditions like BS concentration or pH. Their CMC under our working conditions have been obtained in different works [8] and have shown to be around 10mM (NaTC) and 1mM (NaTDC).

The STAG were synthesized by a continuous enzymatic transesterification process of poly-unsaturated oils and fully hydrogenated fats. This process is described elsewhere [1]. In the present work, they are proceeding from the transesterification of sesame oil (SE) and fully hydrogenated soybean oil (FHSBO) at different concentration ratios (80:20 and 70:30); and from the transesterification of olive oil (OO) and fully hydrogenated palm oil (FHPO) at 90:10, 80:20, 70:30, 50:50 and 30:70.

Fresh solutions were prepared before every experiments set using the buffer solution and different concentrations of BS and MML. The experiments were performed at 30°C and all the solutions were filtered with a 0.2 μm PFTE membrane. The glassware was cleaned by plentiful rinsing of pure water after one day with sulphuric acid (96% purity). All the chemicals were stored according to the manufacturer instructions.

2.2. Emulsions preparation

The emulsions were prepared using a DiAx 900 homogenizer (Heidolph Instruments GmbH&Co., Schwabach, Germany) with a 6G tool. Pre-emulsification was achieved by homogenizing 700mg of STAG in 1 ml of buffer with the correspondent concentration of BS, depending on the experiment. This mixture was let to equilibrate at the treatment temperature and then was submitted, without previous shaking, to a five minutes treatment at a temperature of 60°C. The protocol followed was, one minute at 8000rpm, three minutes at 26000rpm and again one minute at 8000rpm. This protocol showed to produce smaller size and more mono-disperse emulsions than the single speed ones. After this first emulsification the sample was diluted to a final concentration of oil of 10% and different concentrations of BS.

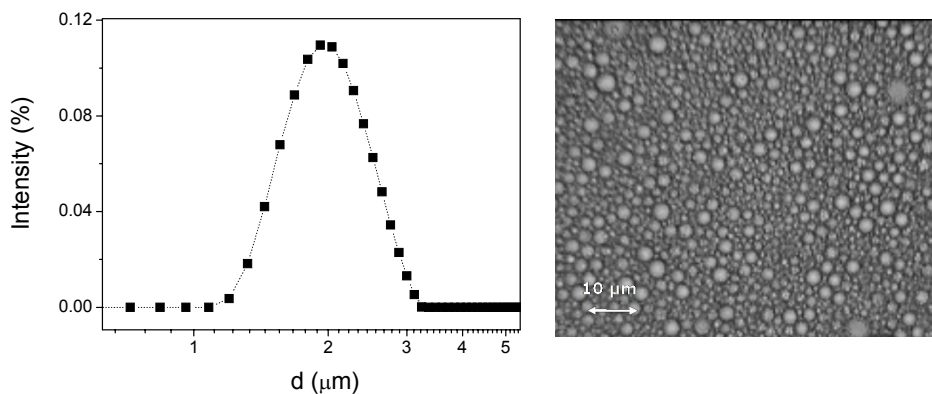


Figure 1. (Left) Size distribution for a triolein (100g/l) in buffer emulsion stabilized with NaTC (20mM) and CaCl₂ (2mM). (Right) Microscopic view (x40) of the former emulsion.

The final emulsions were sealed with a nitrogen atmosphere and kept in the dark in between the turbidity measurement. The droplet size distributions of these emulsions were measured, without dilution by dynamic light scattering (DLS) using an ALV-NIBS/HPPS system (ALV-Laser Vertriebsgesellschaft mbH, Langen, Germany). The size distributions of the emulsions prepared by this procedure were initially very similar, despite the oil substrate employed. They presented a size distribution of approximately 2.0µm weight mean droplet diameter, with slightly higher values for the more saturated STAG. In all the experiments the size distribution was certified by optical inspection (see Fig. 1) using a Motic B3 (Motic, Xiamen, China). No straight states of aggregation were found in the initial optical inspection of the emulsions.

2.3. Theoretical approach

When a light beam crosses a concentrated emulsion sample it will experience multiple scattering phenomena. In this case the light transmitted will be dispersed multiple times and it will become diffusive light. This is occurring when the photon mean path length $l(\varphi, d)$ (Eq.1) is larger than the wavelength of the incident light in the bulk media, λ .

$$l(d, \varphi) = \frac{2d}{3\varphi Q_s} \quad (1)$$

where d is the emulsion droplet mean diameter, φ the particle volume fraction and Q_s the extinction efficiency due to the scattering and adsorption

of the light by the emulsion droplets. Unless otherwise stated, the oil phases employed in this work will present a negligible imaginary part in their refractive index so the values of Q_s will be referred to the scattering efficiency. When the emulsion droplets mean radius is bigger than $\lambda/2\pi m$, being m the relative refractive index between the bulk and dispersed phases, anisotropic scattering of light by the dispersed phase will be occurring. The asymmetry factor, g , is the average cosine $\langle \cos\theta \rangle$ of the scattering angles weighted by the phase function. The light scattering produced by the former big emulsion droplets is characterized by values of g between $0 < g < 1$, where the Mie theory must be used [9]. Under these conditions, the diffusion of light, by the emulsion will be characterized by the photon transport mean free path, l^* , which represents the average distance that travels a photon in the dispersion before acquire a random direction. This photon transport mean free path is a correction of photon mean free path, l , with the asymmetry factor, g , as:

$$l^*(d, \varphi, g) = \frac{l(d, \varphi)}{1 - g} \quad (2)$$

In a system where there is no multiple scattering occurring, the transmittance of light may be related with l using the Lambert–Beer law:

$$T(l, x) = T_0 e^{-\frac{2x}{l}} \quad (3)$$

where x is the emulsion distance crossed and T_0 is the transmittance of the continuous phase, i.e. the fraction of incident light that passes through the sample when no dispersed phase is present.

In a diffusive system, the solution of the diffusion equation for light maybe given by [10]:

$$T(l^*, x) = \frac{\left(\frac{5l^*}{3x}\right)\beta}{\left[1 + \left(\frac{4l^*}{3x}\right)\right] \sinh \beta} \quad \text{with,} \quad \beta = \sqrt{\frac{3x^2}{l^*l_a}} \quad (4)$$

being l_a the absorption length. When the adsorption taking place can be neglected and the width of the sample is much higher than the photon transport mean free path ($x \gg l^*$) the Equation 4 can be approximated to $T(l^*, x) \approx 5l^*/3x$.

In very concentrated emulsions, where the droplet mobility is restricted by the neighbours, the structure of the system can be parameterized with a length scale like the droplet diameter, d , for example [11]. Therefore, in concentrated systems where d is much higher than λ , the photon transport mean free path can be considered as proportional to the mean emulsion droplet diameter, ($l^* \propto d$) [12].

During the breaking process of an emulsion the oil phase concentration and number of droplets are changing along the height of the sample. Therefore, quantitative estimations of the structure of the system at the different heights of the sample are very difficult to obtain from measurements of the static transmitted or backscattered light. However, qualitative information can be obtained if we consider that, after the initial moments of preparation and with relatively high concentrated emulsions, the oil phase concentration at the top of the sample maybe considered as constant and that the changes in the transmitted light in this part of the

system will be due to mainly coalescence phenomena. On the other hand, temporal variations of the transmitted light intensity along the samples height can be offering important qualitative information about how the phase separation is taking place along the time.

2.4. Following the breaking of the emulsions with Turbiscan

Turbiscan is an optical instrument designed to study the processes of aggregation and phase separation in colloidal systems. In this work we have employed a Turbiscan Classic MA 2000 (Formulation, l'Union, France) to obtain qualitative information about the breaking process of emulsions with dispersed phase from different oil and with different concentrations of surfactant. The principles of measurement with this instrument are based on the registration of the light intensity transmitted and backscattered, at an angle of 45° , along the emulsion height, at different times during the emulsion breaking process. The detection head is composed by a pulsed light source ($\lambda = 880\text{nm}$) and two synchronous detectors for transmission and backscattering, which are moving up and down along a cylindrical glass cell containing the emulsion sample. The samples height in our work are around 70mm in all the experiments and the transmission and backscattering data are collected every $40\ \mu\text{m}$. After being converted into electric signal by a photomultiplier in the instrument, the light information is processed by the computer and presented as transmitted or backscattered light intensities

along the samples height by the instrument software. Different curves with this type of information may be overlapped to study the phase separation changes along the time (see Figure 2). In the present work, we have only considered the transmission information due to the special characteristics of our emulsions. The high concentrations and our interest for a clear registration of the position of the limit between the dispersed and aqueous phase, made us to leave the backscattering information for future analysis. In this way we skip the problems observed by the saturation of the backscattering signal at high volume fraction due to the spatial organization of the emulsion droplets. On the other hand, we will also avoid the appearance of fake increments in the backscattering information, due to internal reflections in the measurement cell, which become more important at the low part of the cell were the volume fraction decreases.

During the breaking process of our emulsions simultaneous phase separation by flocculation, coalescence and droplet migration will be occurring simultaneously along the samples height. Qualitative information about the kinetics of the phase separation due to all these effects will be obtained from the temporal increment of the width of the transmission peak appearing at the bottom of the sample. This peak is due to the disappearing of the dispersed oil phase, at this part of the cell, after the creaming of the emulsion droplets or to the drainage of the water phase during their coalescence. Therefore, the very low concentration of droplets appearing at the bottom of the cell increases the values of the photon transport mean free path, allowing the increment of the transmittance values (see Eq. 1 and 3). As we can see in Figure 2, the width of the transmission peak at the bottom

of the emulsion is a very good estimation of the position and sharpness of the interface appearing between the coarsening emulsion and the water phase below, during the creaming process.

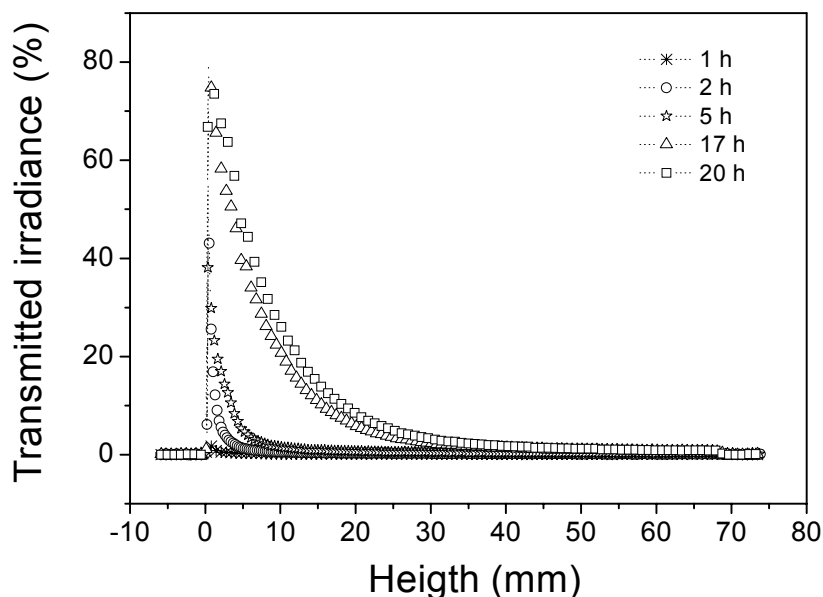


Figure 2. Increase of the width of the transmission peak during the breaking process of a triolein (100g/l) in water emulsion with NaTC (1.5mM).

In our case, we will consider the width of this peak at the 2% of transmitted light intensity, in order to set the position of the limit between the separating phases as closer as possible to the coarsening emulsion phase. This will be done, in all the experiments since the initial values of transmitted light are zero along the whole sample height.

In situations where the main process taking place will be the coalescence, and no differences in the droplet concentration will appear along the emulsions height, the changes in the transmitted light intensity

will occur homogeneously along this height (see the example in Figure 3). These kinds of phenomena are not very common when the bulk and dispersed phases have relatively different densities unless a fast flocculation or coalescence will be taking place. In our case the variations of the transmitted light intensity will be very important in the upper part of the emulsion.

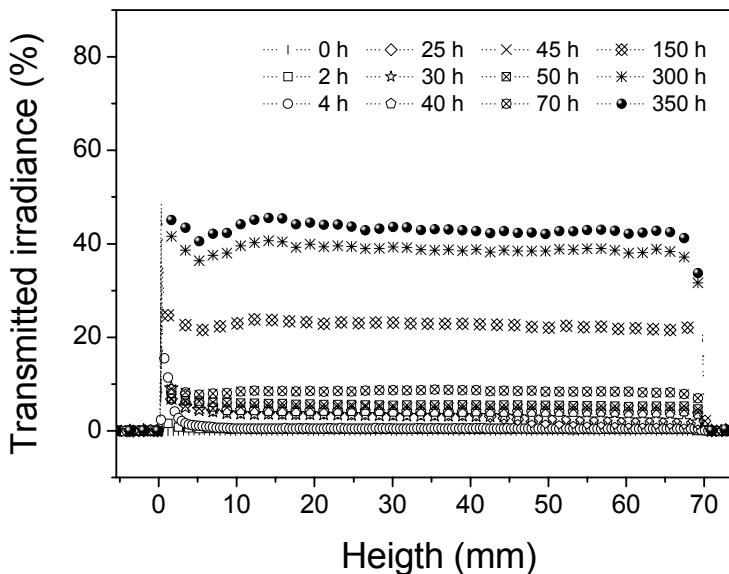


Figure 3. Increase of the mean value of transmitted irradiance during the breaking process of a triolein (100g/l) in water emulsion with NaTC (13mM) and L- α -phosphatidylcholine (6mM).

In this part no further creaming is taking place and the dispersed phase concentration may be considered as constant due to the accumulation of creaming droplets. In this highly concentrated upper part (see Fig. 1), the emulsion droplets arrange themselves in a liquid foam-like organized structure. Consequently, the changes in the transmitted light intensity observed at this part of the sample are only caused by the coalescence of the

emulsion droplets. As we have seen before (Eq. 4), when no light absorption is occurring and the width of the sample is big enough ($x \gg l^*$), these changes in the transmitted can be considered as proportional to the change in the droplet size and, therefore, they will be a good estimation of the kinetics of coalescence. The temporal changes of the mean values of transmitted light intensity, between the positions 6.7mm and 6.9mm, will be considered to estimate the former kinetics of coalescence in the upper part of the sample.

3. Results and Discussion

3.1. Effect of the type and concentration of BS on the stability of emulsions with triolein

In the first part of this work we will analyse the breaking process of triolein (100g/l) in buffer emulsions stabilized with different concentrations of NaTC (1.5mM, 4.5mM and 13.5mM) and NaTDC (1mM, 3mM and 9mM). The overlapping curves with the transmitted light intensity along the emulsion height at different times are presented in the Figure 4 for the different emulsions.

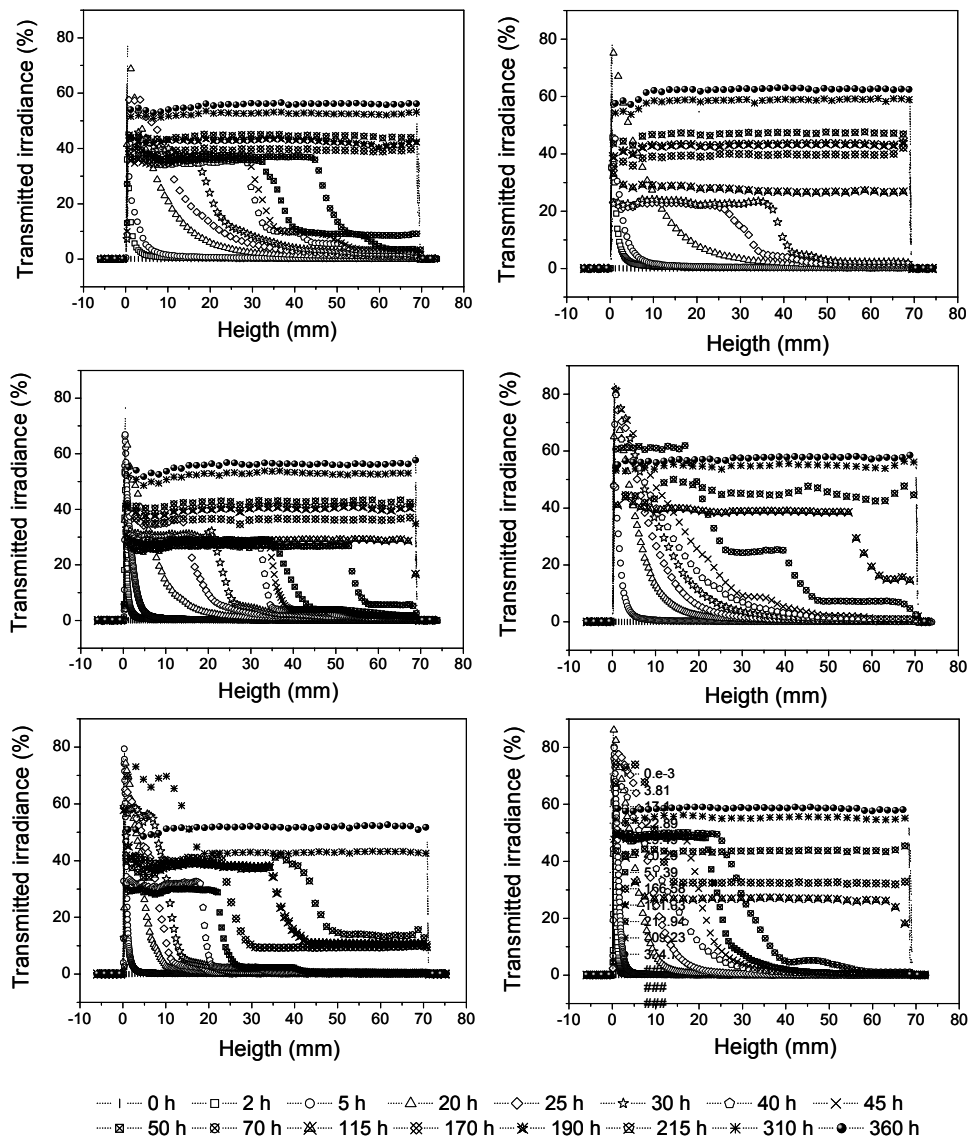


Figure 4. Temporal increase of transmitted irradiance along the height of the emulsion during the breaking process of emulsions with triolein (100g/l) and different concentrations of (left) NaTC (1.5mM, top; 4.5mM, centre; 13.5mM, bottom) and of (right) NaTDC (1mM, top; 3mM, centre; 9mM, bottom)

In these curves is possible to observe how a peak of transmitted light intensity is appearing at the bottom of the cell, increasing its width along the breaking process of the emulsion. In most of the cases, the interface appearing between the creaming emulsion and the water phase below is getting sharper with the time, meaning that the accumulation of droplets in the upper part is obstructing the other droplets ascending movement.

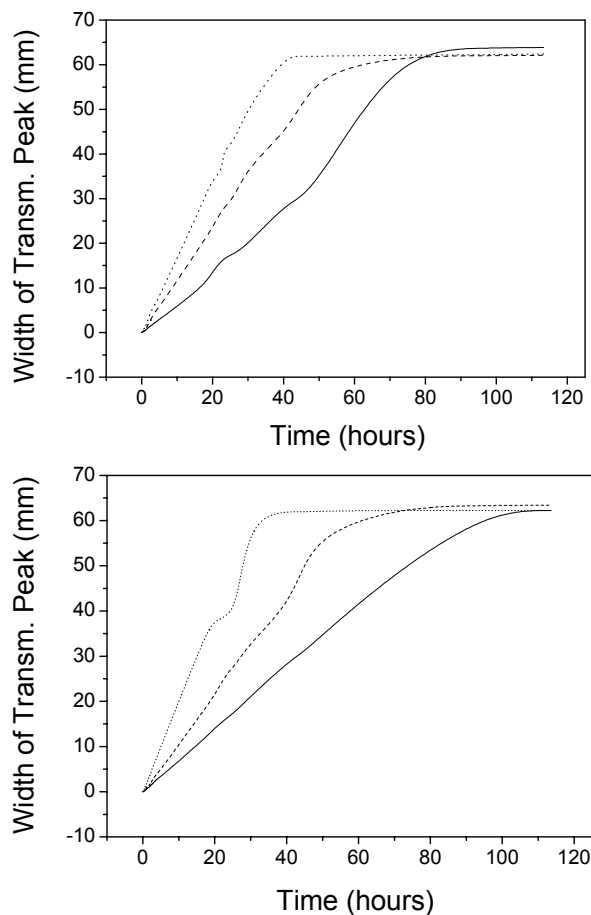


Figure 5. Temporal increase of the width of the transmitted irradiance peak during the breaking process of emulsions with triolein (100g/l) and different concentrations of NaTC (top) at 13.5mM (solid), 4.5 mM (dash) and 1.5mM (dot), and of NaTDC (bottom) at 9mM (solid), 3mM (dash) and 1mM (dot).

In certain cases, before the complete phase separation is accomplished, it is also possible to see the appearance of two steps in the transmission peak (see Figure 4; NaTDC, 3mM). This situation is representative of the appearance of a second, less compact, structure in the organization of the ascending drops. This pseudo phase is finally merged with the upper very organized emulsion phase and we will not analyze it in this work. The temporal increment of the width of the transmission peak at the bottom of the cell for the breaking processes of the emulsions in Figure 4 are shown in Figure 5. As expected, these curves show a clear decrease in the rate of width increment of the transmission peak with the increment of the concentration of BS. The higher concentration of surfactant molecules allows their major adsorption at the oil water interface and therefore offers to the system a higher electrostatic stabilization. This higher stability prevents the flocculation and coalescence and therefore slows down the phase separation during the emulsion breaking process. In order to compare how the type of BS is affecting to the stability of the emulsions lets consider how the slopes of the increment of the transmission peak are changing with the concentration of BS (see Figure 6). The emulsions with NaTC present a slower decrease of the rate of change of the transmission-intensity-peak-width with the concentration of BS than the ones with NaTDC. This is due to the faster formation of micelles in the case of NaTDC that increases the stabilizing effect of this compound. It is precisely due to this lack in the presence of BS micelles that, in all the cases these velocities of droplet migration are faster for NaTC than for NaTDC.

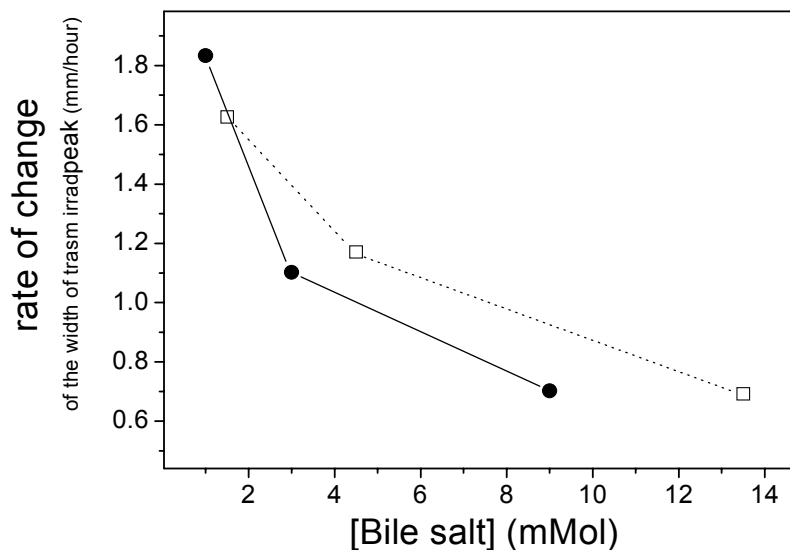


Figure 6. Rate of increase of the width of the transmitted irradiance peak during the breaking process of emulsions without L- α -phosphatidylcholine depending on the concentration of NaTC (empty squares) or of NaTDC (black circles).

This can also be consequence of a possible lower coalescence rate in these emulsions the due to the lack of the extra hydroxyl group that offers to the molecules of NaTDC a higher amphiphilic character.

From the information obtained in the variations of the width of the transmission peak is possible to assess the effect of the BS on the velocity of creaming. However, this information is affected by the flocculation and coalescence effects taking place along the droplets ascending movement. In order to obtain qualitative information about the coalescence phenomena exclusively lets consider the upper part of the sample where the emulsion droplets are confined in a liquid foam-like compact organization and the only reason for the changes observed in the transmitted light will be the

droplet coalescence, increasing the droplets mean diameter. The increment of the even transmission values at the top of the cell, as an estimation of the coalescence in this organized part of the emulsion, are shown in Figure 7 for both BS.

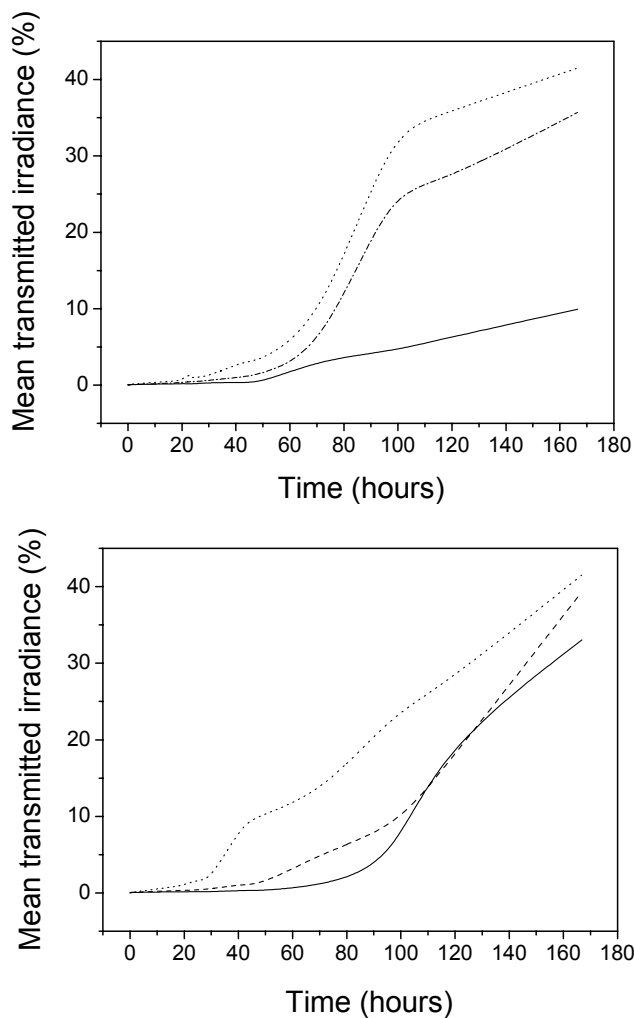


Figure 7. Temporal increase of the mean transmitted irradiance in the upper part of the emulsion during its breaking process of emulsions with triolein (100g/l) and NaTC (up) at 1.5mM (dot), 4.5mM (dash) and 13.5mM (solid) or NaTDC (down) at 1mM (dot), 3mM (dash) and 9mM (stars).

As expected, those emulsions with a higher concentration of BS present a slower increment in the mean transmitted light at this position of the emulsion of the sample. The higher interfacial presence of BS molecules offers an electrostatic interfacial charge that increases the stability of the system slowing down the coalescence rate. Lag periods can be observed before the increment in the droplet diameters will present the characteristic dependence with $t^{1/2}$ predicted by the classical mean field theories for this kind of phenomena [11, 13]. From our point of view, these lag times corresponds to the arrangement of the emulsion droplets at this part of the cell. Even when coalescence phenomena are already taking place, the oil phase concentration is still increasing until the final packing is achieved. After this point, only coalescence phenomena will be occurring. These results seem to show shorter lag periods of droplets arrangement for the emulsions with NaTC that for those with NaTDC. This may be indicative of a lower stability of the first ones that produces a less stable and polydisperse droplets, which position themselves in a faster and less organized way. In the cases with lower concentrations of NaTDC no lag periods are appearing and the dominating effect is the droplet coalescence from the initial moments. A possible coalescence controlled by micellar depletion is suggested as the possible reason for this behaviour. By consideration of the initial rates of change of the transmitted irradiance in the upper part of the emulsion, we can compare how the presence of each BS affects to the stability of the emulsion (see Fig. 8). These rates show that for the lower concentrations, the effect NaTDC on the stability of the emulsions is much smaller than the one of NaTC.

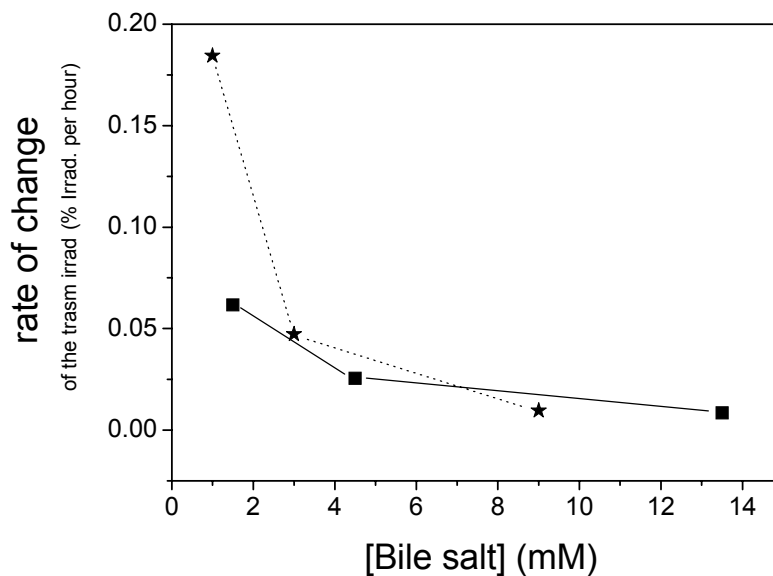


Figure 8. Rate of change of the transmitted irradiance at the top of the emulsion during the breaking process of emulsions with triolein (100g/l), depending on the concentration of NaTC (squares) and of NaTDC (stars).

However, when the concentration of BS is increasing their effects became more similar.

As commented before, the presence of micellar aggregates may be responsible of a higher coalescence enhanced by depletion that decreases with a higher interfacial incorporation of BS molecules for higher bulk concentrations. The small difference between the coalescence occurring at similar concentrations, above the CMC of NaTDC, gives strength to this assumption [14].

3.2. Effect of the STAG type on the stability of emulsions with NaTC

In the second part of this work we have considered the effect of the oil substrate on the stability of the emulsions. NaTC has been chosen for these experiments since it has shown a higher CMC value. The different STAG employed were dispersed in the emulsion at concentrations of 100 g/l using the protocol explained before. The temporal variation of the transmitted light intensities along the emulsion height showed similar tendencies to the ones showed in the last point, with a clear transmission peak appearing at the lower part of the emulsion and a clear coalescence phenomena occurring at the top (not shown).

The temporal increment of the width of the transmission peak for the case of emulsions with STAG from SE and FHSBO are shown in Figure 9. The enhancing of the emulsion stability by the presence of the BS can be clearly observed in these results. However, only for the cases with a lower presence of saturated FA, is possible to observe differences in the stability due to the different concentrations of BS. This can be explained as a higher adsorption of the BS molecules to the more saturated substrates and has been observed in different works [2]. In general, in the cases with less saturated substrates, is possible to observe a slight decrease in the velocity of increment of the transmission peak-width with the increase of the concentration of NaTC. If we consider how the slopes of the increment of the transmission peak are changing with the degree of saturation of these

dispersed STAG, at the different concentrations of BS (see Figure 10) we can see that, in absence of BS, the more stable emulsions are obtained with the more saturated STAG. For the rest of the concentrations of BS, this effect is only perceptible at concentrations below $100\mu\text{M}$. At NaTC ($50\mu\text{M}$) no differences are observed between the emulsions with SE:FHSBO 80:20 and 70:30. This clear improvement of the emulsion stability with the more saturated STAG may be explained by the lower oil water interfacial tensions

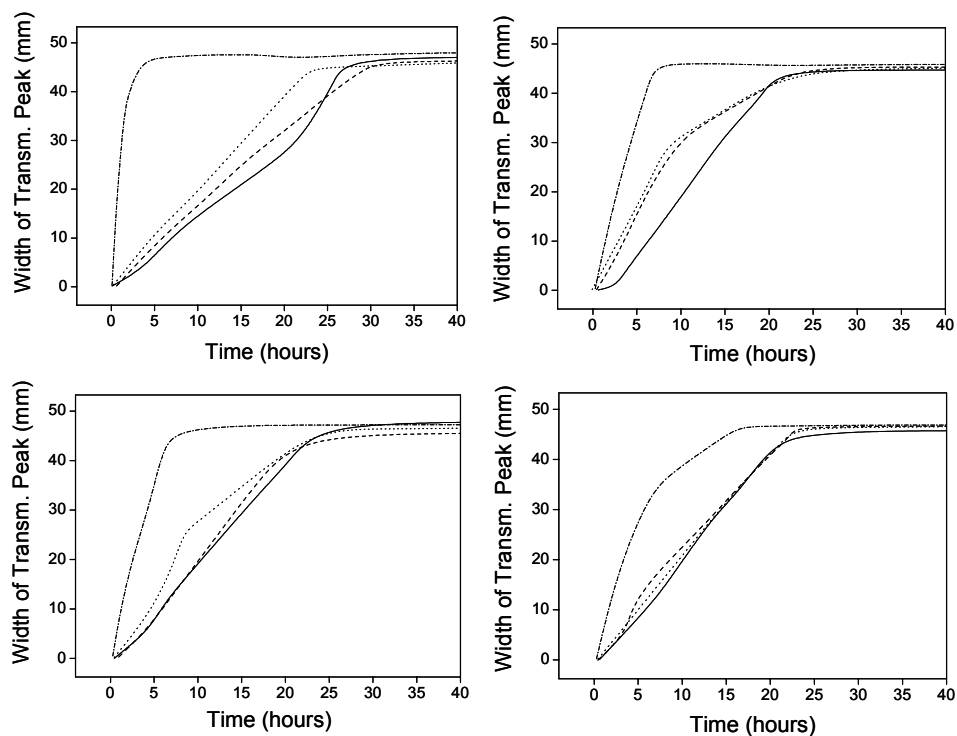


Figure 9. Temporal increase of the width of the transmitted irradiance peak during the breaking process of emulsions with SE:FHSBO (SE, top left; 90:10, top right; 80:20, bottom left; 70:30, bottom right; All 100g/l), depending on the concentration of NaTC (no BS, dash-dot; $10\mu\text{M}$, dot; $50\mu\text{M}$, dash; $100\mu\text{M}$, solid)

and by the slightly higher viscosities of these fats at the temperature at which the breaking process is taking place [15]. However, if we consider now the effect of the type of STAG phase in the breaking process of the emulsions with semisolid structured fats from OO and FHPO we can see that this tendency is not so clear in this type of substrates.

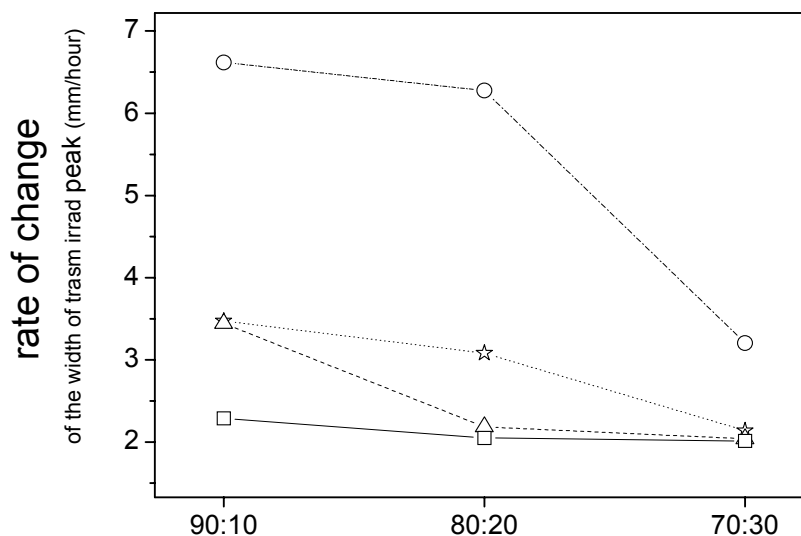


Figure 10. Rate of increase of the width of the transmitted irradiance peak during the breaking process of emulsions with STAG (100g/l) depending on the SE:FHSBO synthesis concentrations ratio in presence of different concentrations of NaTC (no BS, circles; 10µM, stars; 50µM, triangles; 100µM, squares).

The temporal increment of the width of the transmission peak for the case of emulsions with STAG from OO and FHPO are shown in Figure 11. In these cases, the stabilizing effect of the different concentrations of BS is more evident than in the case with SE:FHSBO, especially for the less saturated STAG. A clear slow down in the growth of the transmission peak is appearing as the concentration of BS increases in the system.

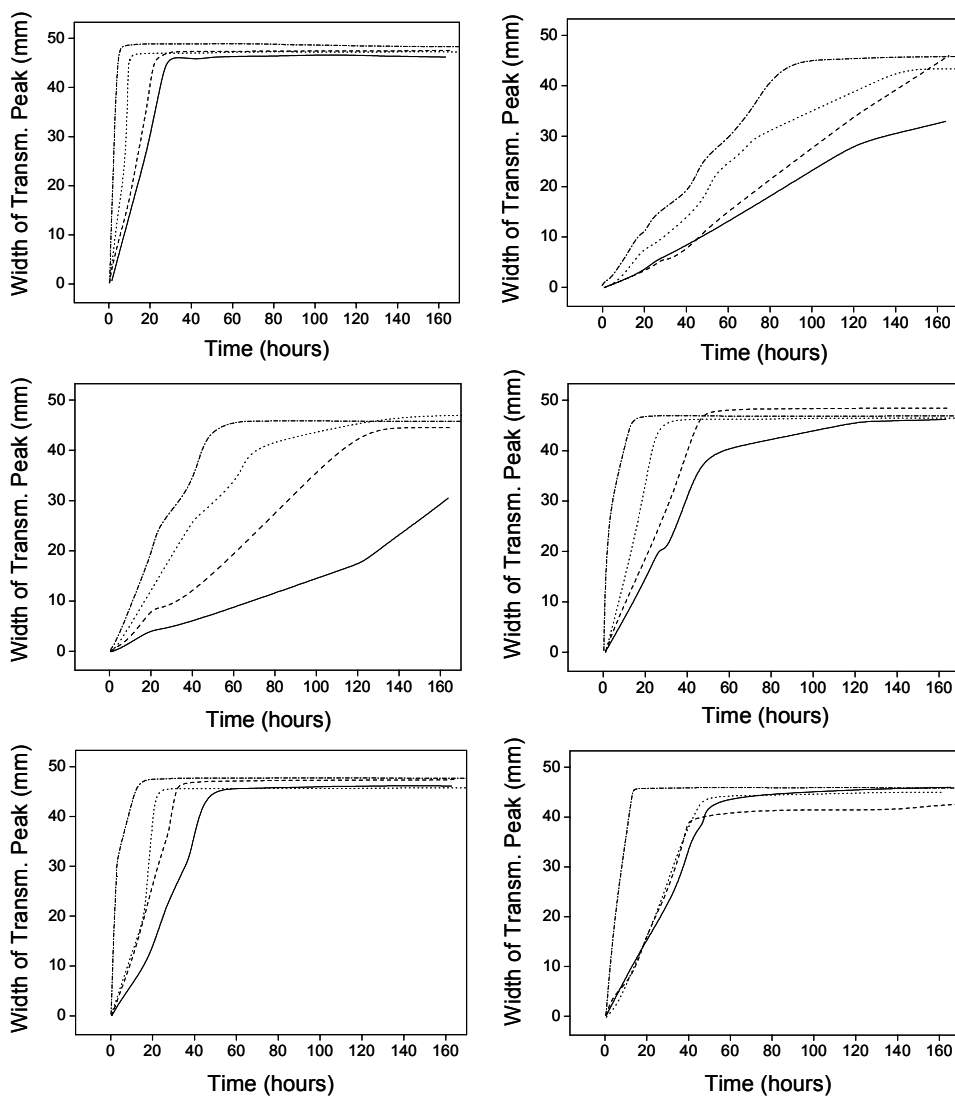


Figure 11. Temporal increase of the width of the transmitted irradiance peak during the breaking process of emulsions with OO:FHPO (OO, top left; 90:10, top right; 80:20, middle left; 70:30, middle right; 50:50 bottom left; 30:70 bottom right; All 100g/l), depending on the concentration of NaTC (no BS, dash-dot; 10µM, dot; 50µM, dash; 100µM, solid)

However, different tendencies are observed in the stability of the emulsion depending on the degree of saturation of the STAG. In this case, it seems that the emulsions are getting less stable when the degree of saturation of the oil increases. In order to have a better estimation of this effect we can observe the variations in the slopes of the increment of the transmission peak produced by the change in the degree of saturation of the dispersed STAG, at the different concentrations of BS (see Figure 12).

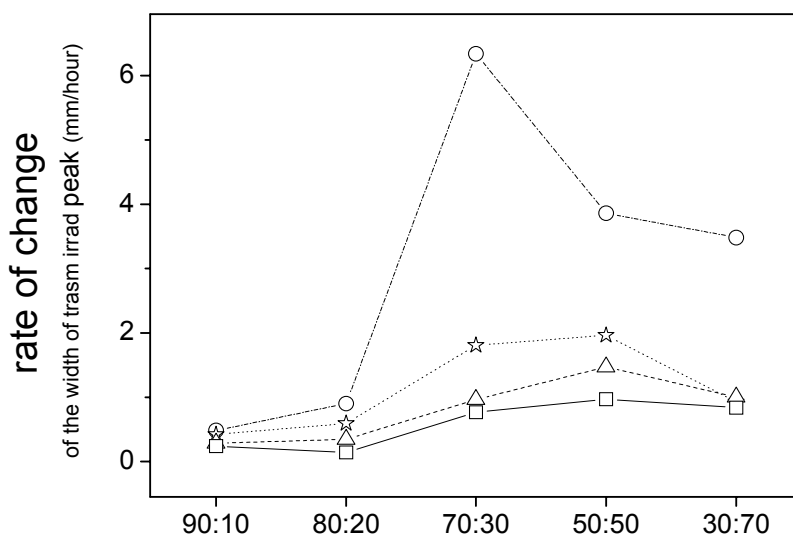


Figure 12. Rate of increase of the width of the transmitted irradiance peak during the breaking process of emulsions with STAG (100g/l) depending on the OO:FHPO synthesis concentrations ratio in presence of different concentrations of NaTC (no BS, circles; 10µM, stars; 50µM, triangles; 100µM, squares).

Especially in absence of BS, a clear maximum in the rate of increment of the transmission peak-width is observed for the emulsions with OO:FHPO (70:30). This means that the less stable emulsions are obtained with this type of STAG. As it would be expected by the decrease in the oil-water

interfacial tension and the increase in the viscosity with the increment in the degree of saturation of the STAG, the emulsions should be more stable with the higher degree of saturation of the STAG. A possible reason for the appearance of this maximum is the little difference in the STAG densities that will cause a faster phase separation for the less dense, more saturated, oil phase. This could explain that even when the coalescence will decrease with the decrease in the saturation degree, the creaming process will occur in a faster way until the increment of the stability will be enough to slow down this effect. Minor differences observed in the size distributions of this emulsions with Sauter diameters slightly higher (~50nm) or the appearance of little fat crystals at this ratios could also be proposed as a possible reason for this behaviour. These last fat crystals have been found to induce coalescence in similar emulsions by different authors [16]. However, further rheological and tensiometric studies are necessary to certify the way in which the oil-water interfacial tensions and the viscosities are decreasing and increasing respectively with the degree of saturation of the STAG. The information about the variations in the transmitted intensity in the upper part of the cell is also showing a similar peak as we will see before (see Figure 16). The increase in the concentration of NaTC helps to reduce the rate of increment of the width of this transmission peak and partially conceal the peak observed in absence of BS. This is particularly clear in the case of OO:FHPO (70:30) where the higher adsorption of the BS molecules helps to reduce the differences in stability with the emulsions with less saturated STAG.

The increment of the transmitted light intensity at the top of the emulsions with these STAG from SE:FHSBO, in presence of different concentrations of NaTC, are shown in Figure 13 as an estimation of the coalescence taking place at this part of the emulsion. A clear increment in the emulsions stability can be observed, as expected, with the higher concentrations of NaTC.

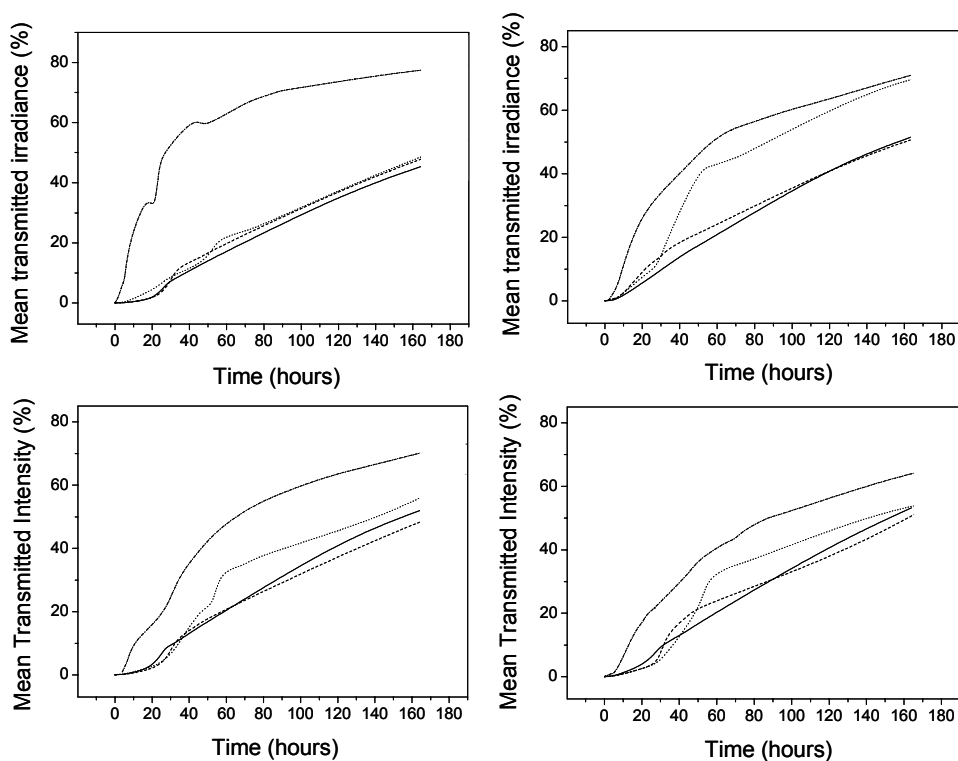


Figure 13. Temporal increase of the mean transmitted irradiance in the upper part of the emulsion during its breaking process depending on the concentration of NaTC (no BS, dash-dot; 10 μ M, dot; 50 μ M, dash; 100 μ M, solid) for emulsions with STAG from SE:FHSBO (SE, top left; 90:10, top right; 80:20, bottom left; 70:30, bottom right; All at 100g/l)

As we saw before, in this case is also difficult to distinguish the effect of the different concentrations of NaTC in the cases with the more saturated STAG due to the higher degree of adsorption observed in these cases. No lag periods are observed as we saw in the case of triolein in the first part of this work. The lower concentration of BS present, in this case, does not offer enough stability to the emulsion as to allow the ascending oil droplets to organize themselves spatially before the coalescence process will dominate the variations in the light transmitted at this position of the emulsion. This effect is particularly clear in the cases where no BS is present, where the coalescence appearing from the initial moments shows an increment of transmitted intensity proportional to the square root of the time [11, 13] according with the increment predicted in the mean droplet diameter [12]. However, the presence of BS offers to the system enough stability as to mix the spatial arrangement and coalescence effects so that is not possible to observe lag times neither $t^{1/2}$ dependencies typical from single coalescence. In order to obtain a qualitative estimation of the effect of the different concentrations of BS on the stability of the emulsions with this type of STAG we can consider the initial rates of change in the former results of transmitted irradiance in the upper part of the emulsion (see Fig. 14). The observed increment of the emulsion stability with the degree of saturation of the STAG, manifested in the decrease of the rate of increment of the transmission peak width, can now be observed in the transmitted intensity in the upper part of the emulsion. These results, therefore, evidence that the slower creaming observed in these more saturated STAG is enhanced mainly by a decrease in the coalescence phenomena taking place

and in a much smaller degree to a decrease in the droplet flocculation. The higher concentration of BS tends to increase the stability to coalescence and at concentrations of NaTC ($100\mu\text{M}$) is already not possible to observe differences between the different STAG.

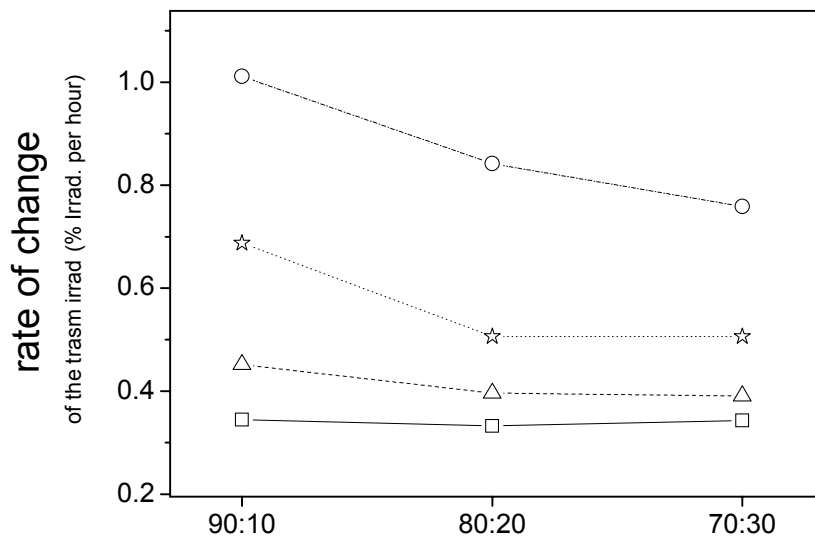


Figure 14. Rate of change of the transmitted irradiance at the top of the emulsion during the breaking process of emulsions with STAG (100g/l) depending on the SE:FHSBO synthesis concentrations ratio in presence of different concentrations of NaTC (no BS, circles; $10\mu\text{M}$, stars; $50\mu\text{M}$, triangles; $100\mu\text{M}$, squares).

If we consider now the effect of the type of STAG phase in the coalescence in the upper part of the emulsions with semisolid structured fats from OO and FHPO we can see again considerable differences with respect to the former STAG. As we can see in Figure 15, small differences appear between the coalescence in the emulsions with triolein and OO. Their similarity in their FA composition makes them to present similar interfacial tensions, viscosities and similar interactions with the BS molecules.

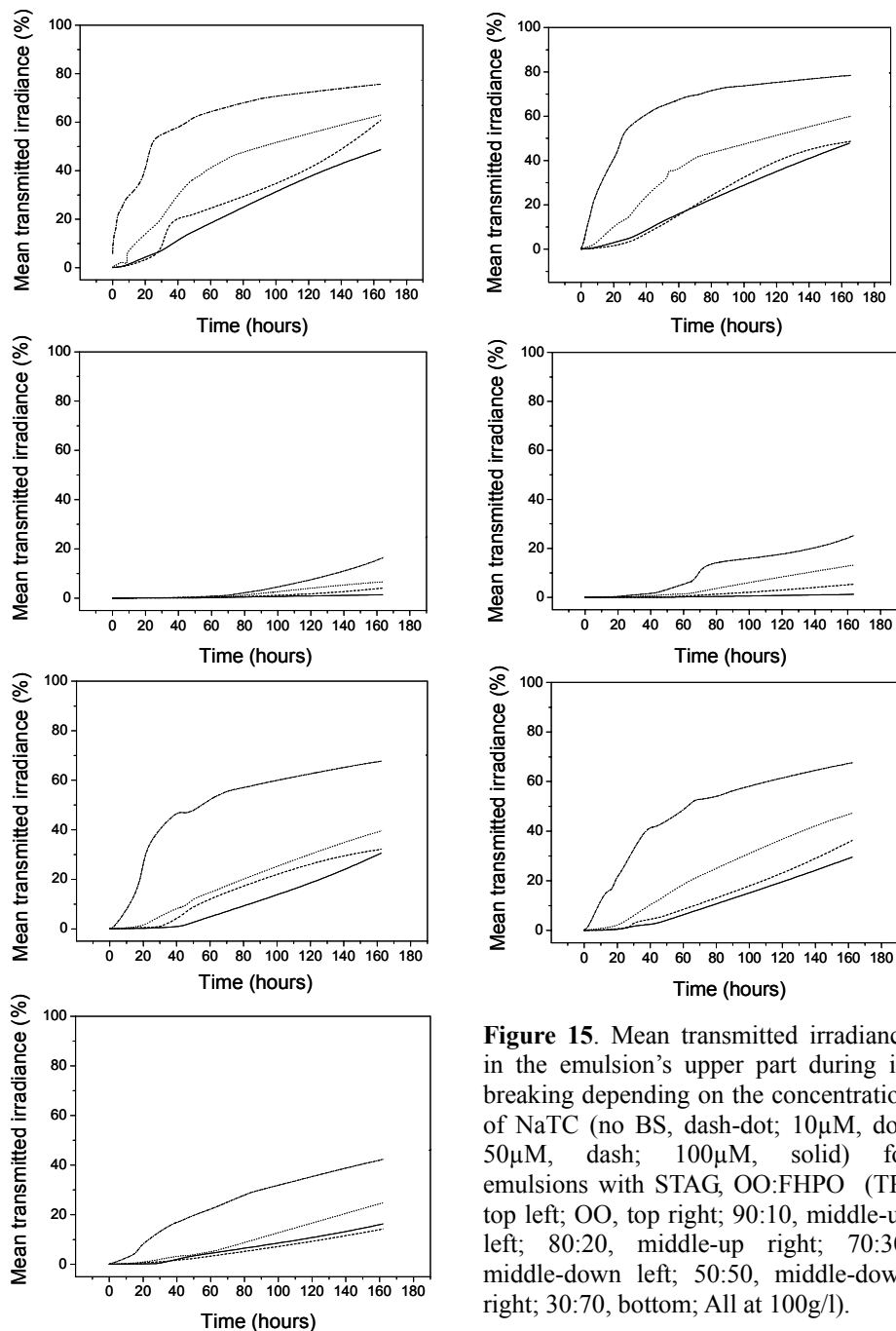


Figure 15. Mean transmitted irradiance in the emulsion's upper part during its breaking depending on the concentration of NaTC (no BS, dash-dot; 10 μ M, dot; 50 μ M, dash; 100 μ M, solid) for emulsions with STAG, OO:FHPO (TR, top left; OO, top right; 90:10, middle-up left; 80:20, middle-up right; 70:30, middle-down left; 50:50, middle-down right; 30:70, bottom; All at 100g/l).

For these oils the coalescence is dominating the increment in transmitted light in absence and at the lower concentration of BS. The STAG from these sources show the same tendencies than the ones in the increments of the transmission peak observed before. Again a peak in the coalescence seems to appear for the STAG with a middle saturation degree. For the less saturated, the coalescence seems to play a secondary roll in the increment of the transmitted light. Especially in the cases with no BS it is possible to observe some lag periods of droplet spatial arrangement before the transmitted light increases due to the droplet coalescence. This fact is manifesting the intrinsic high stability of these less saturated emulsions from OO and FHPO.

It is difficult to explain this stability against coalescence and the only reason that we can propose is small differences during the transesterification process leading to a STAG molecules with a different composition that would affect to the oil-water interfacial conformation, causing a decrease in the interfacial tension values. Further research is necessary to clarify the appearance of this phenomenon. The presence of increasing concentrations of BS tends to reduce the coalescence until non measurable levels. Only in the cases with higher degree of saturation is possible to observe some coalescence appearing after lag periods of droplet organization. In order to have a more clear image to compare the differences appearing between this type of STAG lets consider the rates of change of the transmitted light intensity in this upper part of the emulsion (see Fig. 16). These values show a very similar tendency to the one observed in Figure 12. This means that the faster creaming occurring with the more saturated STAG is causing also

a faster coalescence in the upper part of the emulsion. The fact that this effect is reversed at degrees of saturation above OO:FHPO (70:30) is a clear prove of the enhancement of the emulsion stability versus coalescence obtained with the more saturated substrates.

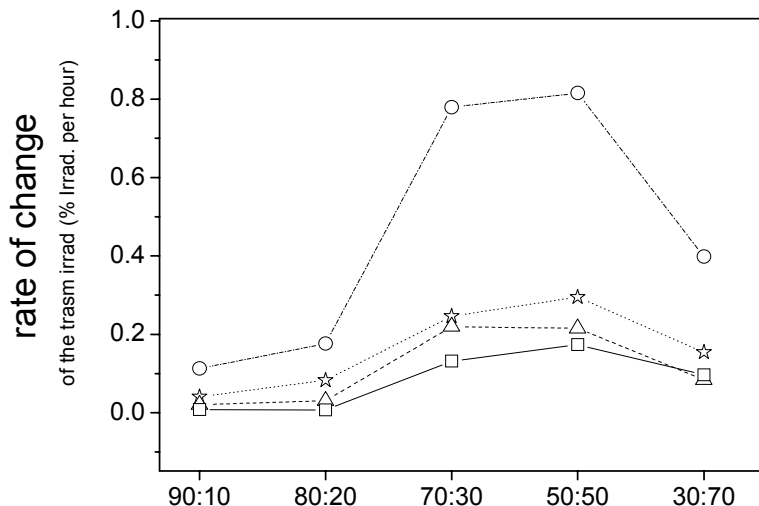


Figure 16. Rate of change of the transmitted irradiance at the top of the emulsion during the breaking process of emulsions with STAG (100g/l) depending on the OO:FHPO synthesis concentrations ratio in presence of different concentrations of NaTC (no BS, circles; 10μM, stars; 50μM, triangles; 100μM, squares).

In these measurements, the clear peak appearing in the rate of increment of the transmitted intensity-peak-width for OO:FHPO (70:30) is not so sharp, in absence of BS. This is reinforcing the hypothesis of the combination of the effects of the less density and interfacial pressure with the higher degree of saturation since, in this case, what in the lower part of the emulsion is a process mainly controlled by little differences in density, in the upper part of the emulsion is mainly controlled by the enhancement of the emulsion stability due to smaller values of interfacial tension.

4. Conclusions

The combination of the qualitative information obtained with Turbiscan about the velocity of creaming and the rate of coalescence in the upper part of the emulsions has shown to be very illustrating about the effect of the different variables on the stability of oil in water emulsions. As we have seen, changes in the type or concentration of the surfactant or even in the type of oil dispersed can be clearly assessed with this technique. Different effects on the stability of the emulsions of triolein were observed in presence of NaTC or NaTDC. The first BS with a lower amphiphilic character has shown to offer more stability to the emulsions at concentrations below its CMC. The appearance of micelles is supposed to reduce significantly the emulsion stability for the case with NaTDC due to a possible depletive enhanced coalescence. This effect, however, is clearly reduced by the increment of the BS bulk concentration due probably to a better incorporation of the BS molecules at the oil water interface.

The type of oil phase has also showed to be a very important factor in the emulsion stability. For the STAG considered we have found differences regarding to their synthesis source type as well as to their degree of saturation. For similar oil:fully-hydrogenated-fat synthesis ratios, the emulsions with STAG from SE and FHSBO showed a clear higher stability versus creaming and coalescence. In the case of STAG from SE and FHSBO the main factor controlling the stability of the emulsions appears to be the degree of saturation. This means that the more saturated substrates, with

lower oil-water interfacial tensions will produce more stable emulsions despite the little differences that may appear in their densities. In the case of STAG from OO and FHPO these little differences became more important dominating the stability of the less saturated emulsions due to a faster creaming that can not be obstructed by the enhancement in the emulsion stability produced by the lower interfacial tensions. All these effects are dissimulated by the increment in the concentration of BS but they are still observable for the lower concentrations. All these findings, suppose important clarifications in the different aspects of the stability of these important systems that may explain differences on the digestibility of functionalized foods and may help to improve their formulations.

References

1. Otero C et al. *Continuous enzymatic transesterification of sesame oil and a fully hydrogenated fat: effects of reaction conditions on product characteristics*. *Biotechnol Bioeng* 2006;94:877
2. Tejera-Garcia R et al. *Turbidimetric and interfacial study of lipolysis in O/W emulsions of triolein or semisolid structured fats stabilized with bile salts*. to be published 2008
3. Tejera-Garcia R et al. *Digestibility of semisolid structured triacylglycerols from olive oil and fully hydrogenated fats - an in vitro study*. to be published 2008
4. Ahmad K et al. *Properties of palm oil-in-water emulsions stabilized by nonionic emulsifiers*. *Journal of Colloid and Interface Science* 1996;181:595
5. ten Grotenhuis E et al. *Phase stability of concentrated dairy products*. *J Dairy Sci* 2003;86:764
6. Borgstrom B. *Dimensions of Bile Salt Micelle . Measurements by Gel Filtration*. *Biochimica et Biophysica Acta* 1965;106:171
7. O'Connor CJ and Wallace RG. *Physico-Chemical Behavior Of Bile Salts*. *Adv Colloid Interface Sci* 1985;22:1
8. Tejera-Garcia R et al. *Interfacial study of interactions between lipases and bile salts*. to be published 2008
9. Kerker M. *The Scattering of Light and Other Electromagnetic Radiation*. Academic Press, New York 1969
10. Ishimaru A. *Wave Propagation and Scattering in Random Media*. Academic Press, New York 1978:1
11. Mullins WW. *The Statistical Self-Similarity Hypothesis in Grain-Growth and Particle Coarsening*. *Journal of Applied Physics* 1986;59:1341
12. Durian DJ et al. *Multiple Light-Scattering Probes of Foam Structure and Dynamics*. *Science* 1991;252:686
13. Bibette J et al. *Emulsions: basic principles*. *Reports on Progress in Physics* 1999;62:969
14. Matubayasi N et al. *Thermodynamic study of gaseous adsorbed films*

-
- of sodium taurocholate at the air water interface.* Langmuir 1996:12:1860
15. Salager JL et al. *Encyclopedic Handbook of Emulsion Technology.* Ed J Sjöblom Marcel Dekker, New York 2001:455
 16. Boode K et al. *Partial Coalescence in Oil-In-Water Emulsions .2. Influence of the Properties of the Fat.* Colloids and Surfaces A-Physicochemical and Engineering Aspects 1993:81:139

Capítulo 3

Turbidimetric and interfacial study of lipolysis in O/W emulsions of triolein and of semisolid structured fats stabilized with bile salts

Abstract

The effect that different variables have on the activity of lipases during the process of lipolysis of triacylglycerides has been extensively studied until nowadays. However, the way in which the effect of one variable is affected by the others is difficult to assess and model due to the lack of perfectly reproducible lipase and substrate standards and to the great variety of techniques employed in the different laboratories. In this work, we present a new and simple protocol for the lipase assay based in the turbidimetric analysis of the reaction combined with final air-water interfacial tension measurements. We have employed this protocol to study the effect of different variables on the activity of one lipase acting on emulsified substrates. A wide scanning have been made over the combined effect of the lipase and substrate concentrations, the bile salts CMC or the Ca^{2+} ionic presence. In a final part, we study the effect of the type of oil on the lipase activity using structured triacylglycerides proceeding from the transesterification of poly-unsaturated oils and fully hydrogenated fats. The

effect of the type and concentration of bile salt on the lipolysis of these semisolid structured fats has also been considered. These results have shown that the concentration of bile salt may have different effects on the lipase activity depending on the type of oil substrate. During the different combination of variables studied, we found some conditions in which fibril-like precipitates were formed during the lipolysis in emulsions with triolein. These precipitated showed some features that suggest their possible amyloid character. The employed methodology appears as a new and promising approach to clarify certain topics about the activation and activity of lipases that still are not completely clear.

1. Introduction

Digestive lipases (triacylglycerol acylhydrolases, EC 3.1.1.3) are biological catalyzers that favors the hydrolyzation of the ingested oil and fat triacylglycerides (TAG) splitting them into monoacylglycerols (MAG), diacylglycerols (DAG) and free fatty acids (FA). As most of the digestive agents, they are water-soluble and, due to the hydrophobic character of the TAG, the hydrolysis must be taking place at the oil-water interface. During the digestion, the ingested hydrophobic TAG is dispersed in water by means, for example, of the mastication or by the stomach peristaltic movements. This dispersion is an emulsification process which main purpose is to increase the TAG-water interface to a maximum area. With a maximum interfacial area, the number of reactions increases to a maximum reaction rate. This maximum area is in part maintained thanks to the stabilizing effect of bile salts (BS) at the oil-water interface. The whole process is a complicate interfacial and colloidal serial of events that are strongly influenced by the many variables involved. The type and arranging of the TAG, the concentration of each digestive agent or the environmental characteristics of reaction are very important factors controlling this whole process. All of these factors make that the type of interactions occurring between the different compounds, or whether they occur at the bulk or interfacial levels [1], will be topics with certain level of controversy still now days. One of the main difficulties is to compare in-vitro results with the

real process, which takes place in presence of multiplicity of aggregates like the elements from the food matrix. All these factors have been studied separately and characterized until nowadays for several lipases and substrates [2, 3, 4, 5, 6]. However, the effects of the combination of the different variables are difficult to model since there is not a perfect standardized form of arranging the substrate for reaction. The complexity of emulsified systems is one of the main reasons. Apart of being by definition thermodynamically unstable systems, their configuration and destabilization process are highly dependent on the emulsification protocol and on the concentration and composition of the stabilizing agents. Tiny differences in the temperature or in the duration or speed of the shear during preparation may end in very different stabilities or size distributions in the final emulsion. Standard substrates and lipases are nowadays commercial available [7], however, several difficulties seems to appear when comparing results [8]. In consequence, there is a continuous searching for reference materials [9, 10, 11]. Among the possible techniques for the assay of the lipase activity [12], titrimetric methods are clearly the most employed and reliable. Nevertheless, these methods are slow [13], being still difficult to obtain enough amount of data without having an ageing effect or using different emulsions between the different sets of experiments. Turbidimetric methods appear as a good alternative for a faster data collection, however they usually requires a calibration step based on different techniques that have inhibited a wider diffusion of these methods [12]. From our point of view, the appearing of standardized universal ways to arrange any substrate for lipase assays is one goal that will require still long time and work to be

achieved. Therefore, in this work we will present one methodology for the assessment of the effects of different variables on the activity of a lipase hydrolyzing the same substrate preparation at the same time. In this way is possible to obtain a maximum amount of information in a fairly and reliable way. This methodology is based on the initial characterization of the emulsified substrate followed by a turbidimetric registration of the changes during the reaction and a final ascertainment of the obtained results by air-water interfacial tensiometry. The sequence of steps followed during the implementation of this protocol is:

- i) The substrate is emulsified following the same procedure before every experiment. In our case, this was done by ultrasonic emulsification in which we had complete control of the different variables involved in the process.
- ii) The size distribution of the prepared emulsion is then obtained. In this work, we have used dynamic light scattering (DLS) for this characterization.
- iii) The changes in the turbidity of the emulsion are registered during the process of lipolysis.
- iv) The estimated size distributions along the process are obtained from the initial size distribution and the registered turbidity changes. After this point, some kinetic parameters are already available.
- v) The obtained kinetic parameters are qualitatively tested and complemented by the estimation of the final accumulation of reaction products, at the air-water interface, on the top of the reacting samples.

For fast reactions, the whole protocol may take less than forty minutes, with the extra advantage of the possibility of obtaining batch results using multi-well plates. Transparent bottom plates also allow the observation of precipitates when this information is considered as relevant.

We have employed this methodology to obtain information about the way in which the effects of different variables like the concentrations of lipase, substrate, BS or calcium ions interfere on the lipase activity.

In a final part of this work, we have studied the effect that the degree of saturation of semisolid-structured fat substrates (STAG) has on the kinetics of the reaction. These type of fats are very important in the present advances in food industry since they are especially designed to obtain similar textures and flavors to the ones obtained by hydrogenation of natural oils but avoiding the presence of the manifestly unhealthy *trans* FA residues [14]. In our work, we employ the proposed methodology to estimate how the type of BS and the concentration of lipase are affecting to the lipolysis on these substrates.

This work is therefore mainly dedicated to the presentation of a lipase assay protocol, based on the batch processing of simultaneous reactions with the same lipase on the same substrate, and to employ it to obtain relevant information about the way in which the effects of different variables interferes on the interfacial velocities of reaction. The final objective is to use this methodology for the characterization of the process of lipolysis on novel semisolid fat substrates with a low presence of *trans* FA.

2. Materials and Methods

2.1. Chemicals

Hepes buffer (0.02M, 0.1mM EDTA) with pH 7.4 was prepared every day using freshly deionized (0.054mS) water (Milli RO/Milli Q, Millipore Inc., Jaffrey, NH). NaCl (150mM) was lately added to the buffer preparation [15]. Sodium chloride was from J. T. Baker (Deventer, Holland). HEPES, EDTA, calcium chloride and triolein were from Sigma (St. Louis, MO).

The lipase employed in all the experiments is the mutant *W89mN33Q* (W117F, W221H, W260H, N33Q) of the fungal lipase *Thermomyces lanuginosa* (TLL) and was obtained from Novo Nordisk (Bagsværd, Denmark). The crystal structure of TLL was initially solved at 1.8Å resolution by Derewenda et al. [16]. Our mutant lacks the carbohydrate moiety present in TLL (S.A. Patkar, personal communication). It has a globular structure with dimensions of 3.5 x 4.5 x 5 nm and its isoelectric point is 4.4 [17]. It is constituted by 269 residues and it has a molecular weight of 55kDa. This lipase presents interfacial activation presenting an active site that contains a Ser(146)–Asp(201)–His(258) catalytic triad covered by a α -helical surface loop (amino acids 86–93) with a high mobility [18]. This lid presents a single tryptophan (Trp) at position 89 that is supposed to play a very important roll in the interfacial activation

of TLL [17, 19]. Its high specific activity rate [20] and the advantage of the absence of the carbohydrate moiety for future lid conformation experiments, made *W89mN33Q* a very appropriate lipase for the present study. The different inhibition of this lipase in presence of NaTC or NaTDC, observed in the preliminary experiments, was taken into account when selecting this lipase. The lipase purity was checked by SDS-PAGE, being higher than 90% (see Fig 1).

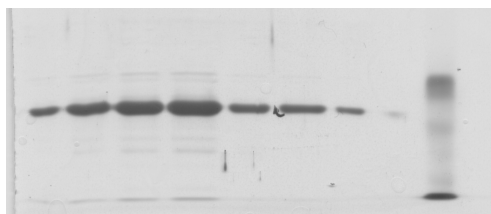


Figure 1. SDS-PAGE Test of the lipase W89mN33Q

The concentrations of *W89mN33Q* were estimated by UV spectrophotometry using a LS 50B (PerkinElmer Inc., Waltham, USA) spectrophotometer and a molar extinction coefficient $\epsilon = 18850\text{cm}^{-1}$ at a wavelength of 280nm.

The STAG were synthesized by a continuous enzymatic transesterification process of poly-unsaturated oils and fully hydrogenated fats. This process is described elsewhere [21]. In this work, they were proceeding from the transesterification of sesame oil (SE) and fully hydrogenated soybean oil (FHSBO) at different concentration ratios (80:20 and 70:30); and from the transesterification of olive oil (OO) and fully hydrogenated palm oil (FHPO) at 90:10, 80:20, 70:30, 50:50 and 30:70.

Sodium taurocholate (NaTC) and sodium taurodeoxycholate (NaTDC) bile salts were purchased from Sigma (St. Louis, MO). Their purity was above 95% and 97% respectively. These water-soluble molecules have a rigid 5 β ring structure and present amphiphilic character with a hydrophilic α -face and a hydrophobic β -face [22]. Due to their structure, they form micelles in a non-usual stepwise way [23]. The micellar sizes, R_h , may vary from 20 \AA^3 to 13x10 $^3\text{\AA}^3$ [24, 22] depending, for example, on the BS concentration or pH. Under most of the conditions of our experiments, NaTDC will be forming bigger micelles than NaTC [25]. The critical micelle concentration (CMC) of these BS was assessed with Delta-8 multichannel microtensiometer (Kibron Inc., Helsinki, Finland) at pH 7.4 and 22°C. Serial dilutions of BS (30mM) with a dilution factor of 0.6 were made in NaCl (150mM) water solution. CMC values of 8mM and 2mM were found for NaTC and NaTDC respectively. These results are similar to those ones presented by different authors [26, 27].

Fresh solutions were prepared before every experiment using the former buffer solution and different concentrations of BS and lipase. The experiments were performed at 23 °C and all the solutions were filtered with a 0.2 μm PFTE membrane. The glassware was cleaned by plentiful rinsing of pure water after one day immersed in sulphuric acid (96% purity). All the chemicals were stored according to the manufacturer instructions.

2.2. Emulsions preparation

Ultrasonic emulsification has experimented a very high increase in popularity in the last decade, especially in the industry but also in science [28, 29, 30]. The main reason is that ultrasonication offers larger interfacial area with smaller mean oil droplet diameter and narrower size distributions than those obtained by mechanical agitation [31]. In an ultrasonication process, mechanical vibrations are produced radiating acoustic energy into one fluid. The acoustic energy is transmitted in form of pressure waves, consisting in alternating expansion and compression cycles. These waves are dependent on the different properties of the media like vapor pressure, surface tension, viscosity or density. Vapor pressure and bulk surface tension are particularly important variables since they are proportional to the energy required for the formation of the cavitation bubbles, basic for the transmission of the ultrasonic waves. These waves may be very energetic causing the necessary shear at the oil-water interface for the oil droplets to cleave being dispersed into the water phase forming a fine emulsion. In spite of all the advantages of ultrasonic emulsification, this method has rarely been used in emulsions for the study of lipolysis of oils.

In the present work, the emulsions have been prepared using adaptive focused acoustic energy with an S-Series device (Covaris, Inc. Woburn, USA). With this instrument, the acoustic frequency can be established in frequency sweeping mode, where it sweeps through a range (500-1000 kHz), or in power tracking mode, where is automatically

optimized for a maximum power generation. The ultrasonic treatment can be modeled by setting three different variables: duty cycle, intensity and cycles per burst. Duty cycle controls the intensity of the ultrasonic power generated by setting the percentage of the treatment time that the transducer is “on”, creating acoustic waves. Intensity is amplitude of the pressure waves as a function of the voltage applied to the acoustic transducer (mV). Cycles per burst are the number of times that the transducer is switched on/off during each burst. A combination of up to four different treatments, of less than one minute, may be programmed sequentially with the Series SonoLab Single software. Pre-emulsification was achieved by sonication of 1.5 ml of the buffer system (20mM HEPES, 0.1mM EDTA and 150mM NaCl at pH 7.5) with 370mM triolein and 20mM of the correspondent BS. This mixture was submitted without previous shaking to 4 minutes of ultrasonic treatment at a temperature of 40°C. The software was adjusted to maximum levels of Duty Cycle, Intensity and Cycles/Burst in frequency sweeping mode. These settings led to an acoustic power on the sample varying from 100W to 130W. After this first sonication, the sample was diluted changing only the concentration of triolein to a final concentration of 16mM. This dilution was then submitted to a second sonication of one minute at the same temperature and software settings. The obtained pre-emulsion was prepared every day and kept in the dark at room temperature under continuous magnetic stirring in a nitrogen atmosphere [32]. It showed no particle size change along 12 h. Final emulsion was achieved by diluting the correspondent volume of the pre-emulsion in the same buffer system and different concentrations of CaCl₂ and BS depending on the experiment. The

droplet size distributions of these emulsions, diluted at concentrations varying from 10 to 100 times, were measured by DLS with a Zetasizer Nano ZS (Malvern Instruments Ltd., Worcestershire, U.K.). For all the prepared emulsions, as in similar polydisperse systems, the distribution of sizes could be effectively adjusted to a Schultz distribution [33]. This size distribution presented minimal variations from one sample to another before the reaction took place. In some experiments, the size distribution was certified (see Fig. 2) using an inverted microscope (Zeiss IM-35, Jena, Germany).

2.3. Following the reaction by turbidimetry

Turbidimetry is a physicochemical method for the registration of the activity of lipases based in the disappearance of substrate. In this process, the lipase hydrolyzes the TAG converting them in soluble products and causing the oil phase to fade. This produces a continuous decrease in the turbidity of the system that can be correlated with the kinetics of the reaction. It has been presented as a faster alternative, of similar sensitivity, to traditional titrimetric methods [2]. Turbidimetric methods have been widely used, for example, for the diagnosis of pancreatitis [34]. Their main advantages are their shorter assay times and the possibility of working with buffered systems. However, historically has presented certain limitations in accuracy and precision [8]. The disregarding of the effect of the droplet size distribution on the light scattering properties of the emulsion has been frequently one of the main reasons [35]. In this way, several methods

attempted erroneously to correlate in a linear way the amount of FA released with the turbidity of the emulsion [36]. Reference materials have been proposed as a solution to these problems [37]. The use of standardized emulsions has been established as the preferred method for the turbidimetric assessment of lipases. Some of these standards have been commercialized in form of lipase assay kits like the one of Boehringer Mannheim Diagnostics (BMD, Indianapolis) [38]. The conditions for the assay with these kits have been improved in several works [34, 11]. However, there are still appearing some works attempting to find a perfect certified reference material (CRM) for the assay of the catalytic activity of lipases [9]. The oil-water interfacial area of the emulsion seems to be a very important factor, difficult to control, affecting to the measured lipase activities [39].

In the present work, we are trying to obtain a maximum amount of information, from the same emulsified substrate, in a minimum time. This is done in order to skip the possible differences in the emulsion structure or composition that may appear during the emulsion preparation or storing and that would be manifested when comparing the results from different experiments. From the measured pre-reaction size distribution and the recorded variations of turbidity along the reaction time, we obtain information about the amount of products released per unit of oil-water interfacial area and per unit of time, at any time of the reaction. The main approximation that is made to obtain our kinetic parameters is to consider the interfacial velocity of reaction as independent of the curvature of the oil-water interface. This means that we assume that the rate of volume loss per unit of interfacial area is independent of the droplet size and therefore, for a

same value of the interfacial velocity of reaction, v_r , all the droplets radii will decrease a same value, r_i , despite their size. This approximation is getting stronger during the final part of the reaction, where the droplet sizes are much smaller, but otherwise it works fine (see Fig. 7). The estimated values of v_r will be therefore equivalent to the temporal variation of the radius of the emulsion droplets, dr/dt , at any time during the reaction.

2.4. Theoretical approach

The extinction of light crossing an emulsion sample will be the sum of the effects of the absorbance of each phase and of the scattering produced by the dispersed phase drops:

$$\sigma_{ext}(r, \lambda, m) = \sigma_{scat}(r, \lambda, m) + \sigma_{abs}(r, \lambda, m) \quad (1)$$

where r is the drop mean radius, λ the incident wave length, m the relative oil to water refractive index and $\sigma_{ext}(r, \lambda, m)$, $\sigma_{scat}(r, \lambda, m)$ and $\sigma_{abs}(r, \lambda, m)$ are the total extinction, scattering and absorbance cross sections respectively. When the light beam crosses the emulsion sample, the light intensity is attenuated following the Lambert's equation [40]:

$$I_{rel} = e^{-\tau(r, \lambda, m)x}; \quad \text{with } \tau = N\sigma_{ext}(r, \lambda, m) \quad (2)$$

being I_{rel} , the relative irradiance, i.e. the ratio between transmitted at a distance x , and incident irradiances, τ the turbidity and N the number density of particles. In the case of a polydisperse emulsion with a size

distribution $f(r)$, the turbidity will be given by the contribution of the different size particles [41] as:

$$\tau = N \int_0^{\infty} \sigma_{ext}(r, \lambda, m) f(r) dr \quad (3)$$

As we said previously, most of the size distribution measurements in our emulsions may be fitted to a Schultz distribution (Fig. 2) which is given by the following expression [42]:

$$f(r) = \frac{(t+1)^{(t+1)} \left(\frac{r}{\langle r \rangle} \right)^t e^{-\left(\frac{r}{\langle r \rangle} \right)^{t+1}}}{\langle r \rangle \Gamma(t+1)} \quad (4)$$

being t a measure of the width of the distribution and $\langle r \rangle$ the mean value of the first moment of the distribution of sizes.

Fitting the initial experimental size distribution to the Schultz distribution (Eq. 4) is a possible way to obtain the estimated turbidity of the emulsion after the calculation the correspondent value of $\sigma_{ext}(r, \lambda, m)$. In our case, this calculation has been done using the Mie theory [43], with an adaptation of the Mathematica (Wolfram Research Inc., Champaign, USA) notebook developed by A. Lompadó [44]. With this approach is possible, given the values of λ and m , to obtain the numerical dependence of the droplet cross sections with the dropped radius, for a defined range of droplet sizes. By integrating this dependence together with Equation 4 in Equation 3 is possible to obtain the estimated value of the emulsion turbidity, τ . The values of m in the original emulsion were difficult to obtain due to the unknown accumulation of BS at the oil water interface. This accumulation

could be estimated by electrophoretic mobility measurements [45] and contemplated in the Mie calculations using the notebook of Lompado [44]. However, in our case and due to the variations in the interfacial concentration of BS during the reaction, they were obtained just by adjusting its value to the correspondent turbidity measured with the initial size distribution. This value of m will fluctuate along the reaction time due to the continuous accumulation and intermittent release of products at the interface [46].

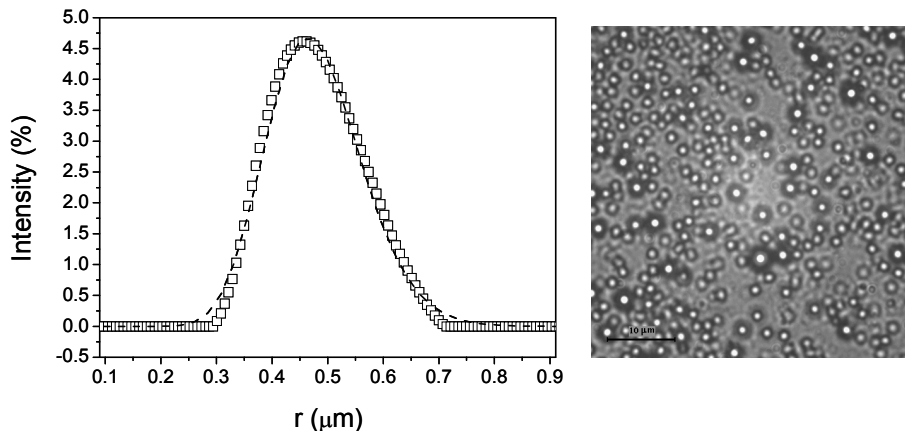


Figure 2. (left) Size distribution (squares) for a triolein (1.6mM) in buffer emulsion stabilized with NaTC (20mM) and CaCl_2 (2mM) fitted to a Schultz's distribution (dash line) with $\langle r \rangle = 0.48\mu\text{m}$ and $t = 30$ where reduced $\chi^2 = 0.011$ and $R^2 = 0.994$. (right) Microscopic view (x63) of the former emulsion.

These fluctuations will occur constantly until the substrate is completely consumed and they will be considered as a systematic error that introduce noise in the results but will not interfere in the practical tendencies observed.

If we consider v_r as independent of the interfacial curvature, we can derive that at any point of the reaction, the temporal decrease of the droplets

radii may be considered as equivalent to the value of v_r . This means that the size distribution will be displaced a distance r_i towards smaller droplet radii keeping its original shape and variance until the complete disappearance of the oil phase. Similar behavior in the size distribution has been observed by another authors for the initial moments of the reaction [47, 48]. As we can see in Figure 7, as soon as we are not at the final stage of the reaction, this assumption is possible according to the measured behavior of the size distributions during some experiments.

The initial number density of drops, N_0 , can be calculated using the initial concentration of oil:

$$N_0 = \frac{[Oil]}{\frac{4}{3}\pi \int_0^{\infty} r^3 f(r) dr} \quad (5)$$

For displacements, r_i , smaller than the minimum sizes of the original distribution, N may be considered as constant equal to N_0 (see Fig. 3). For higher values of r_i , the approximation to estimate $N(r_i)$ could be done by considering the change in N_0 proportional to the change in the volume of the distribution as:

$$N(r_i) = N_0 \frac{\int_0^{\infty} g(r - r_i) dr}{\int_0^{\infty} g(r) dr} \quad (6)$$

where $g(r)$ is the non-normalized initial size distribution. This approximation however will not be used in the results presented in this work. The data collected at values of r_i higher than the minimum sizes of the initial distribution will be disregarded due to the unknown error implicit in the approximations made.

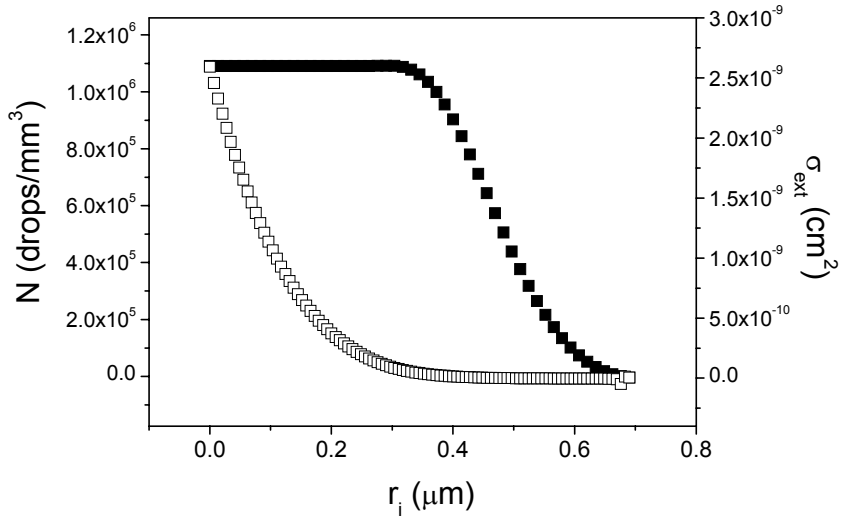


Figure 3. Dependency of the number density of drops (black squares) and the extinction cross section (empty squares) with the decrease the drop radius for the emulsion of Figure 2.

By calculating $\sigma_{\text{ext}}(r-r_i, \lambda, m)$, using the Mie theory, and integrating it (Eq. 3) together with the correspondent displaced size distribution, $f(r-r_i)$ (Eq. 4), is possible to obtain the estimated turbidity of the emulsion, τ , for every decrease in the droplets radii, r_i (see Fig. 4). In our case, this dependence of τ with r_i is calculated using the adapted notebook commented before. To avoid long computer processing times the dependence $\sigma_{\text{ext}}(r-r_i, \lambda, m)$ was interpolated from 400 values obtained numerically before the integration of the Equation 3.

Therefore, in principle, by having access to the original size distribution, and to the values of m and λ , we are able to correlate the measured temporal changes in the emulsion turbidity with the variations in the particles size, and therefore, with the estimated decrease in the droplets radii, r_i (see Fig 5).

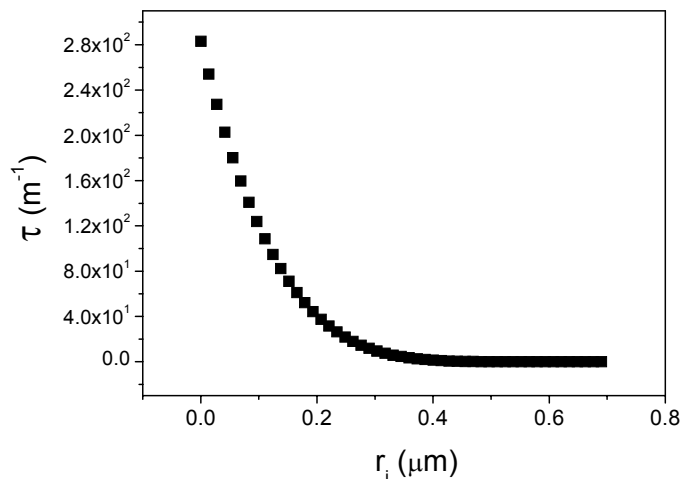


Figure 4. Dependency of turbidity with the decrease the drop radius for the emulsion in Figure 2.

The temporal dependence of the values of $r_i(t)$ is automatically obtained by interpolating the measured values of $\tau(t)$ using the relations between τ and r_i (see Fig. 4) obtained for each experiment.

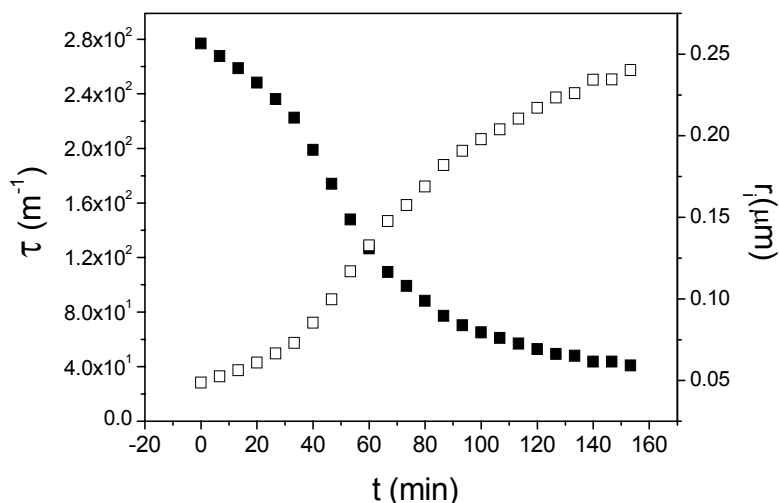


Figure 5. Measured temporal dependency of the turbidity of the emulsion in Figure 2 (black squares), and its correspondent estimated decrease in droplet radius (empty squares), during process of lipolysis with W89mN33Q (200nM).

As mentioned before, the slopes (dr_i/dt), at any moment of the reaction, will correspond with the value of the estimated interfacial velocity of reaction, v_r (See Fig. 6).

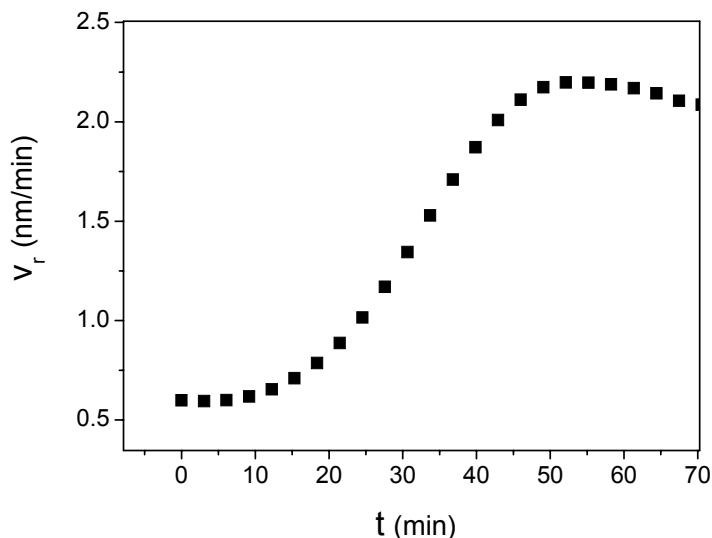


Figure 6. Estimated temporal rates of radius decrease along the process of lipolysis of the emulsion in Figure 2 with *W89mN33Q* (200nM).

In some cases, may appear some decrease in the values of v_r after the maximum. The possible accumulation of sediments from reaction products at the bottom of the cuvette may cause a fake decrease in interfacial velocity of reaction measured. This has been proved by well exchanging after reaction and by optical microscopic inspection (not shown). In some cases, these sediments are the responsible for the lack of zero turbidity records at the end of the experiments (see Fig. 5). As mentioned before, this part of the data will be neglected in our analysis. To assess the reliability of the obtained results, in some experiments, the correlation between the turbidity and the displacement of the size distribution has been confirmed by stopping

the experiment at different stages of the reaction and collecting samples for size distribution analysis using DLS. These results show a reasonable agreement between the expected size distribution estimated by turbidimetry and the measured one (see Fig 7).

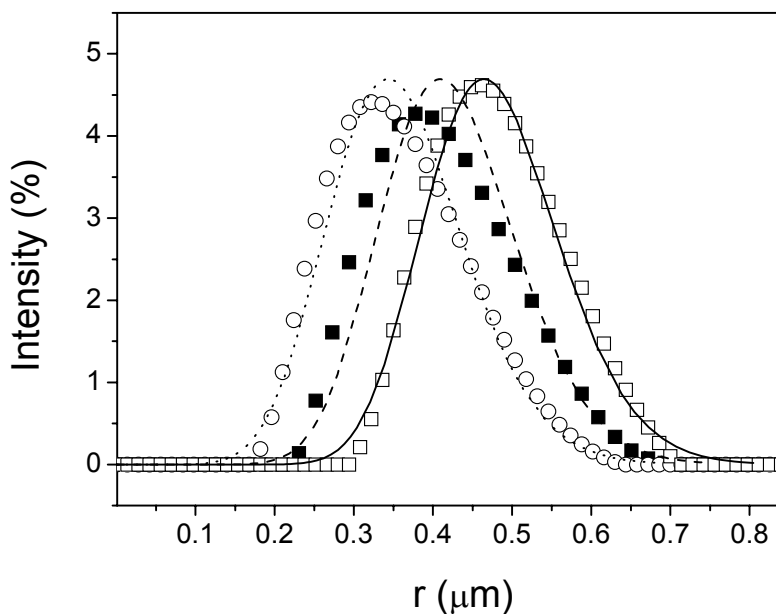


Figure 7. Measured and estimated by turbidimetry size distributions (symbols/lines) for a triolein (1.6mM) in buffer with CaCl_2 (20mM) emulsion stabilized with NaTC (20mM) at different points of the process of lipolysis with W89mN33Q (200nM). (empty squares/straight) Beginning of the reaction with an initial turbidity of 284 m^{-1} ($r_i \approx 0 \mu\text{m}$); (black squares/dash) after forty-five minutes with turbidity of 179 m^{-1} ($r_i \approx 0.055 \mu\text{m}$); (empty circles/dots) after seventy-five minutes with a turbidity of 98 m^{-1} ($r_i \approx 0.121 \mu\text{m}$). The Kolmogorov-Smirnov test for comparison between the measured and expected size distributions gave the following maximum difference between the cumulative distributions, D, and corresponding P values: for $t = 0 \text{ min}$, $D = 0.2040$ and $P = 0.0000$; for $t = 45 \text{ min}$, $D = 0.1443$ and $P = 0.0027$; for $t = 75 \text{ min}$, $D = 0.1692$ and $P = 0.005$.

In the present work, all the turbidity measurements were performed with a 96-well SPECTRAFluor Plus (Tecan AG, Hombrechtikon, Switzerland)

fluorescence plate reader with an extinction filter of 520 nm. The background measured for buffer cells serving as controls, was subtracted from the values recorded for the cells where the reaction was taking place. The samples height was 7 mm so the turbidity values were directly derived from the extinction values dividing them by this height. The concentrations of the compounds were changed by diluting along the rows and columns on transparent flat bottom 96-well plates (Greiner Bio-One, Duesseldorf, Germany). Each variable were diluted separately in different plates and then mixed together just before the experiment started. The experiments were done by measuring the average light intensity after three sequential flashes on each well. This value was stored every five minutes with four minutes of continuous linear shaking of high intensity between every record. The data was collected during four hours keeping the temperature constant at 37°C along the whole process [48].

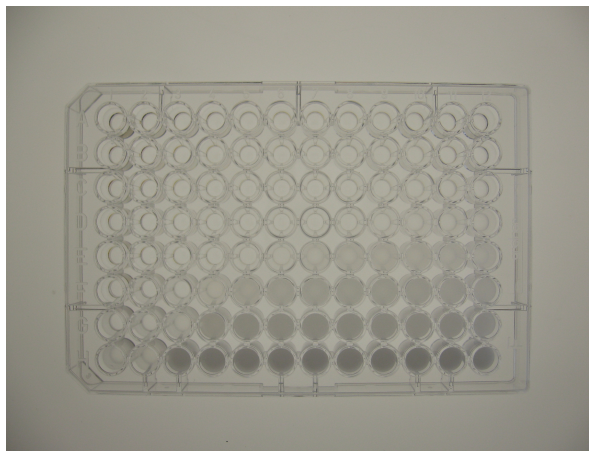


Figure 8. 96-well plate after 4 hours of reaction with concentrations of lipase and oil phase decreasing, by a similar diluting factor, in the horizontal and vertical directions respectively. The top row and right column are test wells with no oil phase and no lipase.

At the end of the reaction is also possible to observe at naked eye the degree of consumption of the substrate (see Fig 8). It must be clear that we do not consider this protocol as a specific assay for the absolute lipase activity quantification. However, from our point of view, this whole protocol appears as a very suitable method for the efficient and comparable study of the combined effect of different variables on the activity of lipases. With this protocol is possible to avoid typical problems appearing when comparing results that usually are due to differences in the substrate organization. As an example of application of the procedure followed, we will consider the study the effect of the lipase concentration on the lipolysis of a triolein in buffer emulsion stabilized with NaTC. First, the emulsion is prepared and let to equilibrate at the temperature at which the reaction will take place (37°C in this case). Then, the size distribution is measured and the plate wells are filled. At this point, is important to mention that the plate wells should not be filled to a higher volume than $\frac{3}{4}$ of their capacity since the shaking in between the intensity readings may mix the wells samples. Straight away, the lipase is added and the plate is placed on the plate reader to begin the reaction registration without losing the very important initial variations in the emulsion turbidity. Once the reaction time has finished the obtained results of “absorbance” are converted into turbidity. The samples height can easily be obtained from the reacting volume and wells diameter. The registered kinetics of turbidity variations from the present case are shown in Figure 9. These data, with the temporal variation of the turbidity

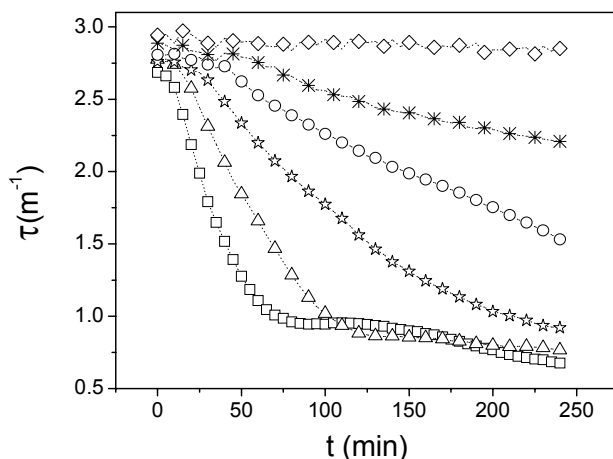


Figure 9. Measured temporal dependency of the turbidity of a triolein (3.2mM) in buffer emulsion stabilized with NaTC (20mM) during the lipolysis with the following W89mN33Q lipase concentrations where: 200nM (squares), 80nM (triangles), 30nM (stars), 10nM (circles), 6nM (asterisks) and 2nM (diamonds).

of the samples, are then introduced, together with the initial size distribution information, in the Mathematica notebook commented before to obtain the correspondent estimated temporal decrease of the droplet radii, r_i , (Fig 10).

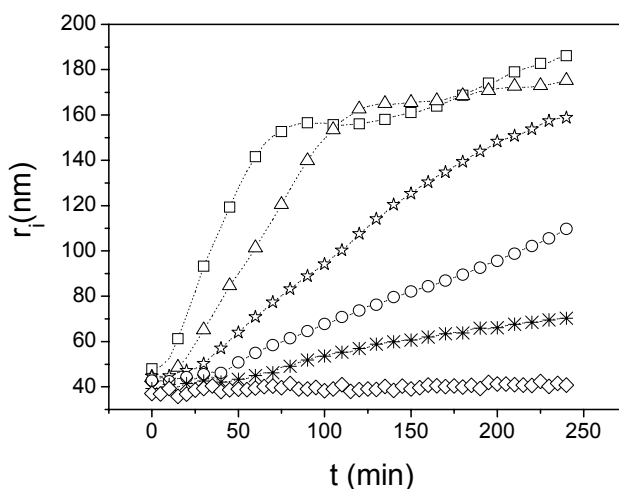


Figure 10. Estimated temporal decrease of the emulsion droplet radii during the process of lipolysis of the emulsion of Figure 9.

By obtaining the slopes of the curves in Figure 10 is possible already to observe how fast the emulsion drops are considered to decrease along the reaction time (see Fig.11).

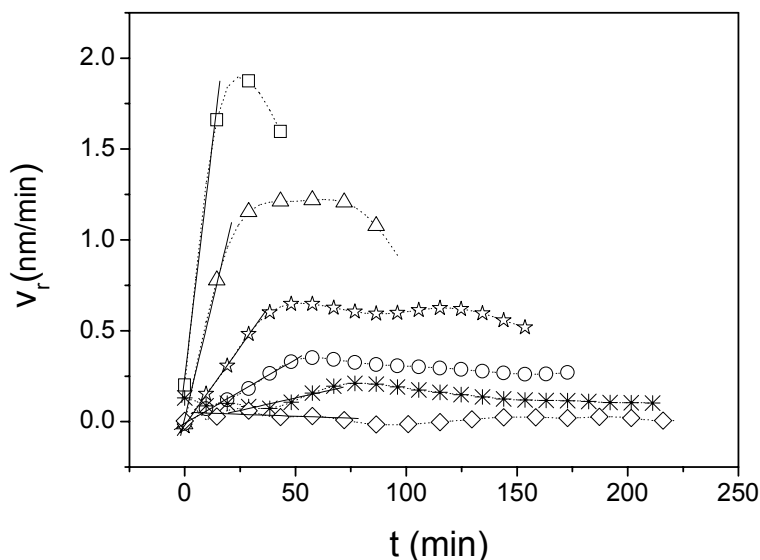


Figure 11. Temporal variations of the rates of the droplet radii change (velocity of reaction) during the process of lipolysis of the emulsion of Figure 9.

This information is already correspondent with the interfacial velocity of reaction, v_r . From the temporal changes in the interfacial velocity of reaction, we can get important information about the kinetics of lipolysis. We obtain two parameters from these changes: the maximum velocity of interfacial reaction, V_r^{Max} , and the initial acceleration of interfacial reaction, $(dv_r/dt)_{\text{ini}}$. The first one, V_r^{Max} , is the maximum value of v_r that will be reached at the beginning of the reaction. It offers important information about how different variables affects to the activity of the lipase.

In the present example, we can observe how, as expected, this velocity is increasing considerably with the concentration of lipase (see Fig.12).

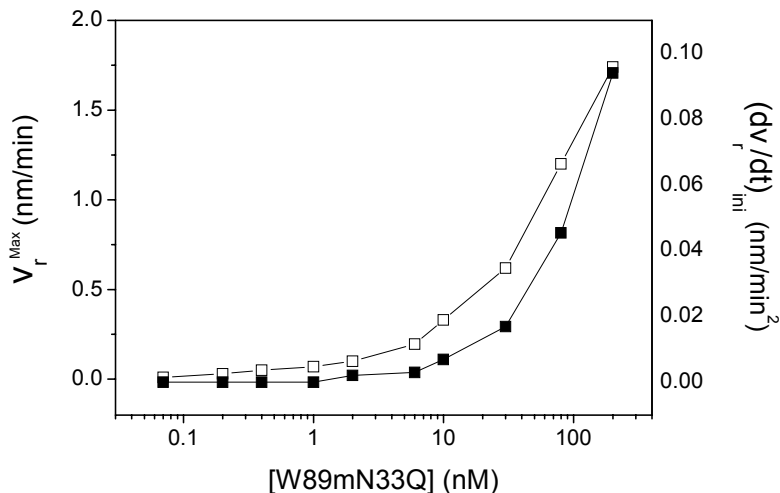


Figure 12. Maximum velocities of reaction (empty squares) and initial accelerations of interfacial reaction (black squares) depending on the lipase concentration for the process of lipolysis of Figure 9.

It is important not to confuse this directly measurable parameter with the traditional maximum rate of product formation, V_{max} , in the Michaelis-Menten kinetics or in its correspondent adaptations for lipases [49]. In our case, V_r^{Max} , is a measurable and straight estimation of the amount of reactions taking place per unit of area and per unit of time at the oil water interface. It can be related with the catalytic rate constant if we consider conditions of pseudo-equilibrium in the rates of lipase adsorption and association with the substrate. The other parameter, $(dv_r/dt)_{\text{ini}}$, offers more information about the events taking place at this initial period of the reaction, were the lipolytic products are beginning to appear in the system. This parameter can be related to the apparition of lag periods of possible activation of the lipase.

2.5. Lag phase

Lag periods before the complete activation of the lipase have been observed in different works. Initially, they were found to be dependent on the interfacial pressure and independent on the concentration of lipase. These periods are supposed to be due to the rate limiting effect of the interfacial pressure on the interfacial adsorption of the lipase [50]. Different lag periods have been reported showing certain dependence on different factors like the lipase concentration, Ca^{2+} presence, pH or even on the type of FA produced [51]. All the last factors have in common their influence in the interfacial presence of reaction products. Some studies have also considered as a lag periods the time that the reaction products remain at the interface before getting desorbed [52]. The interfacial accumulation of reaction products is considered in many cases to have an activating character on the lipase activity [51, 53]. This interfacial appearance of FA produced during the initial moments of the reaction, are supposed to change the properties of the interface making it more accessible to the lipase or to the lipase cofactor [54]. Another authors have proposed the possibility of an activation of the lipase by forming complexes with the amphiphilic compounds on the bulk [55, 56]. The structure of ternary complexes with porcine pancreatic lipase, colipase and BS micelles was obtained using neutron crystallography by Hermoso et al. [57]. These complexes are supposed to be very dependent on the type of BS and the calcium concentration [32]. Unusual forms of lipase activation produced by the

interfacial association of molecules have also been reported in several works [58, 59]. In our case, we propose that the active forms of the lipase may be present at the interface forming oligomers and forming active complexes in the bulk. Therefore, most of the lag times reported in this work will be considered as dependent biophysical lag times, referring to the rate of formation of this lipase activating aggregates. These lag periods will be evaluated in terms of $(dv_r/dt)_{ini}$ due to the configuration of the experiments. This is done in order to ensure that errors produced by a possible later precipitation of reaction products are not affecting to the results. As we can see in our example, the activation of the lipase is getting faster as the lipase concentration increases (see Fig.12).

2.6. Air-water interfacial accumulation of reaction products

The final accumulation of reaction products at the oil water interface on the top of the reacting wells can offer information about the degree of reaction that have been taking place under the different experimental conditions. It can be considered as an indicator of the amount of products released during the reaction. During the lipolysis of TAG some of the reaction products are dispersed in form of mixed micelles together with BS, some of them precipitate, forming crystals for example, and some of the remain dispersed in monomeric form in the bulk [45]. These products are mainly MAG, DAG and FA. The amount of solubilized FA is usually

employed by titrimetric methods to assess the lipase activity during the reaction. Due to their amphiphilic character, they are adsorbed at different interfaces. Big part of these products is forming micelles or re-adsorbed into the very extensive oil-water interface but some of them are adsorbed into the air-water interface. The final amount of reaction products at this air-water interface will depend on their composition and bulk concentrations. It is difficult to assess the real composition of this final air-water interfacial layer. Labeling techniques or compression isotherms at different ratios of BS-lipase-lipolytic products could be used to gain quantitative information [60, 61]. However, in this work, and due to the different concentrations of BS and types of substrates employed, only qualitative information will be obtained from these experiments.

The final air-water interfacial concentration of amphiphilic reaction products was associated with the interfacial pressure measurements made using the Delta-8 multichannel microtensiometer at room temperature. The same plate was passed straight away, after the reaction time, from the SPECTRAFluor plate reader to Delta-8.

2.7. Fibrillar formations

After the turbidity measurements and the subsequent observation of the final air water interfacial pressures, optical microscopic inspection of the bottom of the plate wells was performed in order to observe under which conditions the precipitation of aggregates was higher and what kind of

sediments were forming. Different type of precipitates could be found in some experiments, mainly spherical little clusters. However, under certain conditions, and always depending on the concentration of lipase, fibrillar structures were found at the bottom of the wells. Similar formations have also been observed when they were appearing at the oil-water interface during experiments of lipolysis in the pendant drop tensiometer [62]. Their shape and their formation at high concentrations of protein in the bulk made us to consider their possible amyloid character. This supposition was done since the formation amyloids can be stimulated by lipid-protein interactions [63] and they have been found with similar lipases [64]. Some of the found fibrillar formations presented certain similarity with the ones encountered in certain clinical cases [65]. Under certain conditions, the found fibrillar formations showed certain level of staining with Congo red and presented birefringence under cross-polarized illumination. These observations were performed using an Olympus IX-70 inverted microscope (Olympus America, Inc. Center Valley, USA) equipped with bright-field and differential interference contrast (DIC) optics.

3. Results and Discussion

3.1. Effect of the oil and lipase concentrations on the kinetics of lipolysis

In the first part of this work, we have considered the effect of different oil and lipase concentrations on the kinetics of lipolysis with *W89mN33Q* in emulsions with our buffer system, 20mM CaCl₂ and 20mM of each BS, NaTC and NaTDC, depending on the experiment. As mentioned before, the different concentrations in the reacting wells are obtained by a certain diluting factor. The size distribution of the emulsion was not affected after by this dilution (not shown). An estimation of the values of the classical constants of enzymatic kinetics, V_{\max} and K_M [49], could be done from the variation of the values of V_r^{Max} with the concentration of oil. However, due to the different set of experiments planned, we are not going to perform this analysis in the present work.

3.1.1. Reaction with NaTC

The results for the maximum velocity of reaction, in the case of NaTC (20mM), are shown in Figure 13. By observing the dependence of V_r^{Max} with the concentration of lipase we can see that, as expected, the

reaction increases its velocity with the concentration of lipase. For lipase concentrations below 1nm, it was not possible to measure any reaction. This means the interfacial presence of the lipase was not big enough as to produce visible decrease on the droplets radii. Surprisingly, V_r^{Max} is also increasing with the decrease in the bulk concentration of the oil phase. In principle, with V_r^{Max} , we are considering the lipase activity per unit of interfacial area, and the interfacial concentration of substrate could be considered as constant. Therefore, the value of V_r^{Max} should not be dependent on the bulk concentration of substrate. However, in emulsions the interfacial concentration of lipase is conditioned by the amount of interfacial area available. The dynamic behavior of the emulsion droplets excludes significantly the kinetics of reaction from the more static models. The more extensive oil-water interfacial area will result in a lower the interfacial concentration of the lipase. This is particularly clear in this case, where lack of interfacial concentration of lipase is observed at high concentrations of triolein with an interfacial area too extensive for a visible reaction. In our case, over triolein (270 μ M) the reaction gets clearly slower even for the higher concentrations of lipase (see Figure 13) and, for lower concentrations of triolein, an increase in V_r^{Max} appears with the decrease of substrate concentration. Interestingly, at concentrations of triolein below 20 μ M there is a decrease of V_r^{Max} with this decrease of the oil concentration. This decrease is more intensive for the higher concentrations of lipase. From our point of view, this decrease could be a consequence of a smaller access to the interface of the lipolytic complexes commented before [24]. The reason could be that the smaller amount of droplets would cause a loose in the

depletive enhancement of complex-interface contacts produced for higher amounts of substrate. However, this is just one hypothesis and more information is needed to give it some solidity.

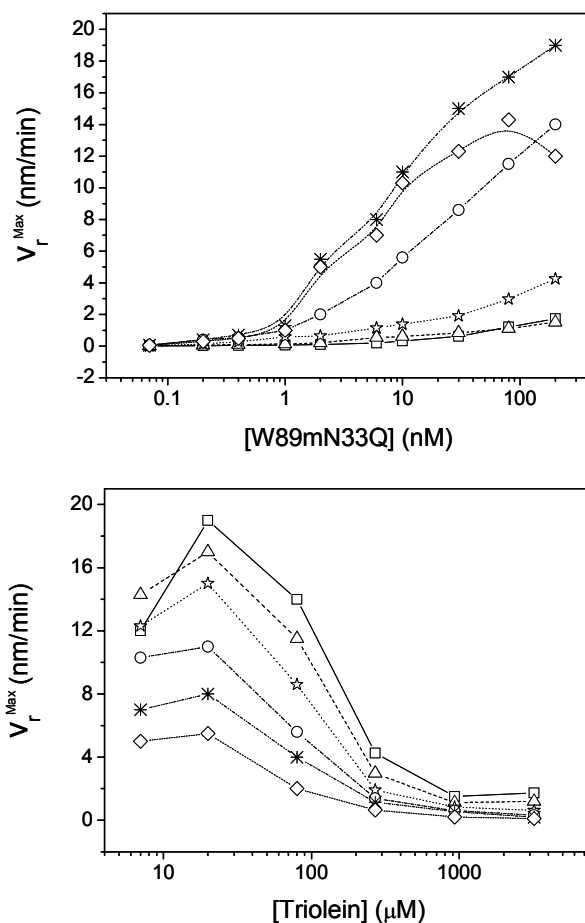


Figure 13. Maximum velocity of reaction for emulsions with $CaCl_2$ (20mM), stabilized with NaTC (20mM), depending on the lipase concentration (top) for the following concentrations of triolein: 3.2mM (squares), 930μM (triangles), 270μM (stars), 80μM (circles), 20μM (asterisks) and 7μM (diamonds); and depending on the triolein concentration (bottom) for the following concentrations of $W89mN33Q$: 200nM (squares), 80nM (triangles), 30nM (stars), 10nM (circles), 6nM (asterisks) and 2nM (diamonds).

In order to obtain more information about these processes taking place in this initial part of the reaction we must consider the initial accelerations of interfacial reaction, $(dv_r/dt)_{ini}$. The values of $(dv_r/dt)_{ini}$ for this experiment are shown in Figure 14.

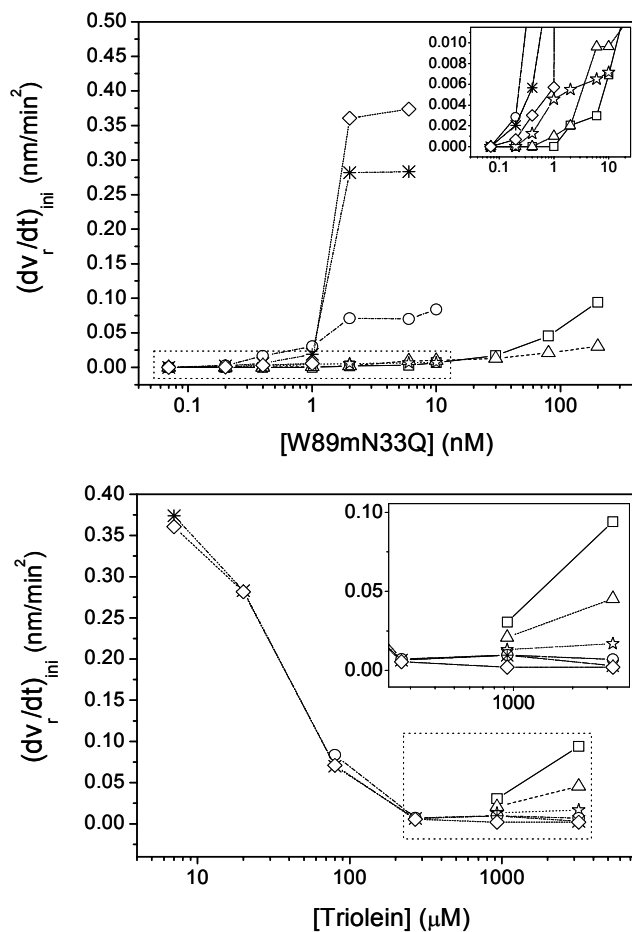


Figure 14. Initial accelerations of interfacial reaction, for the emulsions in Figure 13, depending on the lipase concentration (top) for the following concentrations of triolein: 3.2mM (squares), 930 μM (triangles), 270 μM (stars), 80 μM (circles), 20 μM (asterisks) and 7 μM (diamonds); and depending on the triolein concentration (bottom) for the following concentrations of W80mN33Q : 200nM (squares), 80nM (triangles), 30nM (stars), 10nM (circles), 6nM (asterisks) and 2nM (diamonds).

These results show the same lack of measurable lipase activity that we saw before for the concentrations of lipase below 1nM. Over this concentration, we can see two different behaviors depending on the concentration of oil (see Fig.14 bottom). At concentrations of triolein below 270 μ M, the values of $(dv_r/dt)_{ini}$ decrease clearly with the concentration of oil. This means that the maximum interfacial velocity of reaction is reached in a slower way when the number of droplets is bigger. From our point of view, this can be considered as an effect of the interfacial activation of the lipase by oligomerization [58]. The higher amount of drops will result in a lower interfacial concentration of lipase and therefore in a more sporadic contact between the lipase molecules at the interface, reaching the maximum velocity of reaction in a slower way. For these lower concentrations of triolein, the acceleration of the reaction increases with the concentration of lipase until reach one pseudo-plateau with a steady value of $(dv_r/dt)_{ini}$ (see Fig.14, top). The concentration of lipase corresponding to the appearance of this plateau seems to increase with the concentration of substrate. Over certain concentration of lipase, it is not possible to observe any acceleration at the initial interfacial velocity of reaction since the value V_r^{Max} was reached almost immediately. This behavior can be explained if we consider that, the increment of the bulk concentration of lipase increases its interfacial concentration and, therefore, the formation of the former lipolytic oligomers can occur in a faster way. After certain concentration of lipase, the velocity of interfacial formation of oligomers is not controlled by the interfacial concentration of lipase, i.e. by the frequency of interfacial contacts between the lipase molecules, but by the velocity of

oligomerization itself. At this point, the increment of the interfacial velocity of reaction is not increasing anymore, when increasing the concentration of lipase (see Fig. 14, top). The cut in this plateau may be interpreted as an effect of the faster formation of lipolytic complexes in the bulk, due to the higher presence of lipase, which would accelerate again the reaction until non-measurable values of $(dv_r/dt)_{ini}$. The singularity observed with V_r^{Max} , for the lowest concentration of oil, is not appreciable in the initial acceleration of the reaction. This is reasonable according to our hypothesis since in this case, the interfacial oligomers are formed in a faster way due to the higher concentration of lipase, even when the final number of interactions between the lipolytic complexes and the oil-water interface will not be as high as for slightly higher concentrations of substrate. A different behavior is found at concentrations of triolein over $270\mu\text{M}$, where there is no plateau appearing since the very extensive interfacial area is making the interfacial contacts between the lipase molecules to occur very slowly. Only a little increase in the values of $(dv_r/dt)_{ini}$ can be observed at concentrations of lipase over 30nM due to a slightly faster interaction of the lipase molecules at the interface. At these high concentrations of oil, the former tendency of decrease of $(dv_r/dt)_{ini}$ with the increment of the oil concentration is inverted. Now, $(dv_r/dt)_{ini}$ is increasing leading to the low V_r^{Max} observed for these concentrations. The main reason for this behavior seems to be that the depletion of the BS micelles produced by a higher number of drops would accelerate the formation of the lipolytic complexes in the bulk. In this way, the smaller values of V_r^{Max} would be reached in a faster way when increasing the concentrations of lipase or substrate (see Fig. 14, top). The

degree of reaction under the different former conditions was evaluated by measuring final interfacial pressures produced by the accumulation of reaction products at the air-water interface, on the top of the plate wells (See Figure 15).

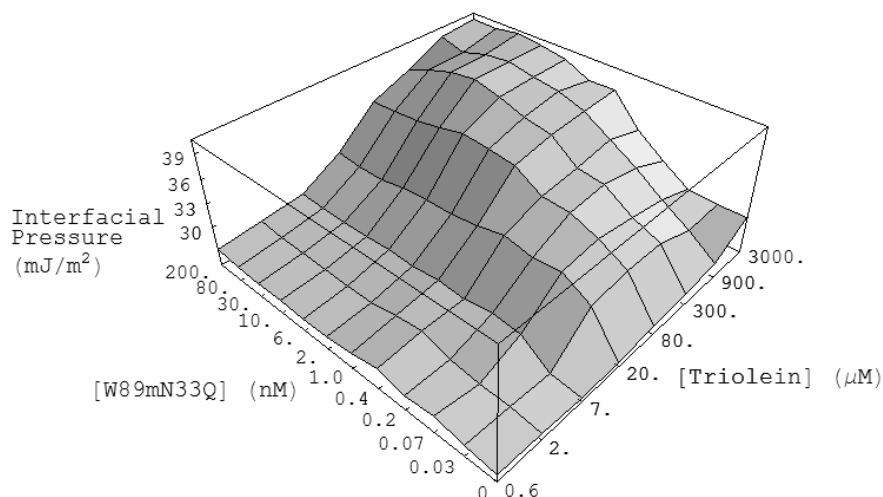


Figure 15. Final air-water interfacial pressure, after four hours of reaction in the emulsions of Figure 13, depending on the oil and lipase concentrations.

In these results, we can see as expected, that the amount of products released after the reaction is much higher for the emulsions with the higher concentration of lipase and triolein. For these higher concentrations of triolein, we found smaller values of V_r^{Max} , however, the more extensive interfacial area where the reaction was taking place gave rise to a much higher amount of reaction products released. This also shows that, even for the very low velocities of reaction, obtained for the concentrations of lipase below 1nM, still there is a significant amount of reaction products released after four hours of reaction, without producing big changes in the droplets size when the interfacial reacting area is big enough.

3.1.2. Reaction with NaTDC

In order to compare the effect of the type of BS on the kinetics of reaction we have performed a similar experiment using NaTDC. In preliminary probes, we have observed that this BS produces some degree of inhibition of our lipase. The results for the maximum velocity of reaction, in the case of NaTDC (20mM), are shown in Figure 16. A clear inhibitory effect of the BS can be observed for concentrations of lipase below 80nM. However, over this concentration it is possible to register lipase activity. At 200nM, the values of V_r^{Max} increases drastically depending on the concentration of the oil phase. For the higher concentrations of oil, these values are slightly higher than the ones found in the same conditions with NaTC. An increment of V_r^{Max} with the decrease of the concentration of oil can be observed at this high concentration of lipase. From our point of view, this situation is very likely produced by the formation of inactive complexes between the lipase and the BS micelles. Their inhibitory character has been proved using fluorescence quenching techniques by other authors [66]. This kind of complexes has shown to be more easily formed than the ones with NaTC [24]. Therefore, when these complexes are forming, a big part of the lipase molecules are in their structure and only smaller part will be competing to penetrate the BS populated interface. The big enhancement that the lipolytic activity is experimenting at high concentrations of lipase may be produced by a rate limiting effect of the concentration of BS micelles on the formation of these inactive complexes. Therefore, when we

increase the bulk concentration of lipase over certain limit, is not possible to form more complexes and the interfacial adsorption of lipase increases leading to the formation of the interfacial oligomers commented before.

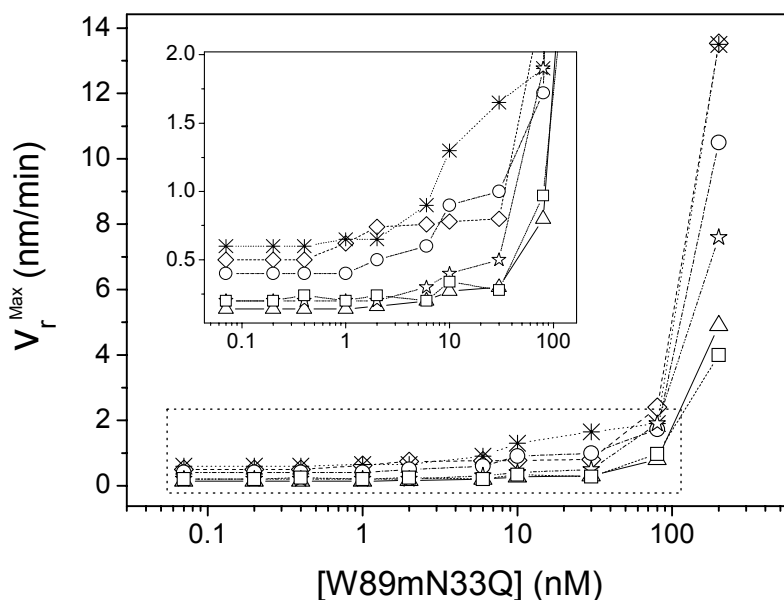


Figure 16. Maximum velocity of reaction for emulsions with CaCl_2 (20mM), stabilized with NaTDC (20mM), depending on the lipase concentration for the following concentrations of triolein: 3.2mM (squares), 930µM (triangles), 270µM (stars), 80µM (circles), 20µM (asterisks) and 7µM (diamonds).

This can also explain the increment of V_r^{Max} with the decrease of the concentration of substrate at these high concentrations of lipase. With the smaller amount of emulsion droplets, the interfacial concentration of lipase will increase, enhancing the interfacial velocity of reaction. Up to this point, is important to notice that the type of complexes appearing with each BS have different structures and they do not form necessarily at the same concentrations of lipase and BS. The fact that for certain high concentrations

of lipase and BS the interfacial velocity of reaction is higher for emulsions with NaTDC than for the ones with NaTC suggests that, even when they are not forming active complexes, their higher amount may produce some displacement or even desorption of some parts of the BS interfacial layer allowing the penetration of the lipase molecules. In order to obtain some information about this whole lipase activating process lets consider now the information about the initial acceleration of interfacial reaction (see Figure 17).

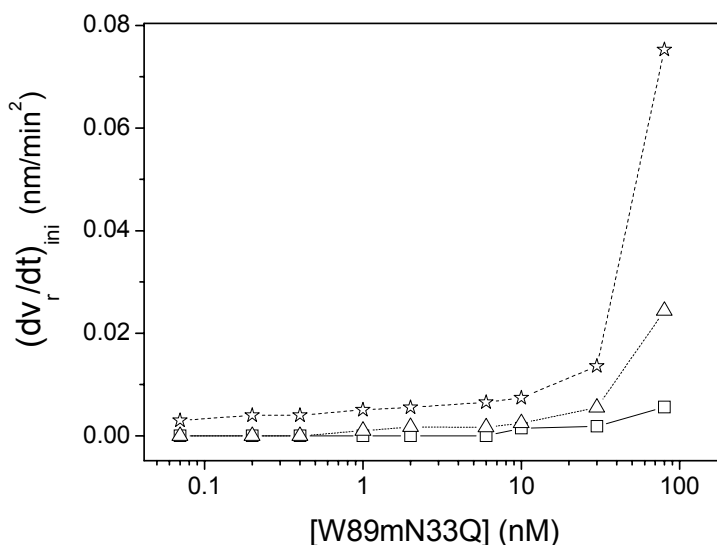


Figure 17. Initial accelerations of interfacial reaction, for the emulsions in Figure 16, depending on the lipase concentration for the following concentrations of triolein: 3.2mM (squares), 930 μ M (triangles) and 270 μ M (stars).

In this case, the initial acceleration of reaction was too fast to be measurable for the case of the smaller concentrations of triolein. For the higher concentrations of substrate, (dv_r/dt)_{ini} is increasing with the lipase concentration, especially for the higher values. This fact supports the

hypothesis that the formation of the inactive complexes may be displacing or desorbing some parts of the layer of BS molecules allowing the interfacial presence of the lipase. In this case, the acceleration of interfacial reaction would be correspondent with the activation of the lipase at the interface by oligomerization. After the displacement of the BS, the interfacial interactions between the lipase molecules may be favored by the interfacial pressure produced by the remaining molecules of BS. For the lower concentrations of substrate, this would occur in a faster way due to higher interfacial presence of lipase and the acceleration of reaction is not registrable. This hypothesis may explain also the fact that the velocities of reaction observed were higher for NaTDC than for NaTC, under similar high concentrations of lipase and substrate. For the high concentrations of substrate, these measurable values of the acceleration are much smaller than in the case of NaTC due to the slower formation of active oligomers. The information about the total degree of reaction is again estimated by observing the final interfacial accumulation of reaction products at the air-water interface on the top of the wells (see Figure 18). Due to the lack of lipolytic activity, there are similar final air-water interfacial pressures, despite the concentration of lipase. Only in the case with a maximum concentration of lipase is possible to observe some differences and perform some analysis. The maximum global release of reaction products occurs at the maximal concentration of lipase and oil. This maximum interfacial pressure at the maximum concentration of substrate is not coinciding with a maximum value of V_r^{Max} but the very extensive interfacial area guarantees a maximum formation of reaction products, as we saw before (Fig. 18).

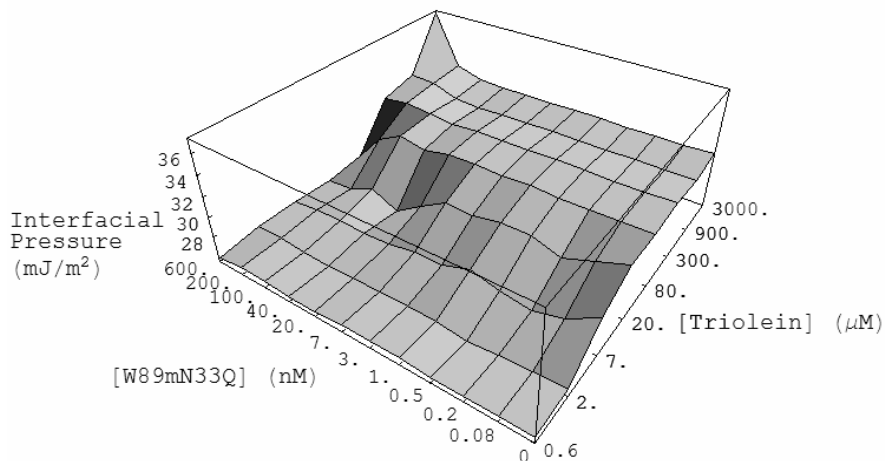


Figure 18. Final air-water interfacial pressure, after four hours of reaction in the emulsions of Figure 16, depending on the oil and lipase concentrations.

For the substrate concentrations of 80 μM and this maximum concentration of lipase, the interfacial pressure is smaller than for lower concentrations of lipase. This can be consistent with the presence of a maximum part of the BS micelles forming complexes.

Some fibrillar aggregates were found forming sediments after the reaction for the conditions of the maximum velocities of reaction. We consider that they may be produced by the interfacial association of different oligomers leading to fibrillar structures that precipitate after the reaction. The conditions of their formation will be considered in a later point of this work.

3.2. Effect of the NaTC and CaCl₂ concentrations on the kinetics of lipolysis

The effect of the CaCl₂⁺ ionic presence and the type of BS are considered two primary factors on the lag periods of activation of the lipases. Wickham et al. state “*No literature is available concerning the variation in binding strength of the lipase/bile salt complex but it would be expected to be affected both by bile salt structure and calcium ion concentration*” [32]. In this part of the work, we have consider the effect of different concentrations of NaTC and CaCl₂ on the reaction of lipolysis with *W89mN33Q* (30nM) in emulsions with triolein (100μM). This means that we are in a region with an intermediate lipolytic activity, as we saw before.

The results for the maximum velocity of reaction are shown in Figure 19. As we can see in these results, there is a clear dominating effect of the concentration of BS in the kinetics of lipolysis. At concentrations of NaTC below 4mM, there is almost no lipase activity. This is probably due to an interfacial presence of BS molecules that is not enough for the formation of micelles, and therefore for the formation of active complexes. This would obstruct the interfacial penetration of these low concentrations of lipase. Interfacial associations between the lipase and the BS molecules have been suggested in other works [1] and could be responsible of the lack of activity of the lipase. When the concentration of BS increases, the values of V_r^{Max} get higher, and over its measured CMC, it is possible to observe a clear enhancement in the lipolytic activity.

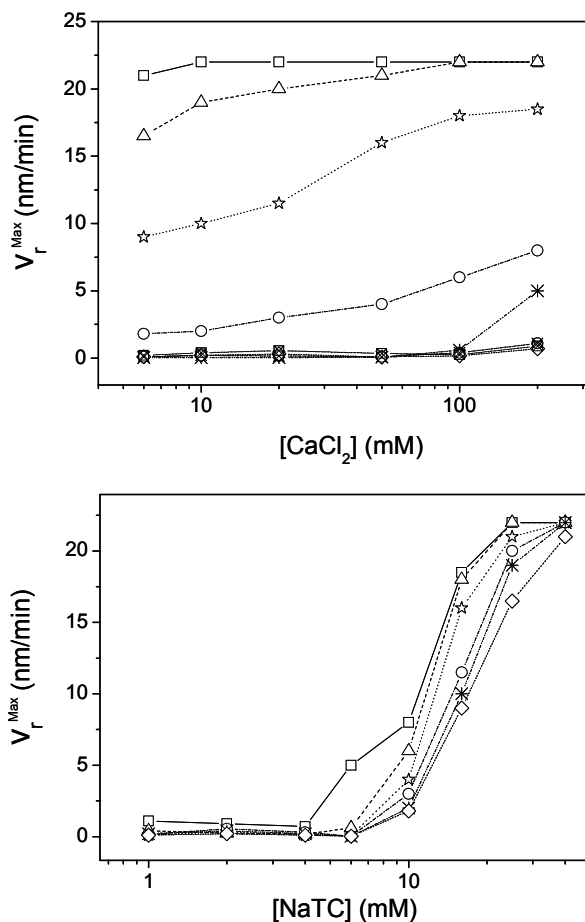


Figure 19. Maximum velocity of reaction with *W80mN33Q* (30nM) in a emulsion with triolein (100 μ M), depending on the CaCl_2 concentration (top) for the following concentrations of NaTC: 40mM (squares), 25mM (triangles), 16mM (stars), 10mM (circles), 6mM (asterisks), 4mM (diamonds), 2mM (crossed squares) and 1mM (crossed circles); and depending on the NaTC concentration (bottom) for the following concentrations of CaCl_2 : 200mM (squares), 100mM (triangles), 50mM (stars), 20mM (circles), 10mM (asterisks) and 6mM (diamonds).

These results are similar to those found by another authors for bovine pancreatic lipase in presence of its correspondent cofactor [67] and, from our point of view, it can be consider as the formation of active complexes

between the lipase and the BS micelles. The increment of the concentration of CaCl_2 produces a clear enhancement in the lipolytic activity that has been reported by different authors and has been attributed to different reasons [7]. Without neglecting any of this possible causes, which may be considered as complementary, we estimate that a very important factor is the one suggested by Gilbert Benzonana [68]. This author proposed a possible screening effect of the Ca^{2+} ions on the electrostatic repulsion between the different compounds taking place in the process of lipolysis. In this case, the formation of aggregates is favored and the values of V_r^{Max} increases considerably. This screening effect is clearly manifested in the displacement towards lower concentrations of BS, in the values of V_r^{Max} , when we increase the presence of Ca^{2+} (see Fig. 19). During this experiment, no lag periods could be recorded.

The final air-water interfacial pressures after the reaction are shown in Figure 20. They show a very small dependence of the global release of lipolytic products on the different presence of Ca^{2+} ions. However, it is possible to observe a strong dependence with the concentration of BS. The maximum interfacial pressures are observed for the minimum concentrations of BS. At the concentrations of BS close to its CMC, where the reaction begins, the final interfacial pressure decreases. The formation of mixed BS micelles solubilizing the reaction products appears to be a logical reason for this phenomenon. For very low concentrations of BS, the residual activity appearing due to the small interfacial penetration and activation of the lipase is able to produce a final amount of reaction products that cannot be solubilized when the concentration of BS is too small.

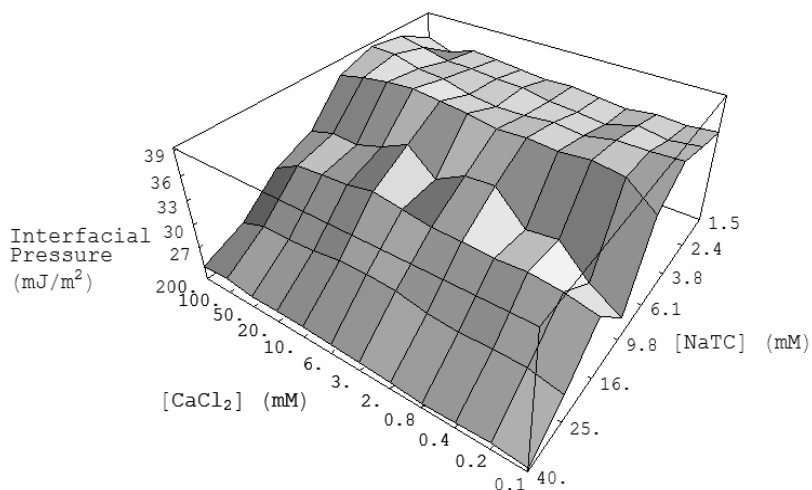


Figure 20. Final air-water interfacial pressure, after four hours of reaction in the emulsion of Figure 19, depending on the CaCl₂ and NaTC concentrations.

Therefore, similar values of final air-water interfacial pressure are found for these low concentrations of BS. The increment in the concentration of BS enhances the production of lipolytic products by forming complexes with the lipase, but also helps to solubilize them, leading to a lower final air-water interfacial pressure. The concentration of BS (10mM), where the micelles are appearing, presents a slightly lower interfacial pressure. This could be representative of an optimum concentration of BS for the formation of the mixed micelles.

3.3. Effect of the lipase and NaTDC concentrations on the kinetics of lipolysis

In former experiments, we have observed the appearance of lipase activating lag times. The formation of interfacial lipolytic oligomers of lipase has been proposed to explain these times [58]. However, the presence of complexes in the bulk between BS micelles and the lipase molecules appears to influence this phenomenon. When they are active, like in the case of NaTC, they may increase the interfacial acceleration of reaction. However, when they were inhibiting like in the case of NaTDC, they may favor the acceleration of the interfacial formation of active oligomers by facilitating the interfacial access to the lipase after displacing or desorbing the BS at certain areas on the interface. In some cases, under optimum reaction conditions, the precipitation of fibril-like aggregates was found. As mentioned before, these structures are supposed to be composed by a considerably part of the lipase. Different shapes could be found depending of the reacting conditions. Since the BS plays a very important roll in the kinetics of reaction due to its way of aggregation, we will consider the effect of this variable and the lipase concentration on the formation of these fibril-like aggregates in the next experiment. The results for the maximum velocity of reaction, in emulsions with our buffer, triolein (0.5mM), CaCl_2 (2mM) and different concentrations of NaTDC and *W89mN33Q* are shown in Figure 21.

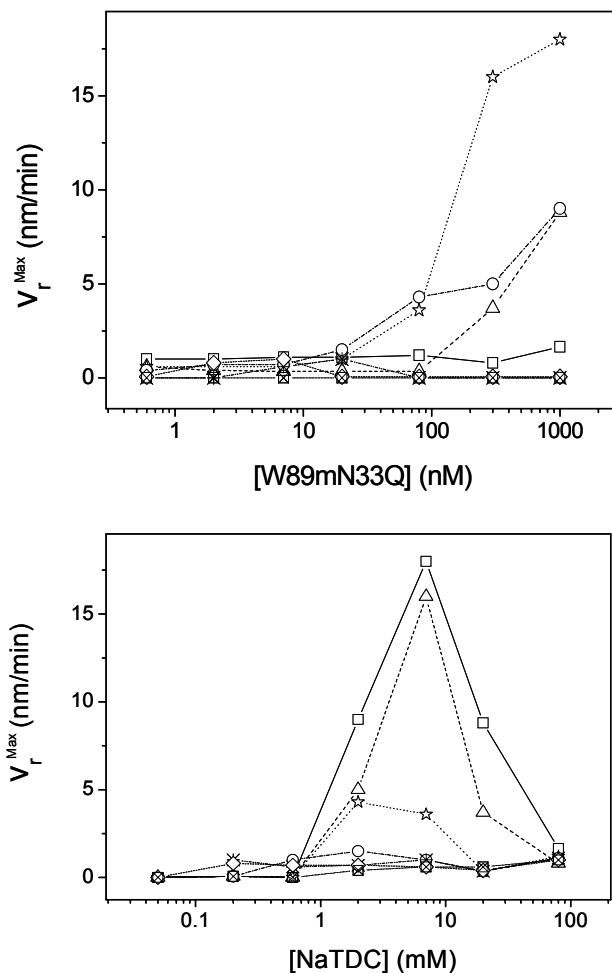


Figure 21. Maximum velocity of reaction in a emulsion with triolein (0.5mM) and CaCl_2 (20mM), depending on the lipase concentration (top) for the following concentrations of NaTDC: 80mM (squares), 20mM (triangles), 7mM (stars), 2mM (circles), 600 μM (asterisks), 200 μM (diamonds) and 50 μM (crossed squares); and depending on the NaTDC concentration (bottom) for the following concentrations of *W80mN33Q*: 1 μM (squares), 300nM (triangles), 80nM (stars), 20nM (circles), 7nM (asterisks), 2nM (diamonds) and 0.6nM (crossed squares).

These results show, as expected, an increment in the values of V_r^{Max} with the concentration of lipase. At concentrations of *W89mM33Q* below 20nM,

there is no observable lipase activity. The interfacial presence of BS seems to obstruct the penetration or to inhibit the activity of the lipase for these low concentrations.

The degree of increment of the reaction for higher concentrations is strongly influenced by the concentration of BS (see Figure 22). Only at concentrations of BS over 2mM, is possible to observe a measurable decrease in the emulsion droplet radii. These concentrations are very close to the CMC of this BS. A bell-like shape is observed in the dependence of V_r^{Max} with the concentration of BS for the higher concentrations of lipase. This kind of dependency has also been reported by other authors using different lipases and BS [69, 2], but no clear explanation was given to this behavior.

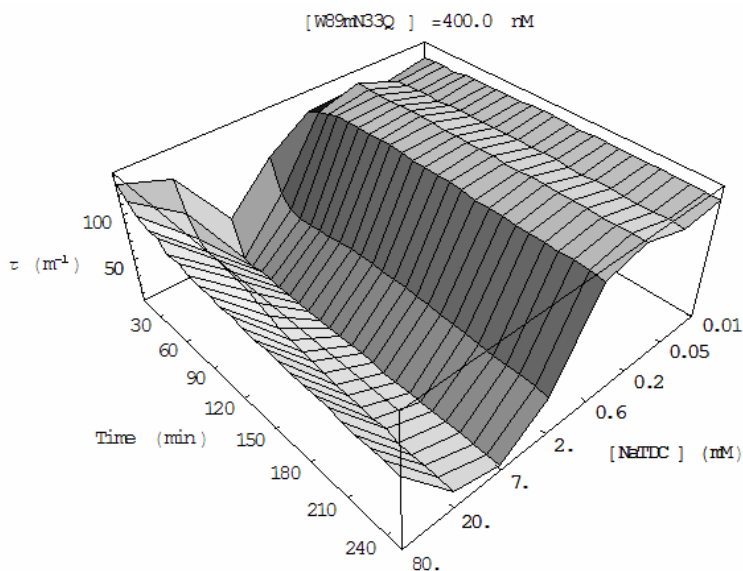


Figure 22. Temporal dependence of the turbidity of an emulsion with triolein (0.5mM), CaCl₂ (2mM) and different concentrations of NaTDC and during the reaction of lipolysis with different concentrations of *W89mN33Q*.

The BS concentration correspondent to this maximum decreases slightly with the concentration of lipase. For the higher concentrations of lipase this maximum is reached around NaTDC (7mM) whereas for concentrations close to *W89mM33Q* (80nM) this maximum activity is already observed at NaTDC (3mM). This behavior is consequent with the hypothesis that we proposed, when we considered the variation of V_r^{Max} with the concentrations of lipase and substrate for NaTDC (20mM). The formation of the inactive complexes in the bulk may be displacing or desorbing some parts of the interfacial layer of BS allowing the penetration of the lipase. In this case, the activation of the lipase molecules at the interface by oligomerization would be enhanced by the interfacial pressure of the BS molecules. For the lower concentrations of BS, still over its CMC, the concentration of micelles is enough to form inactive complexes able to clean small areas of the interface for the lipase penetration. When we increase the concentration of BS this phenomenon is increasing and the values of V_r^{Max} are getting higher until certain concentration. At this point, the bulk concentration of BS is too high to form this type of micelles and higher order aggregates begin to appear. These bigger BS aggregates are unable to form complexes and may be adsorbed at the interface decreasing the interfacial area available for the lipase. Higher order BS micelles have been studied in many works and they are supposed to form cylindrical aggregates that eventually may collapse forming long crystals with a fibrillar appearance [70]. In this case, the increment in the concentration of BS after this maximum results in a decrease of the values of V_r^{Max} (see Fig. 21). Therefore, the maximum appearing for the variation of V_r^{Max} with the

concentration of NaTDC may be explained as the concentration of BS where it changes its way of aggregation due to its step-wise process of micellization [23]. It would correspond with an optimum concentration of BS for the formation of inactive complexes that would interact with the BS molecules at the interface. The higher concentration of lipase shifts slightly this concentration of BS to higher values due to the major number of lipase interactions occurring at the oil-water interface. No lag periods were observed during these experiments. The information about the final concentration of reaction products in the bulk is estimated, as before, from the final air-water interfacial pressure after reaction (see Fig. 23). As we saw in the case of the variation of the concentration of NaTC, the final interfacial pressure is decreasing with the increment of the BS concentration.

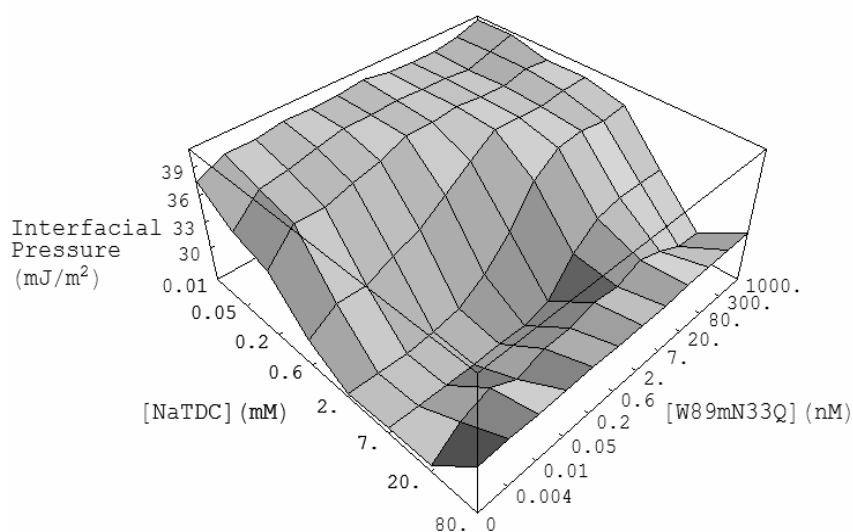


Figure 23. Final air-water interfacial pressure, after four hours of reaction in the emulsion of Figure 21, depending on the BS and lipase concentrations.

Especially in the cases where the reaction is fully completed, this is a clear prove that the BS micelles are solubilizing the products of lipolysis. Otherwise, there would be a higher interfacial presence of these compounds at the air-water interface, increasing the interfacial pressure values. For the maximum BS concentrations, where very low lipolytic activity was taking place and the solubilization of products is maximum, is possible to observe normal saturating values of interfacial pressure in presence of BS and lipase [1]. In this case is also possible to observe how for low concentrations of BS, the residual activity of the lipase may produce a considerable final amount of reaction products after four hours without possible solubilization.

By microscopic inspection of the bottom of the different reacting wells, different shape aggregates were found forming sediments (see Figure 24). For the wells with the higher concentration of BS, where no lipolytic activity was registered, globules of intertwined fibril-like structures were found independently of the concentration of lipase. These globules are supposed to be composed by BS aggregating on their highest order of aggregation. This type of structures has been extensively studied in the literature [23]. As we can see in Figure 24, they presented certain level of birefringence under cross-polarized illumination. However, we were unable to stain them with Congo red diazo dye so their possible amyloid nature was discarded. At low concentrations of NaTDC, straight fibril like shapes began to appear at the bottom of the wells when increasing the concentration of lipase. They presented a branched structure and formed globules in some cases (see Fig. 24 middle). These sediments also showed some birefringence but again were not stainable with Congo red. Only in the case of optimum

conditions of reaction, certain aggregates were found that were birefringent and able to be stained with this dye (see Fig. 24 bottom).

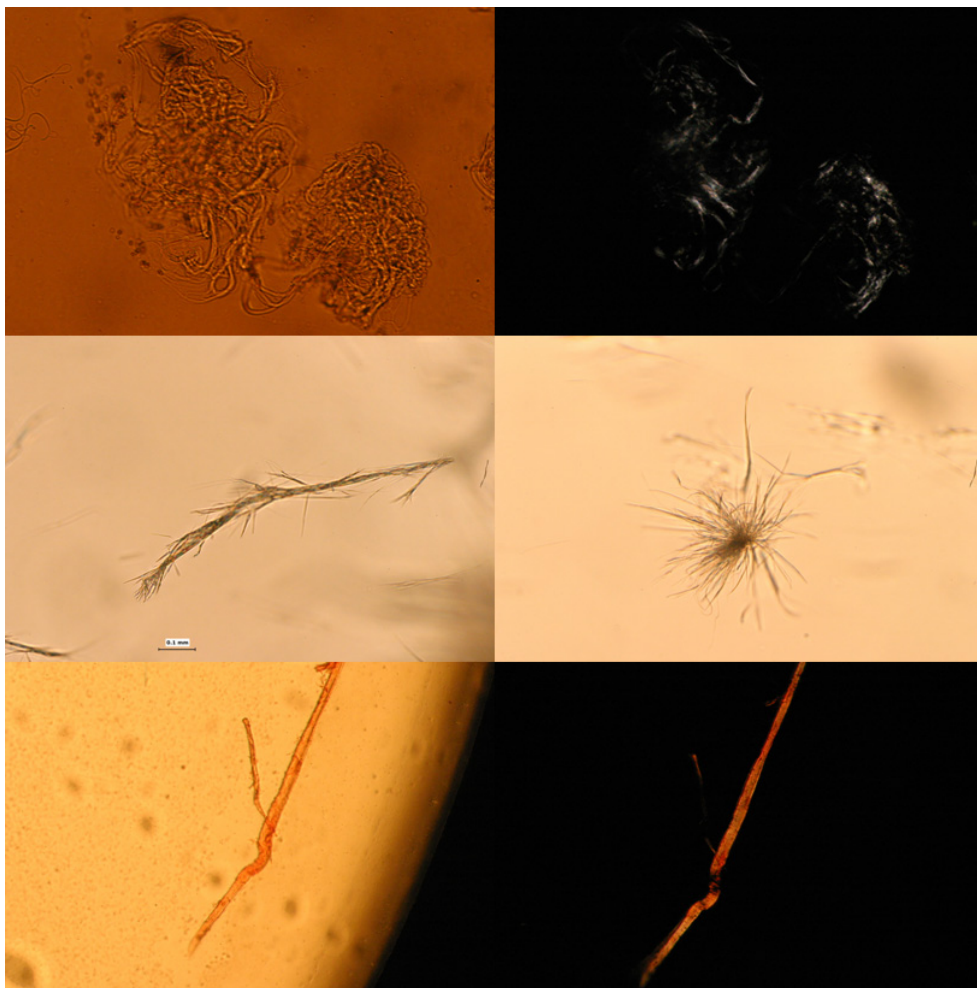


Figure 24. Fibrillar aggregates precipitated after four hours of reaction in the emulsion of Figure 21, when (top) $[\text{NaTDC}] = 20\text{mM}–80\text{mM}$ and $[\text{W89mN33Q}] = 0.3\mu\text{M}$; (middle) $[\text{W89mN33Q}] = 1\mu\text{M}$ and $[\text{NaTDC}] = 600\mu\text{M}$; (bottom) $[\text{W89mN33Q}] = 1\mu\text{M}$ and $[\text{NaTDC}] = 6.7\text{mM}$. (All pictures $\times 10$; top and bottom right ones under cross-polarized illumination and Congo red stained)

These optimum conditions are very close to the ones of maximum estimated formation of inactive complexes that would help to offer appropriate zones at the oil-water interface for the lipase oligomerization and activation. The aggregates found under this conditions were less numerous than the ones found for slightly higher concentrations of BS and appeared in random positions at the bottom of the wells. Even when they showed certain characteristics proper of amyloids, we are not able to certify their amyloid condition until further studies will be carried out like Thioflavin staining or some other probes. This kind of confirmation studies will be performed in future works.

3.4. Effect of the type of STAG on the kinetics of lipolysis

As a final part of this work, we have employed the proposed methodology to study the effect of the type of substrate and the concentration of lipase on the lipolysis of STAG obtained from transesterification of poly-unsaturated oils and fully hydrogenated fats [21]. Specifically, they were obtained from sesame oil (SE) and fully hydrogenated soybean oil (FHSBO) at concentration ratios (SE: FHSBO) 80:20 and 70:30; and from olive oil (OO) and fully hydrogenated palm oil (FHPO) at (OO:FHPO) 90:10, 80:20, 70:30, 50:50 and 30:70.

3.4.1. Reaction with STAG from sesame oil and fully hydrogenated soybean oil

The values of V_r^{Max} for the lipolysis of different STAG from SE and FHSBO are shown in Figure 25.

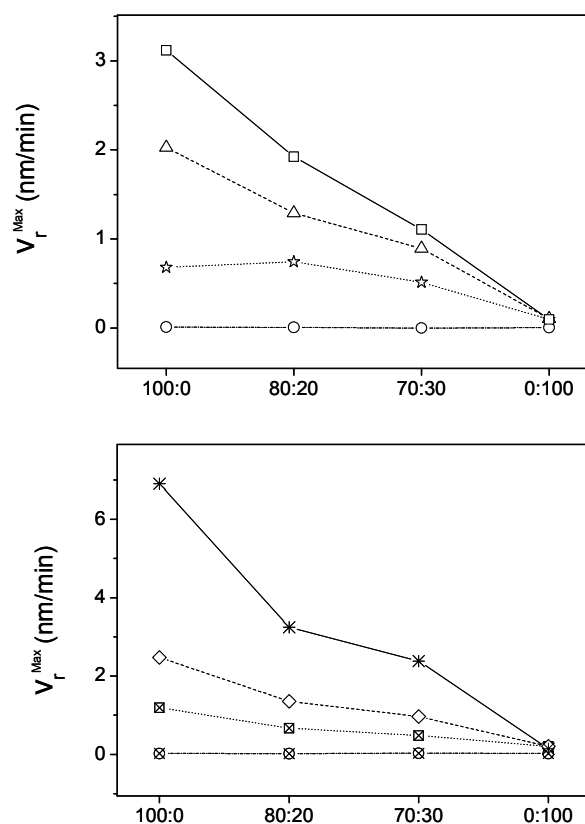


Figure 25. Maximum velocity of reaction in emulsions with STAG (80mg/l) from SE and FHSBO, BS (20mM) and CaCl_2 (20mM), depending on the SE:FHSBO concentrations ratio during transesterification, for the following concentrations of *W80mN33Q*: (NaTC, top) 100nM (squares), 10nM (triangles), 1nM (stars) and no lipase (circles); and (NaTDC, bottom) 500nM (asterisks), 150nM (diamonds), 45nM (crossed squares) and no lipase (crossed circles).

As expected, these results show a clear increase in the interfacial velocity of reaction with the concentration of lipase. However, for these STAG the values of the maximum interfacial velocity of reaction are smaller than the correspondents obtained when reacting with triolein. *W89mN33Q* showed a smaller specificity for this kind of substrates probably because of their different composition in FA.

NaTC, with lower concentrations of lipase reacting, presented a higher enhancement on the reaction of lipolysis than NaTDC. As we saw before this fact can be explained as consequence of the different mechanism of the lipase activation that appears depending of the type of BS. The possibility of formation of lipolytic complexes with NaTC increases the maximum velocity of reaction more than the interfacial access than the inactive complexes with NaTDC may offer to the lipase. No lag periods were observed during the present experiment. In all the cases is possible to observe a clear decrease in V_r^{Max} with the degree of saturation of the STAG. This decrease followed similar linear tendencies with for both BS having, as mentioned, higher slopes for NaTC than for NaTDC. The influence of degree of saturation of the STAG on the interfacial quality, i.e. on the interfacial tension and on the concentration and orientation of the substrate molecules at the interface, seems to be one of the main reasons for this decrease. The highly saturated STAG are more voluminous and the interfacial area per molecule will increase with the degree of saturation, reducing therefore, the values interfacial velocity of reaction. These molecules will present a much smaller mobility presenting a worse interfacial orientation and packing. Consequently, a less specific contact

between the lipase molecules, and between them and the substrate, will occur. Another possible effect is the different composition of the mixed micelles formed, which eventually may affect to the lipolytic complexes formed at the initial stage of the reaction.

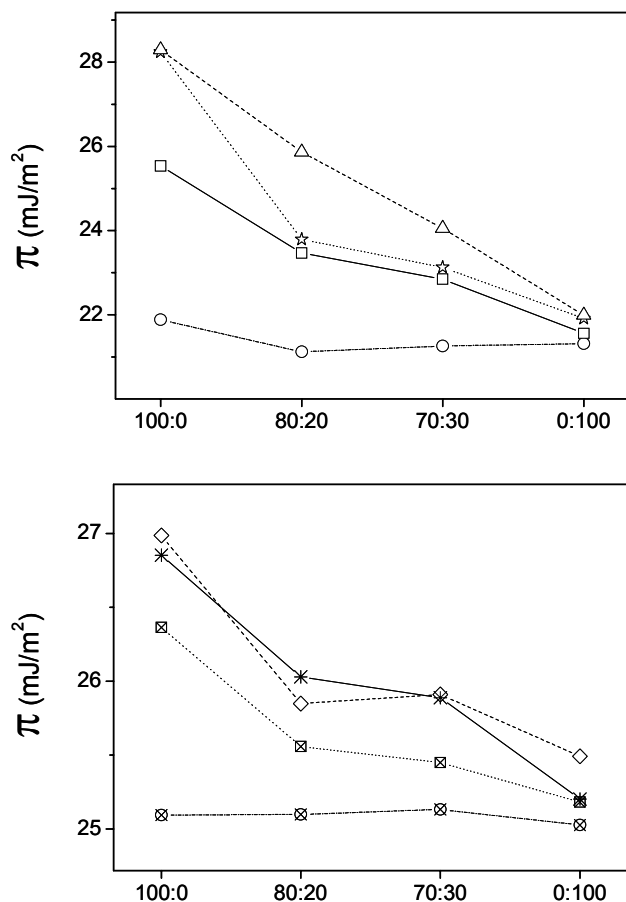


Figure 26. Final air-water interfacial pressure, after four hours of reaction in the emulsions in Figure 25, depending on the SE:FHSBO concentrations ratio during transesterification, for the following concentrations of *W80mN33Q*: (NaTC, top) 100nM (squares), 10nM (triangles), 1nM (stars) and no lipase (circles); and (NaTDC, bottom) 500nM (asterisks), 150nM (diamonds), 45nM (crossed squares) and no lipase (crossed circles).

At this point, we may consider the final air-water interfacial pressures (see Fig. 26) in order to obtain some information about the former hypothesis. These results indicate a decrease of the final air-water interfacial pressure with the increment of the saturation of the STAG. Very small differences are appearing at the final interfacial pressures, after four hours of adsorption, depending on the concentration of lipase. This means that the variations in their value depend mostly on the type of reaction products released and on the way that they are solubilized by the BS micelles. The lower final interfacial pressures observed for the emulsions with NaTDC, even when the interfacial velocity of reaction was higher due to the higher concentration of lipase, seems to show that the reaction products from this type of STAG are more efficiently solubilized with NaTDC than with NaTC. For both BS the final interfacial pressure is minimum when no lipase was present, proving the increment in the interfacial pressure is due only to the accumulation of products of reaction. The very low interfacial pressures and the lack of lipolysis, when no reaction is taking place, suggests that most of the BS molecules are adsorbed at the oil water interface in this case. In these emulsions without lipase, the similar interfacial pressures measured for the different substrates suggest that the type of STAG is not influencing the interfacial adsorption of the BS. At the end of these experiments, it was not possible to find any kind of aggregates forming sediments after reaction. Therefore, the formed complexes may be dispersed in the bulk after reaction.

4.3.2. Reaction with STAG from olive oil and fully hydrogenated palm oil

The values of V_r^{Max} for the lipolysis of different STAG from OO and FHPO are shown in Figure 27.

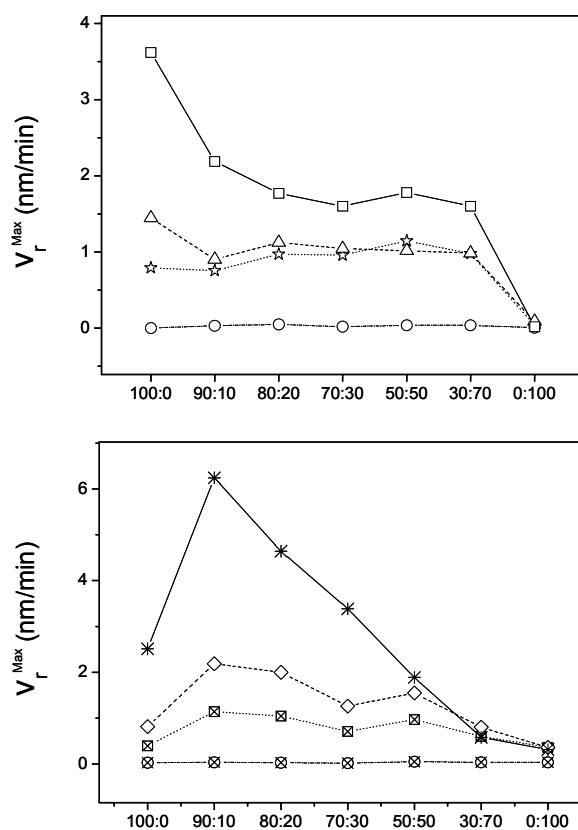


Figure 27. Maximum velocity of reaction in emulsions with STAG (80mg/l) from OO and FHPO, BS (20mM) and CaCl_2 (20mM), depending on the OO:FHPO concentrations ratio during transesterification, for the following concentrations of *W80mN33Q*: (NaTC, top) 100nM (squares), 10nM (triangles), 1nM (stars) and no lipase (circles); and (NaTDC, bottom) 500nM (asterisks), 150nM (diamonds), 45nM (crossed squares) and no lipase (crossed circles).

For these different substrates, the reaction is again slower than the measured with triolein in similar conditions of reaction. The values V_r^{Max} are in the same order of magnitude than in the reactions with STAG from SE and FHSBO and, if we consider the concentrations of lipase, they are again higher for NaTC than for NaTDC. This is again probing the different mechanism of lipase activation depending on the BS. The interfacial velocities of reaction are also increasing with the concentration of lipase but, in the case of NaTC, they seem to be very similar for the lower concentrations of lipase. This effect is not so strong in the case of NaTDC and we consider that it may be caused by a poor adsorption of the lipase molecules at the oil-water interface due to a lower interfacial quality in these substrates. Only over certain limit in the concentration of lipase, the interfacial penetration becomes high enough as to increase the velocities of reaction in a significant manner. Again, in this experiment no lag periods could be found. The decrease of the maximum velocity of reaction with the degree of saturation, observed for the case of STAG with SE, is also reproduced with the present substrates. However, some odd behaviors may be contemplated in this case. For example, in the case of the emulsions with NaTC, this decrease is only manifested at the substrates with maximum and minimum degrees of saturation. The rest of the substrates show no variations in V_r^{Max} with the degree of saturation. In the reactions with NaTDC, this behavior is only observable for the lower concentrations of lipase. The interfacial quality seems to be the responsible for this phenomenon. A possible similar interfacial organization in the substrates with medium saturation degree may be the main reason.

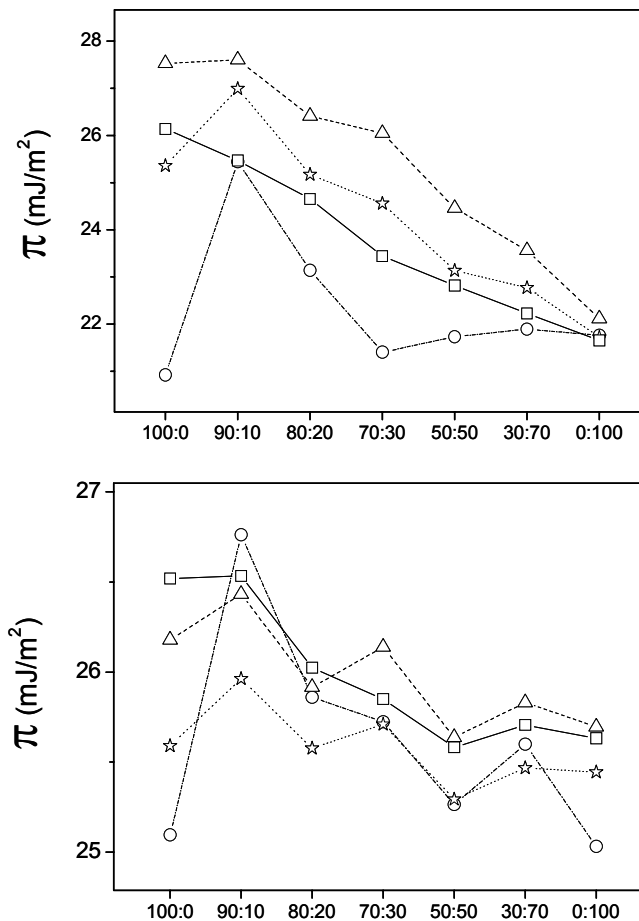


Figure 28. Final air-water interfacial pressure, after four hours of reaction in the emulsions in Figure 27, depending on the OO:FHPO concentrations ratio during transesterification, for the following concentrations of *W80mN33Q*: (NaTC, top) 100nM (squares), 10nM (triangles), 1nM (stars) and no lipase (circles); and (NaTDC, bottom) 500nM (squares), 150nM (triangles), 45nM (stars) and no lipase (circles).

Another singularity of these substrates is the lower values of V_r^{Max} found for the emulsions with only OO, in the case of NaTDC. As we can see in the information from the final air-water interfacial pressures (Fig. 28), the differences in the BS interfacial concentrations may be the responsible of

these lower values of V_r^{Max} in this case (100:0). If we consider the values of the final air-water interfacial pressures after the reaction, we can see that they tend to decrease with the increment of the degree of saturation of the substrate even for the emulsions where no reaction was taking place. This means that, for this type of STAG, the BS molecules are adsorbed more efficiently at the interfaces with a higher degree of saturation. Only in the case of completely unsaturated substrate, is possible to observe a higher adsorption of the BS molecules, separating themselves from this tendency. This seems to be the reason for the differences observed in the tendencies of reaction between the STAG with SE and the ones with OO. The similar values obtained for the reaction in STAG from OO with different degrees of saturation may be a consequence of the effects of a lower specificity of our lipase for this type of substrate together with lower presence of BS molecules at the interface slowing down the interfacial access of the lipase to the interface. This would also explain that, in the case of emulsions with only OO the reaction would be much lower. The differences observed, in this case of unsaturated substrate, for the velocity of reaction with both BS, are very representative of the different way in which the lipase is activated when they are present. In the case of the emulsions with NaTC, the lipolytic complexes may be able to penetrate and hydrolyze the STAG in a much efficient way. However, the inactive complexes from NaTDC, in this case with a higher interfacial concentration of lipase (100:0), are displacing parts of the BS layer in a more difficult way and the formation of interfacial active lipase-oligomers is obstructed considerably. In any case, all of the former hypotheses strongly require further studies to clarify their solidity.

4. Conclusions

In this work, we have proposed a new protocol for the assay of the lipase activity based in the combination of turbidimetric and tensiometric measurements. The main advantages of this method are its simplicity and the possibility of performing batch measurements of several samples simultaneously. In this way, is possible to skip traditional problems observed when comparing different results. These problems are usually due to the ageing of the emulsion or to minor differences during its preparation that may propagate causing bigger changes in the final characteristics of the system. Especially interesting is the possibility of compare the effect in the changes of two variables simultaneously on the very same system. With this protocol is possible to obtain the traditional constants of enzymatic kinetics with just one experiment and also can offer straight information about the maximum interfacial velocity of reaction and, when corresponding, about the lag periods of lipase activation that may appear. The final measurement of the air-water interfacial tensions at the top of the reacting samples offers important qualitative information about the global amount of amphiphilic products released during the reaction and help to clarify the results obtained by turbidimetry. Being more accurate than traditional turbidimetric methods, this protocol allows obtaining a great amount of information in a very fast and efficient way.

We have used this protocol to study the reactions of lipolysis in triolein emulsions stabilized with two different BS. The emulsions were prepared using ultrasounds and the influence of different variables like the lipase, substrate, BS or Ca^{2+} concentration on the kinetics of reaction have been reported. Similar results to those found in other works have been reported and new effects have been found. For example, a different mechanism of the lipase activation seems to appear depending on the type of BS. The formation of lipolytic lipase oligomers at the interface, enhanced by the BS displacing effect of inactive complexes formed by the lipase and BS micelles, appears as a suitable hypothesis to explain the obtained results in emulsions with NaTDC. On the other hand, in emulsions with NaTC, the study of the activating periods seems to show the formation of active complexes in the bulk that are able to act in conjunction with the active interfacial oligomers commented before. The appearance of optimum concentrations of lipase for certain low concentrations of BS, have showed the important roll that the concentration of the different compounds may play in this whole process. The kind of lipase-BS interactions proposed in this work are based in the findings of different authors in the bibliography but some of them have been just hypothesized from the analysis of our experimental results. Therefore further work must be done to clarify whether or not they are appropriate. Some of these interactions, for example, could explain some of the last findings about the lipolysis in the human digestive tract [71].

One of the main findings in this work, is the formation of fibril-like precipitates at the end of the reaction that, from our point of view, are a consequence of the interfacial aggregation of lipolytic oligomers composed mainly by lipase molecules, following a stepwise scheme similar to the one proposed by different authors [58]. Under optimum conditions these aggregated seemed to have an amyloid character that must be certified in future works.

In a final stage, we have observed the differences observed in the kinetics of lipolysis of several STAG proceeding from reactions of transesterification of different oils and fully hydrogenated fats. A very interesting relation between the kinetics of reaction and the degree of saturation of the substrate or the type of BS present during the reaction has been found.

References

1. Tejera-Garcia R et al. *Interfacial study of interactions between lipases and bile salts*. to be published 2008
2. Vogel WC and Zieve L. *A rapid and sensitive turbidimetric method for serum lipase based upon differences between the lipases of normal and pancreatitis serum*. Clin Chem 1963;9:168
3. Nano JL and Savary P. *Hydrolysis of an aliphatic monoester in emulsion by swine pancreas lipase: influence of interfacial bile salts molecules upon reaction rate*. Biochimie 1976;58:917
4. Borgstrom B et al. *Pancreatic colipase: chemistry and physiology*. J Lipid Res 1979;20:805
5. Schandl A and Pittner F. *The role of Na⁺ and Ca²⁺ ions on the action of pancreatic lipase studied with the help of immobilisation techniques*. Eur J Biochem 1984;140:547
6. Granon S. *Spectrofluorimetric study of the bile salt micelle binding site of pig and horse colipases*. Biochim Biophys Acta 1986;874:54
7. Tietz NW and Shuey DF. *Lipase in serum--the elusive enzyme: an overview*. Clin Chem 1993;39:746
8. Tietz NW. *Accuracy in Clinical-Chemistry Does Anybody Care*. Clinical Chemistry 1994;40:859
9. Lessinger JM et al. *Preparation and characterization of reference materials for human pancreatic lipase: BCR 693 (from human pancreatic juice) and BCR 694 (recombinant)*. Clin Chem Lab Med 2003;41:169
10. Ferard G et al. *Interassay calibration as a major contribution to the comparability of results in clinical enzymology*. Clin Biochem 1998;31:489
11. Tietz NW. *Support of the diagnosis of pancreatitis by enzyme tests--old problems, new techniques*. Clin Chim Acta 1997;257:85
12. Beisson F et al. *Methods for lipase detection and assay: a critical review*. European Journal of Lipid Science and Technology 2000;102:133

13. Lott JA et al. *Assays of Serum Lipase - Analytical and Clinical Considerations*. Clinical Chemistry 1986;32:1290
14. List GR et al. *Preparation and Properties of Zero Trans Soybean Oil Margarines*. Journal of the American Oil Chemists Society 1995;72:383
15. Arzoglou PL et al. *Conditions for Assay of Pancreatic Lipase from Human-Plasma Using A Nephelometric Technique*. Clinica Chimica Acta 1982;119:329
16. Derewenda U et al. *Current progress in crystallographic studies of new lipases from filamentous fungi*. Protein Eng 1994;7:551
17. Martinelle M et al. *On the interfacial activation of Candida antarctica lipase A and B as compared with Humicola lanuginosa lipase*. Biochim Biophys Acta 1995;1258:272
18. Derewenda U et al. *An unusual buried polar cluster in a family of fungal lipases*. Nat Struct Biol 1994;1:36
19. Svendsen A et al. *Protein engineering of microbial lipase of industrial interest*. Methods Enzymol 1997;284:317
20. Jutila A et al. *Fluorescence spectroscopic characterization of Humicola lanuginosa lipase dissolved in its substrate*. Biochim Biophys Acta 2004;1702:181
21. Otero C et al. *Continuous enzymatic transesterification of sesame oil and a fully hydrogenated fat: effects of reaction conditions on product characteristics*. Biotechnol Bioeng 2006;94:877
22. Borgstrom B. *Dimensions of Bile Salt Micelle . Measurements by Gel Filtration*. Biochimica et Biophysica Acta 1965;106:171
23. O'Connor CJ and Wallace RG. *Physico-Chemical Behavior Of Bile Salts*. Adv Colloid Interface Sci 1985;22:1
24. Pignol D et al. *Critical role of micelles in pancreatic lipase activation revealed by small angle neutron scattering*. J Biol Chem 2000;275:4220
25. Mazer NA et al. *Quasielastic light scattering studies of aqueous biliary lipid systems. Size, shape, and thermodynamics of bile salt micelles*. Biochemistry 1979;18:3064
26. Roda A et al. *The influence of bile salt structure on self-association in aqueous solutions*. J Biol Chem 1983;258:6362

27. Kratochvil JP et al. *Concentration-Dependent Aggregation Patterns of Conjugated Bile-Salts in Aqueous Sodium-Chloride Solutions - A Comparison Between Sodium Taurodeoxycholate and Sodium Taurocholate*. Colloid and Polymer Science 1983:261:781
28. Chanamai R et al. *Effect of temperature on the ultrasonic properties of oil-in-water emulsions*. Colloids and Surfaces A-Physicochemical and Engineering Aspects 1998:139:241
29. Behrend O et al. *Influence of continuous phase viscosity on emulsification by ultrasound*. Ultrason Sonochem 2000:7:77
30. Behrend O and Schubert H. *Influence of hydrostatic pressure and gas content on continuous ultrasound emulsification*. Ultrason Sonochem 2001:8:271
31. Abismail B et al. *Emulsification by ultrasound: drop size distribution and stability*. Ultrasonics Sonochemistry 1999:6:75
32. Wickham M et al. *Modification of a phospholipid stabilized emulsion interface by bile salt: effect on pancreatic lipase activity*. J Lipid Res 1998:39:623
33. Wagner NJ et al. *The Microstructure of Polydisperse, Charged Colloidal Suspensions by Light and Neutron-Scattering*. Journal of Chemical Physics 1991:95:494
34. Tietz NW et al. *Turbidimetric measurement of lipase activity--problems and some solutions*. Clin Chem 1987:33:1624
35. Shihabi ZK and Bishop C. *Simplified turbidimetric assay for lipase activity*. Clin Chem 1971:17:1150
36. Verduin PA et al. *Studies on the determination of lipase activity*. Clin Chim Acta 1973:46:11
37. Moss DW. *The place of reference materials in clinical enzymology*. Clin Chim Acta 1988:173:1
38. Ziegenhorn J et al. *Determination of Serum Lipase*. Clinical Chemistry 1979:25:1067
39. Harkins WD and Beeman N. *Emulsions: stability, area per molecule in the interfacial film, distribution of sizes and the oriented wedge theory*. J Am Chem Soc 1929:51:1674
40. Bohren CF and Huffman DR. *Absorption and Scattering of Light by Small Particles*. John Wiley & Sons, New York, 1998
41. Kerker M. *The Scattering of Light and Other Electromagnetic Radiation*. Academic Press, New York 1969

42. Pandey RK and Tripathi DN. *Schulz distribution function and the polydispersity of the binary suspension of charged macroions*. Colloids and Surfaces A-Physicochemical and Engineering Aspects 2001:190:217
43. Melik DH and Fogler HS. *Turbidimetric Determination of Particle-Size Distributions of Colloidal Systems*. Journal of Colloid and Interface Science 1983:92:161
44. Lompadó A. *Light Scattering by a Spherical Particle*. Dept of Physics, The University of Alabama in Huntsville: LompadóA@email.uah.edu
45. Fillery-Travis A and Wickham M. *Colloidal aspects of lipid digestion and absorption*. Curr Top Colloid Interface Sci 1999:3:103
46. Patton JS and Carey MC. *Watching fat digestion*. Science 1979:204:145
47. Kannisto H et al. *Characterization and elimination of a factor in serum that interferes with turbidimetry and nephelometry of lipase*. Clin Chem 1983:29:96
48. Jurado E et al. *Kinetic model for the enzymatic hydrolysis of tributyrin in O/W emulsions*. Chemical Engineering Science 2006:61:5010
49. de Haas GH et al. *Studies on phospholipase A and its zymogen from porcine pancreas. Action of the enzyme on short-chain lecithins*. Biochim Biophys Acta 1971:239:252
50. Verger R et al. *Action of phospholipase A at interfaces*. J Biol Chem 1973:248:4023
51. Wieloch T et al. *Product activation of pancreatic lipase. Lipolytic enzymes as probes for lipid/water interfaces*. J Biol Chem 1982:257:11523
52. Snabe T and Petersen SB. *Lag phase and hydrolysis mechanisms of triacylglycerol film lipolysis*. Chem Phys Lipids 2003:125:69
53. Nielsen LK et al. *Lag-burst kinetics in phospholipase A(2) hydrolysis of DPPC bilayers visualized by atomic force microscopy*. Biochim Biophys Acta 1999:1420:266
54. Borgstrom B. *Importance of phospholipids, pancreatic phospholipase A2, and fatty acid for the digestion of dietary fat: in vitro experiments with the porcine enzymes*. Gastroenterology 1980:78:954
55. Antonov VK et al. *Catalytic activity and association of pancreatic lipase*. Biochimie 1988:70:1235

56. Pignol D et al. *The lipase/colipase complex is activated by a micelle: neutron crystallographic evidence.* Chem Phys Lipids 1998;93:123
57. Hermoso J et al. *Neutron crystallographic evidence of lipase-colipase complex activation by a micelle.* EMBO J 1997;16:5531
58. Code C et al. *Amyloid-type Fiber Formation in Control of Enzyme Action: Interfacial Activation of Phospholipase A₂.* Biophys J 2008:accepted
59. Hedin EM et al. *Implications of surface charge and curvature for the binding orientation of Thermomyces lanuginosus lipase on negatively charged or zwitterionic phospholipid vesicles as studied by ESR spectroscopy.* Biochemistry 2005;44:16658
60. Labourdenne S et al. *Surface behaviour of long-chain lipolytic products (a 1-to-1 mixture of oleic acid and diolein) spread as monomolecular films in the presence of long-chain triglycerides.* Colloids and Surfaces B-Biointerfaces 1996;6:173
61. Dreher KD et al. *Surface Chemistry of Monoglyceride-Bile Salt System - Its Relationship to Function of Bile Salts in Fat Absorption.* Journal of Colloid and Interface Science 1967;25:71
62. Tejera-Garcia R et al. *Interfacial study of the effect of the oil type on the activity of the Mucor Miehei Lipase.* to be published 2008
63. Gorbenko GP and Kinnunen PK. *The role of lipid-protein interactions in amyloid-type protein fibril formation.* Chem Phys Lipids 2006;141:72
64. Kallberg Y et al. *Prediction of amyloid fibril-forming proteins.* Journal of Biological Chemistry 2001;276:12945
65. Hayden MR and Tyagi SC. *A is for Amylin and Amyloid in Type 2 Diabetes Mellitus.* J Pancreas (Online) 2001;2:124
66. Stobiecka A. *The conformational changes of the fungal lipase from Humicola lanuginosa induced by the formation of bile salt and mixed micelles.* Journal of Fluorescence 2000;10:307
67. Rathelot J et al. *Studies on the effect of bile salt and colipase on enzymatic lipolysis. Improved method for the determination of pancreatic lipase and colipase.* Biochimie 1975;57:1117
68. Benzonana.G. *On Role of Ca²⁺ During Hydrolysis of Insoluble Triglycerides by Pancreatic Lipase in Presence of Bile Salts.* Biochimica et Biophysica Acta 1968;151:137
69. Lessinger JM et al. *Catalytic properties and stability of lipase purified from human pancreatic juice.* Clin Chim Acta 1996;251:119

70. Rich A and Blow DM. *Formation of a helical steroid complex.* Nature 1958;182:423
71. Armand M. *Lipases and lipolysis in the human digestive tract: where do we stand?* Curr Opin Clin Nutr Metab Care 2007;10:156

Apéndice A

Basic Concepts

A.1. Interfacial Energy

We call phase to each one of the homogeneous parts composing a heterogeneous system. Therefore, a pure solution may be considered as a homogeneous, single phase, system meanwhile a dispersion of particles, like the coffee or one spray, is a heterogeneous multiphase system. Interphase is the region between two different phases and is composed by the molecules of both of them. If these phases are immiscible and the interphase can be approximated to a bidimensional space the term interface is employed instead. Interface is referring to the narrow region through which the properties of one phase are changing continuously to the other phase. In order to apply the thermodynamic formalism to these systems there are different models but one of the most employed is to consider the interface as a Gibbs surface. A Gibbs surface is the geometric surface, with zero thickness, that keeps the shape of the interface and is placed in zone of the interface where the densities of both phases is equal.

The interfaces may be classified as fixed interfaces, if both of the phases are solid; rigid interfaces, if one of the phases is solid and the other is fluid (commonly known as surfaces); and flexible interfaces, if both phases are immiscible fluids. In the last two cases the interfaces may change their

extension and the flexible interfaces can change also their shape. If these changes are taking place the interfacial energy of the system will vary as well. Interfacial energy is the potential energy per unit of area of the molecules forming an interface and has units of J/m^2 in the International System. A common terminology for the interfacial energy between two phases A and B is σ_{AB} .

The interfacial energy of a phase dispersed in a second one is dependent on the rate area-volume, i.e. on the amount of area generated during the dispersion. The smaller the size of the aggregates, for a same total volume of dispersed phase, the bigger the interfacial area. When one phase is dispersed in a second one, an area of interface is created setting a big amount of molecules at a region where they experiment attractive cohesion forces from their same molecules, within the aggregate, and forces from the molecules of the second phase. This is producing an excess of potential energy in the system that tends to decrease reducing the interfacial area. The minimum interfacial area for a given aggregated volume is a sphere.

Any attempt to increase the interfacial area by deforming or dividing the interface results in the appearance of new molecules at this interface. This means that the molecules already at the interface must separate to let the new molecules to enter. The force, tangent to the interface, necessary to separate two molecules a unit of distance is called interfacial tension, γ_{AB} , and its units in the International System are N/m . Even when interfacial energy and interfacial tension are dimensionally equal and even have the same value, they refer to different concepts as we have seen. However, the

term interfacial tension is more commonly used at flexible interfaces in order to manifest the potential mechanic nature of its changes. The term of surface tension is commonly used as a particular case of interfacial tension in which one phase A is in equilibrium with its vapour (phase B).

A.2. Young-Laplace equation

The interfacial energy tends to a minimum by decreasing the interfacial area. As we have commented before, for a fixed volume and a flexible interface, this is achieved with a spherical shape. However, when the phases are in presence of external forces, the interface may be deformed by their effect. The shape of a flexible interface is described by the Young-Laplace equation. This equation describes the mean curvature at any point of the interface as proportional to the difference of pressure, between both phases at this point, and inversely proportional to the interfacial energy:

$$H_{AB} = \frac{1}{2} \frac{P_A - P_B}{\sigma_{AB}} \quad (1)$$

where H_{AB} is the mean curvature at any point of the interface between two fluids A and B, σ_{AB} is the interfacial energy and P_A and P_B are the pressures at each one of the phases. In absence of external forces this difference of pressures will remain constant along the interface, which will keep the same curvature leading to the spherical shape commented before. However, in presence of an external vector force field, for example, this difference of

pressures will change in the direction of this field and so will do the curvature of the interface.

The concept present in Equation 1 was proposed almost simultaneously by Thomas Young and by Pierre Simon de Laplace at the early XIX century. Both works made a written similar description of the former expression. The work of Young was published in 1805 “*Young T. An Essay on the Cohesion of Fluids. Phil Trans Roy Soc London 1805:95:65*” whereas the one of Laplace was published one year later “*de Laplace PS. Supplément a la théorie de l'action capillaire in Traité de la Mécanique Céleste. Gauthier-Villars, Paris 1806:419*”. This fact caused certain controversy about the real author and Thomas Young showed his unconformity with the authority of Laplace considering that his work had been copied.

This equation can be easily deduced for the case in absence of external field. If we consider a liquid dispersed into its vapor and we take into account that the minimal energy will correspond with the minimal interfacial area for the given volume of liquid, we can deduce that the shape of the dispersed aggregates will be spheres. The equilibrium of this system implies that the neat force acting on the equatorial perimeter of any of these spheres must be the same on both sides of this curve. For one of the hemispheres, this neat force would be given by,

$$F = 2\pi r\sigma \quad (2)$$

where r is the sphere radius. If now we consider that the difference between the internal and external pressures is always perpendicular to the interface,

the neat contribution of this pressure difference, ΔP , on one of the hemispheres will be given by,

$$F = \Delta P \pi r^2 \quad (3)$$

From the equilibrium of these neat forces we obtain,

$$\frac{1}{r} = \frac{\Delta P}{2\sigma} \quad (4)$$

which is the solution of the Young-Laplace equation for a spherical interface, i.e. an interface in absence of external fields.

A.3. Pendant Drops

In presence of a gravitational field the interfacial pressure difference, on both sides of the interface, will change along the height of the interface according with the fundamental law of the hydrostatic:

$$\Delta P = -\rho g h \quad (5)$$

where ΔP is the pressure difference between two points with a difference of height h , in a fluid with density ρ and with a gravity g .

In we consider a flexible interface in presence of a gravitational field, the difference in pressure between both phases, at any height h , will be given by,

$$\Delta P(h) = \Delta P_0 - \Delta\rho g h \quad (6)$$

being $\Delta\rho$ de difference of densities and ΔP_0 the pressure difference between

both phases at the point of the interface taken as reference of heights. Therefore, Equation 6 shows that the difference of pressures between both faces of the interface changes depending on the height. By including Eq. 6 in Eq. 1 we obtain the equation of Young-Laplace in presence of a gravitational field:

$$H = \frac{\Delta P_0}{2\sigma} - \frac{\Delta\rho g h}{2\sigma} \quad (7)$$

where H is the mean curvature at any point of the interface and h is the height of this point.

Equation 7 is a differential equation of second order in partial derivatives with respect to the parameters used to define the geometry of the interface. At the point of the interface taken as the origin of heights, the mean interfacial curvature radius, r_0 , can be defined as,

$$\frac{1}{r_0} \equiv \frac{\Delta P_0}{2\sigma} \quad (8)$$

At interfaces with an axisymmetric geometry, the apex is defined as the point of the interface with a single radius of curvature. Therefore, the apex is usually taken as the origin of heights for flexible axisymmetric interfaces in presence of a gravitational field.

By considering the Equation 8 and the length of capillarity, l_0 , the Equation 7 can be simplified to:

$$H = \frac{1}{r_0} - \frac{h}{2l_0^2} \quad \text{with} \quad l_0 \equiv \sqrt{\frac{\sigma}{\Delta\rho g}} \quad (9)$$

The mean curvature, H_Σ , at one point of a surface Σ , is defined as half of the trace of the shape operator, or curvature tensor, S_Σ :

$$H_\Sigma(u, v) = \frac{1}{2} \text{Tr}(\tilde{S}_\Sigma(u, v)) \quad (10)$$

If we describe the surface by a parametrization like $\mathbf{r}_\Sigma(u, v)$ the mean curvature will present the following form:

$$H_r(u, v) = \frac{[\mathbf{r}_{uu}, \mathbf{r}_u, \mathbf{r}_v]|\mathbf{r}_v|^2 + [\mathbf{r}_{vv}, \mathbf{r}_u, \mathbf{r}_v]|\mathbf{r}_u|^2 - 2[\mathbf{r}_{uv}, \mathbf{r}_u, \mathbf{r}_v](\mathbf{r}_u \cdot \mathbf{r}_v)}{2\left(|\mathbf{r}_u|^2|\mathbf{r}_v|^2 - (\mathbf{r}_u \cdot \mathbf{r}_v)^2\right)^{3/2}} \quad (11)$$

where the subscripts are the partial derivatives with respect to the variables u and/or v and the box brackets refer to the mixed vector product given by, $[\mathbf{a}, \mathbf{b}, \mathbf{c}] \equiv \mathbf{a} \cdot (\mathbf{b} \times \mathbf{c})$.

On an interface of revolution, Σ , like the one of a pendant drop, the parametrization of the surface, using cylindrical coordinates, may be made as: $\mathbf{r}_\Sigma(r, \varphi) = (r\cos(\varphi), r\sin(\varphi), z(r))$. Therefore, the Equation 11 may be expressed as:

$$H_z(r, \varphi) = \frac{z_r}{2r\sqrt{1+z_r^2}} + \frac{z_{rr}}{2(1+z_r^2)^{3/2}} \quad (12)$$

where each term corresponds with the inverse of the main curvature radii and the derivatives with respect to φ are zero due to the symmetry of revolution of the interface.

By substituting Equation 12 in Equation 9 we obtain an expression of the second order differential equation of Young-Laplace.

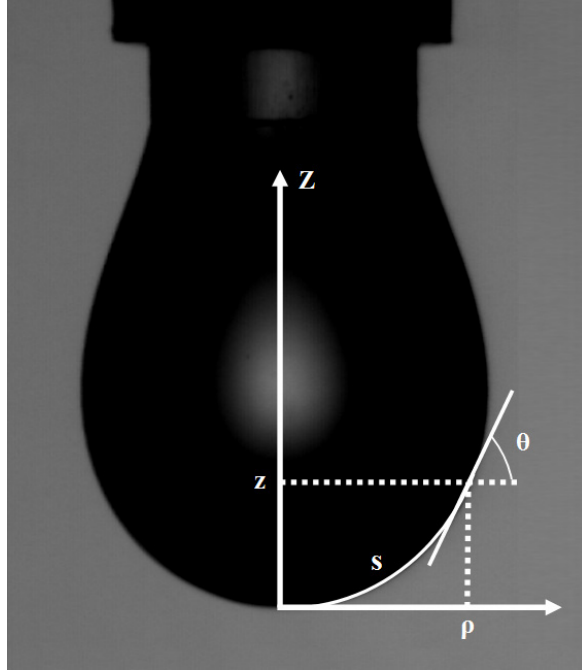


Figure A1. An axisymmetric pendant drop and the different variables defining its interfacial geometry

This expression may be simplified to a system of differential equations of first order (see Eq. 13) by introducing the variable θ , defined as: $\tan\theta = z'(r)$ (see Figure A1).

$$\begin{cases} \theta'(r) = \frac{1}{\cos\theta(r)} \left(\frac{2}{r_0} - \frac{z(r)}{l_0^2} - \frac{\sin\theta(r)}{r} \right) \\ z'(r) = \tan\theta(r) \end{cases} \quad (13)$$

Numerical methods are necessary to integrate the solution of this system of differential equations. The main inconvenience is the divergence of the derivative of $z(r)$ for $\theta=90^\circ$. In order to make it more accessible, a new

parameter, s , is included that may be interpreted as the arc length of the interface profile. This parameter is given by,

$$s = \int \sqrt{1 + z'(r)^2} dr \quad (14)$$

By including this parameter in Equation 13 we obtain the equation of Young-Laplace for revolution interfaces, like the one of a pendant drop, as the following system of first order differential equations:

$$\begin{cases} \theta'(s) = \theta'(r)r'(s) = \frac{2}{r_0} - \frac{z(s)}{l_0^2} - \frac{\sin \theta(s)}{r(s)} \\ z'(r) = z'(r)r'(s) = \sin \theta(s) \\ r'(s) = \cos \theta(s) \end{cases} \quad (15)$$

A.4. Interfacial Adsorption

A tensioactive or surfactant is a substance that is able to decrease the interfacial tension of the solvent in which it is dissolved or dispersed. The activity of surfactants is based on the adsorption at the interface of its molecules showing a simultaneous liophilic and liophobic character i.e. an amphiphilic character. The term adsorption refers to the change in the concentration of one compound at one interface. Thermodynamically it is defined as the way to reach equilibrium in a heterogeneous system by simultaneous interactions that increase or decrease the concentration of the

components at the interface. The interfacial activity of different molecules appears as a consequence of the difference between the cohesion works of the molecules of the solvent and the ones of the solute. However, the amphiphilic molecules are dissolved in water due to the presence of a hydrophilic part in their structure and the presence of a different hydrophobic part favours their interfacial activity. The decrease in the interfacial tension by the presence of a surfactant is closely related to the substitution of the solvent molecules at the interface by the molecules of the surfactant. Therefore, the interfacial tension in presence of a surfactant is dependent of the interfacial excess concentration of surfactant molecules as described by the Gibbs equation (Equation 5 in Capítulo 1). When the surfactant molecules displace the solvent molecules at an interface, the interactions between the solvent molecules and the external phase may be replaced by molecular interactions like solvent-surfactant and surfactant-external phase. These kinds of new interactions are more frequent and therefore the interfacial energy is reduced.

The adsorption of a surfactant at an interface is a dynamic process which kinetics are very important, for example in industrial processes. In these cases, the kinetics of adsorption are always studied before the equilibrium properties are characterized. The properties of surfactant solutions are a result of the adsorption and aggregation of the surfactant molecules. Therefore, the equilibrium state is determined by the rate of diffusion, orientation and aggregation of these molecules. The process of adsorption of surfactant molecules at an interface takes place in two parts: a diffusive part where the concentration gradient in the bulk transports the

surfactant molecules towards the interface, and the adsorption itself where the surfactant molecules take contact with the interface. In this second part is where takes place the approach to the equilibrium between the excess interfacial concentration and the solution concentration. This occurs by the transference of molecules between the subfase and the area immediately close to the interface (subsurface, with width close to the molecular diameter) and by the transference between this subsurface and the interface. The first is a mass transfer process controlled by diffusion (or possible convection) whereas the second is a pure adsorption/desorption process. This adsorption reduces a surfactant concentration at the subsurface that is restored by the diffusion in the subphase. As the interface gets saturated with molecules of surfactant the transfer of mass decreases approaching the equilibrium.

A.5. Emulsions

An emulsion (from Latin *emulsus*, pp. of *emulgere* ~ to milk) is a metastable system formed by two (or more) immiscible liquids and tensioactive agents, where one of the liquids is forming droplets dispersed into the other. Emulsions can be considered as two phase systems with a dispersed phase, formed by the liquid droplets, and a continuous phase, the liquid surrounding. The emulsion droplet dimensions are generally in the mesoscopic scale but in certain cases they may exceed these colloidal typical sizes. They present the characteristic behaviour of metastable

colloids like Brownian motion and reversible or irreversible phase transitions. Depending on the nature of each liquid they can be defined as oil in water (O/W), if an organic liquid is dispersed in an aqueous solution or water in oil (W/O) otherwise. In some cases it is possible to obtain double, or multiple, emulsions in which the dispersed phase is one emulsion forming droplets on another liquid. In this case, they can be defined as O/W/O or O/W/O. Emulsions are prepared by inducing energy to the system in terms of mechanic shear, for example. This will increase the interfacial free energy of the system and the phases will tend to separate. The emulsions suffer a fast coalescence (irreversible fusion of two droplets) unless a surfactant is added to the system to avoid the droplet-droplet contact, reducing the instability of the emulsion. Depending on the higher or lower solubility of this surfactant on each phase, O/W or W/O emulsions will be formed. The Bancroft rule states that a surfactant which is more soluble in the water phase will tend to form O/W emulsions meanwhile the more hydrophobic surfactant will tend to form W/O emulsions. The stability of an emulsion is dependent of many factors, like the type or concentration of the liquids and surfactant, the instrument employed for the fabrication or the temperature, duration and energy of the dispersing process. All these factors have some influence in the final distribution of droplet sizes and therefore on the stability of the emulsion. An emulsion can be relatively polydisperse and is common to define its average size using the mean Sauter diameter, which can be defined as the diameter of a drop having the same volume/surface area ratio as the entire emulsion.

The stability, or lifetime, of an emulsion may be defined by a combination of the coalescence/flocculation and/or the sedimentation or creaming (inverse sedimentation) responsables of the phase separation in the system (see Figure A2).

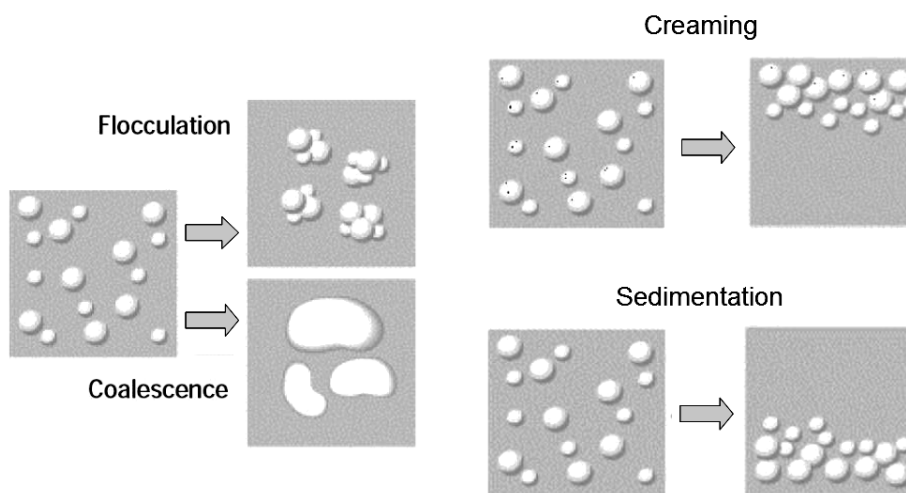


Figure A2. Different processes taking place during the breaking of an emulsion

This phase separation is often defined as the breaking of the emulsion and may be considered suitable when its duration ranges from a few minutes to several years, depending on the purpose of application of the emulsion. It is this flexibility what makes emulsions as the preferred candidates for commercial applications like food, adhesives, ink, paints and especially in medicine and cosmetic. This wide range of applications has caused a very fast development in the design and control of these materials and has enhanced the knowledge about the basics of their formation and breaking.

In some cases emulsions may be stabilized by the interfacial presence of solid colloids that attach to the interface reducing the interfacial energy and offering to the system a higher stability through a sterical mechanism. This type of emulsions is known as solid stabilized or Pickering emulsions. Very dense emulsions are often called biliquid foams. A very special type of emulsions are the microemulsions which are clear thermodynamically stable emulsions that forms spontaneously with very high concentrations of surfactant and under precise conditions. The droplet diameters of these systems range from around 5nm to 100nm depending on factors like the components concentration or temperature.

Apéndice B

Experimental Techniques

B.1. Axisymmetric Drop Shape Analysis: ADSA

The analysis of the shape of axisymmetric drops to obtain information about the surface tension of a liquid is a methodology that has been in continuous development since long time ago *Andreas JM et al. Boundary tension by pendant drops. Journal of Physical Chemistry 1938:42:1001*. However, it was at the early eighties, when the complete analysis of the shape of the drop began to be used for this purpose *Rotenberg Y et al. Determination of surface tension and contact angle from the shapes of axisymmetric fluid interfaces. J Colloid Interface Sci 1983:93:169*. This technique was highly improved with the increment in the velocity of analysis of computers and became more popular during the 90's decade. The initials A.D.S.A. (Axisymmetric Drop Shape Analysis) are commonly used nowadays to refer to the technique as well as to its methodology. With this technique is possible to obtain a straight measurement of the length of capillarity, l_0 , from a drop liquid. However, as we can see in Equation 9 of Apéndice 1, we will need to know the values of the local gravity acceleration and the difference of densities between the drop and the surrounding fluid, in order to obtain a final value of the interfacial tension.

During a modern measurement of the interfacial tension, using ADSA, the profile image of one drop, with back illumination, is registered with a camera and recorded in the memory of one computer. Then, image analysis software uses edge detection algorithms at the drop profile image to extract the positions of the points belonging to the interface. Finally, these points are adjusted to one of the possible solutions, known as laplacian revolution surfaces or laplacian curves, of the Young-Laplace equation (see Equation 15 in Apéndice 1). There are different possibilities for the algorithms used for the interface profile detection and different ways to find the best fit of these points to a laplacian curve. A very good review about the historic evolution of the algorithms and error parameters employed in this technique can be obtained in the PhD thesis of Juan Antonio Holgado Terriza, *Medida de magnitudes dinámicas por análisis digital de interfases curvas*, Universidad de Granada. Tesis Doctoral 2002. This work also shows all the possibilities of the method including the complete automatization of the whole procedure, the real time measurement of interfacial tensions and the possible utilization of these values to fix the interfacial pressure at variable interfacial area during the adsorption of a surfactant, for example.

B.2. Emulsions stability

The stability of emulsions has been characterized traditionally by observing the phase separation during processes of creaming or sedimentation. The temporal variation of position of the boundary between the separating emulsion and the remaining dispersant liquid is a common parameter employed to define the stability of one emulsion. However, there are two main problems associated with the interpretation of the measurements of this parameter. First, the location of the position of this boundary is usually made by optical inspection that may be dependent of the human factor. This position is particularly difficult to estimate during the initial part of the rupture process when the boundary appearing is more diffuse. A second difficulty is to estimate the degree of aggregation taking place along the process or whether this aggregation is reversible (flocculation) or irreversible (coalescence). For a sharp emulsion-dispersant boundary, it is possible to obtain a good estimation of the dynamics of droplet migration and therefore, employ approximately the Stokes Law to estimate the rate of aggregation taking place. However, the polydispersity of the emulsions and the increasing gradient of droplet concentration make this estimation not very accurate. The use of ultrasonic techniques allows assessing the concentration of each phase along the height of the emulsion but, in certain cases, this technique may interfere with the emulsion stability itself. In this work, we have characterized the stability of the emulsions

using a Turbiscan Classic MA 2000 (Formulaction, l'Union, France) optical analyzer. With this instrument is possible to estimate the rate of droplet migration and the coalescence taking place at certain parts of the emulsion in a non-invasive form.

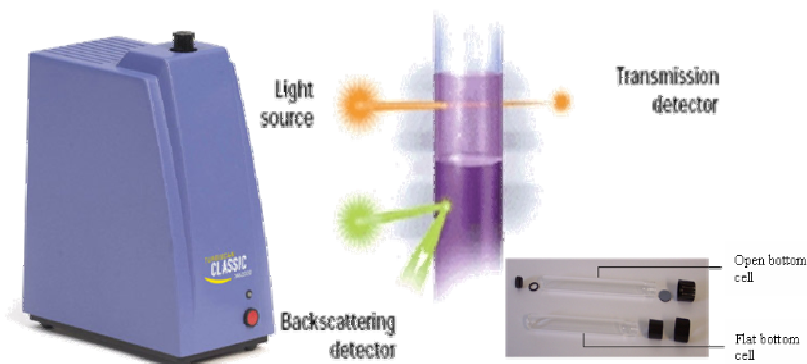


Figure B1. Principles of measurement with Turbiscan Classic MA 2000.

This is done considering the independent and anisotropic scattering of light from an emulsion in a cylindrical glass measurement cell. The measurement of the changes in the turbidity along the time allows, considering the Beer-Lambert law and the Mie theory, the estimation of the concentration and degree of aggregation of each liquid at different positions of the sample. In this instrument, the detection head is composed of a pulsed near infrared light source (wavelength $\lambda \sim 850$ nm) and two detectors which moves synchronously scanning along the height of the glass cylindrical cell containing the emulsion sample. The transmission detector receives the light which goes through the sample ($\theta = 0^\circ$) while the backscattering detector receives the light scattered by the sample at $\theta = 135^\circ$ (see Figure B1). The

length of the sample may vary up to seven centimetres and the turbidity information is collected every 40 μ m. In certain cases it is recommendable to use the initial transmittance or backscattered intensity as a reference to facilitate some parts of the data analysis.

The temporal changes of the turbidity as a function of the sample height (in mm) are presented in form of overlapping curves (for the different times of scanning) providing the transmitted and backscattered light flux in % relative to standards (suspension of monodisperse spheres and silicone oil) or to a reference curve. Migration phenomena are monitored through the increment of transmitted light at the lower, or higher, part of the measurement cell depending on the type of migration being creaming or sedimentation respectively. Two possible working modes may be employed: An automatic mode, which follows the evolution of the product with time through the total height of the sample with the acquisitions being periodically executed by the instrument in a time sequence defined by the operator; Or a “one scan” mode, where the acquisitions are manually activated by the operator. This mode is interesting for the measurement of several samples with long breaking processes. However, the boundary between the separating emulsion and the dispersant is particularly sensible to the movements of the emulsion, losing sharpness if they are brusque. Especial care must be taken to not interfere with this phase separation evolution when inserting and extracting the different samples from the instrument. The latest versions of this instrument incorporate a robotic mechanism for the automatic batch processing of different samples guarantying a minimum perturbation of the emulsion rupture process. In this

work, due to the clear/turbid character of the emulsions analyzed, we have considered exclusively transmission information and all the measurements have been performed in “one scan” mode after taking into account all the precautions commented before.

B.3. Emulsions preparation

Depending on the conditions of the experiments the emulsions were prepared using a Diax 900 homogenizer (Heidolph Instruments GmbH&Co., Schwabach, Germany), with a 6G tool, or a S-Series device (Covaris, Inc. Woburn, USA) for adaptive focused acoustic energy treatments (see Figure B2).

Diax 900 is a homogenizer that offers the possibility of up to six different homogenizing speeds ranging from 8000rpm to 26000rpm. The 6G dispersion tool is specially designed for the homogenization of small volumes (0,6ml-50ml). It has a diameter of 6mm, a maximum working depth of and 45mm and a groove width of 0.5mm. With this instrument is possible to achieve emulsions with mean droplet diameters of around 2 μ m.

The instrument S-Series from Covaris is defined as a single tube system developed for high performance sample preparation using adaptive focused acoustic energy. It can treat samples of up to one gram and volumes of less than 10ml. The instrument is composed of an acoustic assembly (transducer and sample holder), a temperature control system for water bath with cooling loop, a degassing system with water level sensor and a safety

interlock system. The acoustic energy generated causes precisely controlled cavitation and acoustic streaming at a focal point within the sample tube in a noncontact, isothermal process.

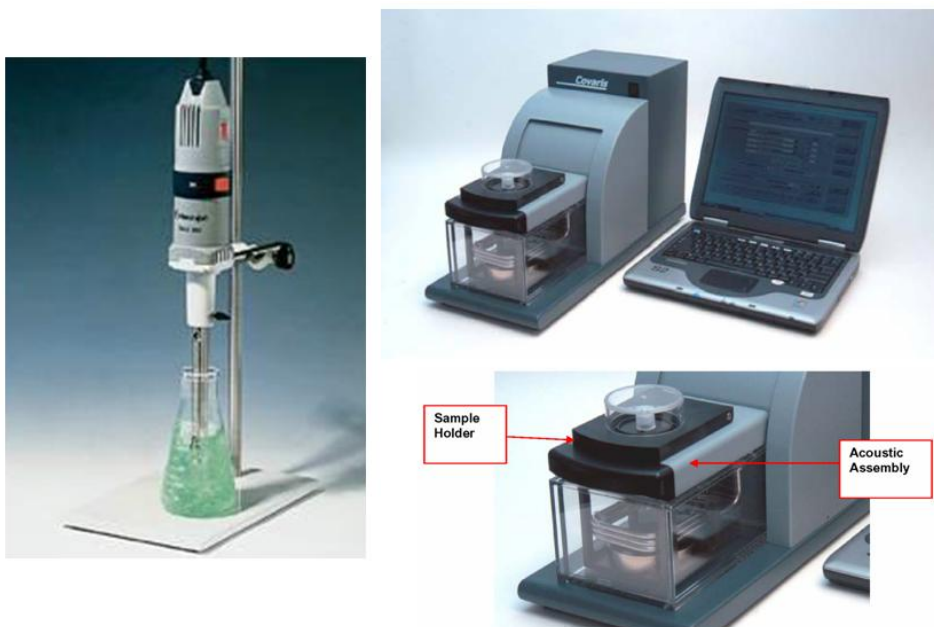


Figure B2. Diax 900 homogenizer with 6G tool (left) and S-Series device for adaptive focused acoustic energy treatment.

These focused acoustics are computer generated and the mechanical energy imparted on the sample results in a controlled series of compression events. The degassing system guarantees a maximum efficiency in the energy transmission and consists of a dip tube with six small holes, a positive displacement pump, and an outlet nozzle. Dissolved gasses and vapors are reduced in the water by pulling the water through the small holes in the dip tube and pumping the resulting coalesced bubbles out the outlet nozzle before they can re-dissolve.

When ultrasound is applied to a sample, containing two immiscible liquids the pressure waves generated disrupts the liquid-liquid interface and allows the cleavage and dispersion of small droplets from one of the liquids into the other. After a proper treatment time, the dispersion is complete and the emulsion is produced. The size distribution and stability of this emulsion is controlled by the concentration of each component, the temperature and the acoustic treatment characteristics. The treatment variables controlled with the S-Series device are frequency mode, duty cycle, intensity and cycles per burst. A complete description of these parameters is given in *Capítulo 2* of this work. With a proper emulsion composition and combination of the treatment variables is possible to obtain size distributions with a mean droplet diameter of less than 300nm.

B.4. Batch turbidity measurements

The simultaneous measurement of the temporal changes in the turbidity of several emulsion samples have been performed using a 96-well SPECTRAFluor Plus (Tecan AG, Hombrechtikon, Switzerland) fluorescence plate reader. This instrument allows the automatic, computer controlled, measurement of absorbance and fluorescence from up to 96 samples in a microplate. Four excitation/absorbance and four emission filters can be arranged in the correspondent slides. The absorbance spectral range may vary from 230nm to 750nm. The light intensity is generated by a high intensity High energy Xenon flash lamp and the transmitted intensity is

measured by a sensitive photomultiplier tube (PMT). The information is processed and stored in the computer by the system software.

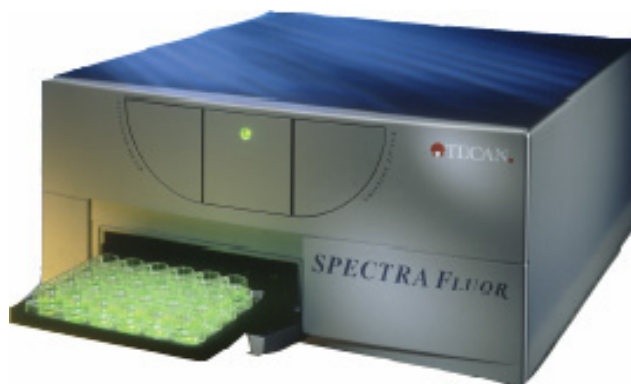


Figure B3. TECAN SpectraFluor fluorescence and absorbance plate reader

This software is also controlling the measurement conditions allowing to set the temperature from 5°C to 40°C, and to produce sample agitation with three different velocities for orbital or linear shaking. These conditions must be established before every experiment together with the experiment duration, time gap between measurements, shaking duration, filters selection and wells positions. More information about the protocol followed in this work can be obtained in *Capítulo 3* of this work.

B.5. Batch interfacial tension measurements

In this work, the dynamic changes in the air-water interfacial tension have been measured using the ADSA technique as explained in *Capítulo 1*. However, to obtain the surface-tension/bulk-concentration adsorption isotherms, the final interfacial pressure of saturation at different surfactant concentrations is the more relevant information. In these cases, the use of ADSA becomes tedious due to the time consuming individual preparation of each experiment. For this type of measurements, we have employed the Delta-8 multichannel microtensiometer (Kibron Inc., Helsinki, Finland). This automatic tensiometer counts with eight parallel microbalances, positioned to match the wells of a standard 96 well plate, in order to measure simultaneously the surface tension of different samples. It uses replaceable wire probes, disposable standard footprint 96-well plates and counts with an automatic system for the probes cleaning based on their heating to approximately 1000°C for 10 seconds in an electric resistor oven. This auto-cleaning system has proven to be effective for removing residual organic compounds that may be adsorbed on the probes after the previous measurement cycle. To obtain the surface tension values a wire is immersed on each sample and subsequently withdrawn from the solution. The maximum force exerted by the interface, just before it disrupts, is recorded by the system software and used to calculate the surface tension. This can be done straight away by considering that the energy balance, just before the interfacial rupture, establish that this force divided by the wire probe

perimeter must correspond with the surface tension value.

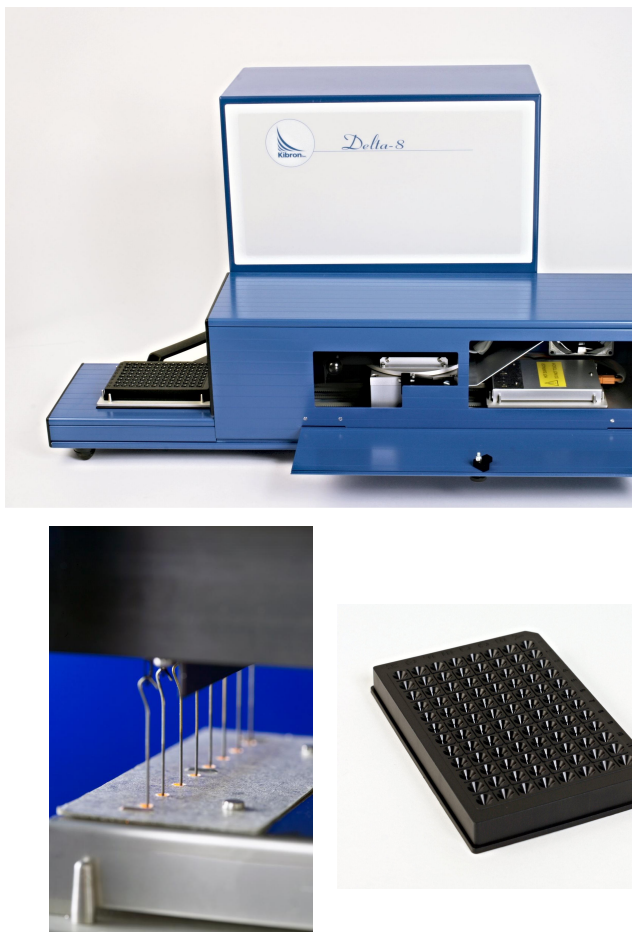


Figure B4. (up) Delta-8 multichannel microtensiometer. (bottom) Auto-cleaning overheating system and 96 wells (50µl) plate.

The precision of this technique is around 0.1mJ/m^2 and serial dilutions may be performed along the wells rows in order to obtain a gradient of concentrations suitable the desired isotherm acquisition. In these dilutions, the concentration may decrease by a dilution factor for every column using

a transfer-and-mix protocol. This dilution factor corresponds with the volumetric ratio between the transferred volume and the initial volume of buffer in the well and can range between zero and one. In this way, up to twelve dilutions can be performed for eight different surfactants. In order to avoid interferences from well to well in the same row, the measurements are always performed from lower to higher concentrations. All the measurements must be performed after the pertinent adsorption time for a maximum approach to the equilibrium between the surface and bulk phases. In our case, this time was obtained with ADSA for the lower concentrations.

B.6. Emulsion droplet sizing

The usual methods employed to obtain the size distribution of relatively concentrated emulsions consist in light scattering studies at certain transmission angles. Due to the big size of the droplets in some emulsions, multiple dispersion phenomena are very common giving raise to erroneous results. However, the information obtained from the backscattered light allows to obtain correct results in the cases where dispersion multiple is affecting to the measurement. The instrument ALV-NIBS/HPPS (Non Invasive Back Scattering/High Performance Particle Sizer) (ALV-Laser Vertriebsgesellschaft mbH, Langen, Germany) uses a combination of the transmitted light (at $\theta = 0^\circ$) and the backscattered at $\theta = 173^\circ$ to allow the measurement of droplet diameters ranging from 5nm to 5 μ m and for dispersed phase concentrations from 0.0001% to 5% in mass. For the

determination of the droplet size distribution, this instrument performs dynamic light scattering analysis (DLS) of the backscattered light.

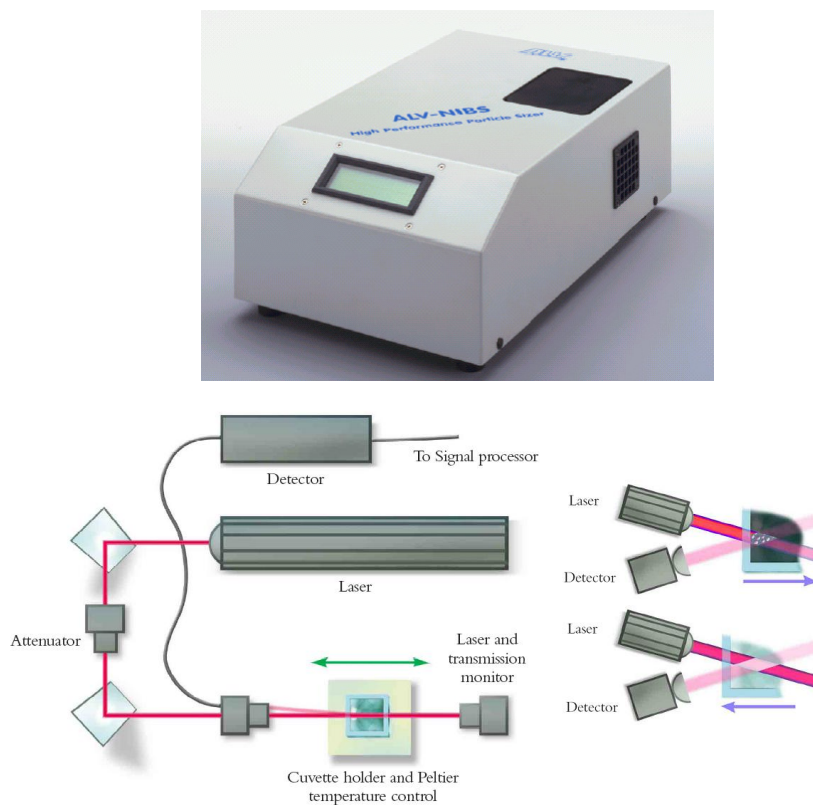


Figure B5. ALV-NIBS/HPPS device (top) and its schematic working principles (bottom).

This instrument therefore facilitate the measurement of concentrated emulsions since it does not need the complete penetration of the incident light beam and minimizes the effect of the multiple dispersion with a very high measurement angle of light detection. A He–Ne polarized laser of 2.5mW and a wavelength of 633nm is employed together with a selective optic fiber detector and a highly efficient avalanche photodiode, to perform

the sample measurement. The photodiode transforms the received photons into electric pulses that are employed by a multiple digital correlator to obtain the autocorrelation function. The transmission detector is employed only for sample and system diagnostics and the intensity of the incident light is controlled by one attenuator that offers a very wide dynamic range. Measurements are performed in polystyrene cuvettes that guaranty the lack of contact of any optical part with the sample. The position of the cuvette is adjusted using auto cell-positioning (see Figure B5) to optimize settings for different sample types and the temperature is controlled along the whole measurement process.

